

University of Southern Queensland  
Faculty of Engineering and Surveying

**Testing of Robotic Total Stations  
For Dynamic Tracking**

**A dissertation submitted by**

**Dennis Garget**

In fulfilment of the requirements of

**Course ENG4112 Research Project**

Towards the degree of

**Bachelor of Spatial Sciences (Surveying)**

Submitted: October, 2005

## **Abstract**

Robotic Total Stations (RTSs) were first introduced by Geodimeter in 1990. These instruments incorporated servomotors and advanced tracking sensor's which allowed the instrument to track a target. This development meant that with the use of a radio link, the instrument could now be completely controlled via remote by a single operator.

Automated machine guidance was the major new application of this advancement in technology. RTS's are now utilised in the construction and extractive industries for the guidance of major earthworks machinery as well as in the agricultural industry for the guidance of machinery such as tractors and harvesters. However, the accuracy and latency of this dynamic application is still not well understood.

Therefore, with the application of RTS's now moving into real-time automated machine guidance it has become critical to understand the exact accuracies that these instruments are capable of achieving whilst operating in the dynamic tracking mode. Thus, upon the completion of this project my aim is to have a better understanding of both the dynamic tracking operational accuracies of several instruments, as well as a better understanding of under what conditions an RTS best performs.

University of Southern Queensland

Faculty of Engineering and Surveying

**ENG 4111 and ENG 4112 Research Project**

**Limitations of Use**

The Council of the University of Southern Queensland, its Faculty of Engineering and Surveying, and the staff of the University of Southern Queensland, do not accept any responsibility for the material associated with or contained in this dissertation.

Persons using all or any part of this dissertation do so at their own risk, and not at the risk of the Council of the University of Southern Queensland, its Faculty of Engineering and Surveying or the staff of the University of Southern Queensland. The sole purpose of the unit entitled “Project” is to contribute to the overall education process designed to assist the graduate enter the workforce at a level appropriate to the award.

The project dissertation is the report of an educational exercise and the document, associated hardware, drawings, and other appendices or parts of the project should not be used for any other purpose. If they are so used, it is entirely at the risk of the user.

*Graham Baker*

Prof G Baker

Dean

Faculty of Engineering and Surveying

# Certification

I certify that the ideas, designs and experimental work, results, analyses and conclusions set out in this dissertation are entirely my own effort, except where otherwise indicated and acknowledged.

I further certify that the work is original and has not been previously submitted for assessment in any other course or institution, except where specifically stated.

Dennis James Garget

Student Number: Q9822921

A handwritten signature in black ink, appearing to be 'Dj Garget', written over a horizontal line.

---

Signature

---

Date

## Acknowledgements

The author wishes to acknowledge the support and guidance received from Mr. Kevin McDougall of University of Southern Queensland, throughout the course of the research project.

Special thanks must also be made to C.R. Kennedy & Co for the loan of the Leica instrument used throughout this project.

In particular Mr. Brett Connolly for his tutoring in the use of the instrument.

Dennis J Garget

*University of Southern Queensland*  
*October, 2005*

# Contents

|                                    |          |
|------------------------------------|----------|
| Abstract                           | i        |
| Limitations of Use                 | ii       |
| Certification                      | iii      |
| Acknowledgements                   | iv       |
| Appendices                         | ix       |
| List of Figures                    | x        |
| List of Tables                     | xiii     |
| <b>CHAPTER 1: INTRODUCTION</b>     | <b>1</b> |
| 1.1 Background of Research         | 1        |
| 1.2 Aim                            | 2        |
| 1.3 Objectives                     | 2        |
| 1.4 Justification                  | 2        |
| 1.5 Overview of Dissertation       | 3        |
| 1.6 Conclusion                     | 4        |
| <b>CHAPTER 2 LITERATURE REVIEW</b> | <b>5</b> |
| 2.1 Introduction                   | 5        |
| 2.2 Trimble S6                     | 6        |

|        |   |    |
|--------|---|----|
| 2.2.1  | Servo Drive                                       | 6  |
| 2.2.2  | Angle Sensor                                      | 8  |
| 2.2.3  | Deviation of the plumb axis                       | 9  |
| 2.2.4  | Collimation errors                                | 10 |
| 2.2.5  | Trunnion axis tilt                                | 10 |
| 2.2.6  | Arithmetic averaging for reducing sighting errors | 10 |
| 2.2.7  | Distances   | 11 |
| 2.2.8  | DR300+: Time of Flight Method (TOF)               | 11 |
| 2.2.9  | DR Standard                                       | 12 |
| 2.2.10 | Comparison of DR300+ and the DR Standard          | 13 |
| 2.2.11 | ATS (Advanced Tracking Sensor)                    | 13 |
| 2.3    | Leica TPS1200                                     | 15 |
| 2.3.1  | Servo Drive                                       | 15 |
| 2.3.2  | Angles  | 15 |
| 2.3.3  | Distance Measurement                              | 16 |
| 2.3.4  | ATS   | 17 |
| 2.4    | Topcon GPT-8200                                   | 18 |
| 2.4.1  | Servo Drive                                       | 18 |
| 2.4.2  | Distance Measurement                              | 18 |
| 2.4.3  | ATS   | 19 |
| 2.5    | Comparison of RTS Specifications                  | 20 |
| 2.6    | Previous Testing Undertaken                       | 21 |
| 2.6.1  | Chua 2004   | 21 |

|                                    |  |           |
|------------------------------------|--|-----------|
| 2.6.2                              | Ceryova                                    | 22        |
| 2.6.3                              | Conclusion                                 | 23        |
| 2.7                                | The Kalman Filter                          | 24        |
| 2.7.1                              | Kalman Filter Description                  | 24        |
| 2.8                                | Conclusion                                 | 25        |
| <b>CHAPTER 3 RESEARCH APPROACH</b> |  | <b>26</b> |
| 3.1                                | Introduction                               | 26        |
| 3.1.1                              | Project Planning                           | 26        |
| 3.2                                | Research Method                            | 27        |
| 3.2.1                              | Literature Contribution to Research Method | 27        |
| 3.2.2                              | Data Collection and Testing                | 28        |
| 3.2.2.1                            | Equipment Utilised                         | 28        |
| 3.2.2.2                            | Components of an RTS                       | 29        |
| 3.2.2.3                            | Operation of an RTS System                 | 29        |
| 3.2.2.4                            | Field Testing                              | 30        |
| 3.2.3                              | Data Analysis and Discussion               | 35        |
| 3.2.3.1                            | Data Transfer                              | 35        |
| 3.2.3.2                            | Software Utilised                          | 35        |
| 3.2.3.3                            | Analysis of Results                        | 36        |
| 3.3                                | Conclusion                                 | 37        |



|  |           |
|--|-----------|
| <b>CHAPTER 4 RESULTS AND DISCUSSIONS</b>         | <b>38</b> |
| 4.1 Introduction                                 | 38        |
| 4.2 Analysis of Results                          | 40        |
| 4.3 Circular Path Test Results                   | 41        |
| 4.3.1 Leica TPS1205 at 0.1 second record time    | 42        |
| 4.3.2 Leica TPS1205 at 0.5 second record time    | 44        |
| 4.3.3 Trimble S6 at 1.0 second record time       | 46        |
| 4.4 Straight-Line Test Results                   | 48        |
| 4.4.1 Leica TPS1205 at 0.1 second record time    | 49        |
| 4.4.2 Leica TPS1205 at 0.5 second record time    | 51        |
| 4.4.3 Trimble S6 at 1.0 second record time       | 53        |
| 4.5 Discussion                                   | 55        |
| 4.5.1 Circular Path results summary              | 55        |
| 4.5.2 Straight-line results summary              | 58        |
| 4.5.3 Accuracy                                   | 60        |
| 4.5.4 Reliability                                | 61        |
| 4.6 Conclusion                                   | 61        |
| <br>   |           |
| <b>CHAPTER 5 CONCLUSIONS AND RECOMMENDATIONS</b> | <b>62</b> |
| 5.1 Recommendations                              | 62        |
| 5.2 Conclusions                                  | 63        |
| <br>   |           |
| <b>REFERENCES</b>                                | <b>65</b> |

## Appendices

|             |  |     |
|-------------|--|-----|
| Appendix A. | Project Specification  | 67  |
| Appendix B. | Circular Path Test Results for Leica TPS1205 at a recording speed of 0.1 seconds | 69  |
| Appendix C. | Circular Path Test Results for Leica TPS1205 at a recording speed of 0.5 seconds | 78  |
| Appendix D. | Circular Path Test Results for Trimble S6 at a recording speed of 1.0 seconds    | 87  |
| Appendix E. | Straight-line Test Results for Leica TPS1205 at a recording speed of 0.1 seconds | 96  |
| Appendix F. | Straight-line Test Results for Leica TPS1205 at a recording speed of 0.5 seconds | 103 |
| Appendix G. | Straight-line Test Results for Trimble S6 at a recording speed of 0.1 seconds    | 110 |

## List of Figures

|      |   |    |
|------|---|----|
| 1.1  | RTS being used for the guidance of scrapers (Trimble, 2005)   | 1  |
| 2.1  | Three current RTS's   | 5  |
| 2.2  | Intergrated angle and servo system (Lemmon & Jung, 2005)  | 6  |
| 2.3  | Servo drive operation (Lemmon & Jung, 2005)   | 7  |
| 2.4  | Cross-section of Angle Sensor Unit (Lemmon & Jung, 2005)  | 8  |
| 2.5  | S6 automatic corrections (Lemmon & Jung, 2005)  | 9  |
| 2.6  | Optical Principles for Pulsed Laser (Hoglund and Large, 2003)   | 11 |
| 2.7  | Optical Principle for Phase Shift EDM (Hoglund and Large, 2003)   | 12 |
| 2.8  | Diagram of the Synchronization process (Trimble, 2005)  | 14 |
| 2.9  | Diagram showing several RTS's operating on a construction site (Geodimeter, 2004)   | 15 |
| 2.10 | GPT-8200 communicating via infrared with a RC-211w (Topcon, 2004)   | 19 |
| 2.11 | The purpose of Kalman Filter is to estimate the values of variables describing the state of a system from a multidimensional signal contaminated by noise | 24 |

## List of Figures

---

|     |  |    |
|-----|--|----|
| 3.1 | Leica TPS1205  | 28 |
| 3.2 | Trimble S6   | 28 |
| 3.3 | Operation and Components of an RTS   | 30 |
| 3.4 | Circular Path target assembly  | 31 |
| 3.5 | Straight-line rail and target assembly                                     | 33 |
| 3.6 | Analysis Process   | 36 |
| 4.1 | Data analysis process with in Microsoft excel                              | 40 |
| 4.2 | Circular Path test results for the Leica TPS1205 at 0.1 second record time | 42 |
| 4.3 | Offset error associated with each point captured by the Leica TPS1205      | 43 |
| 4.4 | Error associated with angular movement speeds to Pillar 1                  | 43 |
| 4.5 | Circular Path test results for the Leica TPS1205 at 0.5 second record time | 44 |
| 4.6 | Offset error associated with each point captured by the Leica TPS1205      | 45 |
| 4.7 | Error associated with angular movement speeds to Pillar 4                  | 45 |
| 4.8 | Circular Path test results for the Trimble S6 at 1.0 second record time    | 46 |
| 4.9 | Offset error associated with each point captured by the Trimble S6         | 47 |

## List of Figures

---

|      |   |    |
|------|---|----|
| 4.10 | Error associated with angular movement speeds to Pillar 3                             | 47 |
| 4.11 | Straight-line test results for the Leica TPS1205 at 0.1 second record time            | 49 |
| 4.12 | Offset error associated with each point captured by the Leica TPS1205                 | 50 |
| 4.13 | Error associated with angular movement speeds from Stn 1                              | 50 |
| 4.14 | Portion of Circular Path test results for the Leica TPS1205 at 0.5 second record time | 51 |
| 4.15 | Offset error associated with each point captured by the Leica TPS1205                 | 52 |
| 4.16 | Error associated with angular movement speeds from Stn 1                              | 52 |
| 4.17 | Portion of Circular Path test results for the Trimble S6 at 1.0 second record time    | 53 |
| 4.18 | Offset error associated with each point captured by the Leica TPS1205                 | 54 |
| 4.19 | Error associated with angular movement speeds from Stn 1                              | 54 |
| 4.20 | Standard Deviation vs Tracking Speed, Pillar 4  | 57 |
| 4.21 | Standard Deviation vs Distance, Speed 1   | 57 |
| 4.22 | Standard Deviation vs Instrument tracking speed                                       | 59 |
| 4.23 | Standard Deviation vs RTS – target distance   | 60 |

## List of Tables

|     |  |    |
|-----|--|----|
| 2.1 | Comparison of RTS instrument turning speeds                          | 7  |
| 2.2 | Comparison of accuracies of both measurement systems                 | 13 |
| 2.3 | Trimble DR Ranges to Various Target Surfaces (Hoglund & Large, 2005) | 13 |
| 2.4 | TPS1200 series angle accuracies (Std Dev) (Leica Geosystems, 2005)   | 16 |
| 2.5 | Leica ATR specifications (Leica, 2005)                               | 17 |
| 2.6 | Leica PowerSearch specifications (Leica, 2005)                       | 17 |
| 2.7 | Accuracy specifications of the GPT-8200 (Topcon, 2004)               | 19 |
| 2.8 | Comparison between the three RTS systems (Product Survey, 2005)      | 20 |
|     |  |    |
| 3.1 | Circular Path testing undertaken                                     | 32 |
| 3.2 | Approximate distance of target from the RTS                          | 32 |
| 3.3 | Approximate target movement speeds                                   | 32 |
| 3.4 | Straight-line testing undertaken                                     | 34 |
| 3.5 | Approximate distance from RTS to target                              | 34 |

|     |  |    |
|-----|--|----|
| 3.6 | Approximate speed of moving target                           | 34 |
| 4.1 | Results summary for the Leica TPS1205 working at 0.1 seconds | 55 |
| 4.2 | Results summary for the Leica TPS1205 working at 0.5 seconds | 56 |
| 4.3 | Results summary for the Trimble S6 working at 1.0 seconds    | 56 |
| 4.4 | Results summary for the Leica TPS1205 working at 0.1 seconds | 58 |
| 4.5 | Results summary for the Leica TPS1205 working at 0.5 seconds | 58 |
| 4.6 | Results summary for the Trimble S6 working at 1.0 seconds    | 59 |

## CHAPTER 1

### INTRODUCTION

#### 1.1 Background of Research

Robotic Total Stations (RTS) were first introduced by Geodimeter in 1990 with the System 4000. This system, as with many current systems incorporated servomotors for the automatic rotation of the instrument and an Advanced Tracking Sensor (ATS) to allow the instrument to track a given target (i.e. prism). This development meant that with the use of a radio link between the instrument and the prism pole, the instrument could now be completely controlled by a single operator from the prism pole.

This advancement significantly increased the RTSs operating capacity in DTM surveys, as-constructed surveys and hydrographic surveys.

Automated machine guidance however was the major new application, with the RTS now being used in the construction and extractive industries for the guidance of dozers, graders, excavators and scrapers (see Figure 1.1) as well as in the agricultural industry for tractor and harvester guidance.



**Figure 1.1:** RTS being used for the guidance of scrapers.  
(Trimble, 2005)



## 1.2 Aim

The aim of this project is to test the accuracy and reliability of robotic total stations when used in the dynamic tracking mode.

## 1.3 Objectives

The objectives of this project are:

1. To review existing literature concerned with RTSs;
2. Establish a testing regime in order to determine the dynamic accuracy of several RTS's;
3. Conduct a series of tests on several RTSs under various conditions;
4. Undertake comprehensive analysis of test results; and
5. Determine the final accuracies of the RTSs.

## 1.4 Justification

With the application of RTS's now moving into real-time automated machine guidance it has become critical to understand the exact accuracies that these machines are capable of achieving whilst operating in the dynamic tracking mode.

This is because on major construction sites (eg road construction) the earthworks are often required to be within tolerances of  $\pm 0.02\text{m}$ . In order to utilise this dynamic tracking technology for such work we must first determine whether this technology is capable of meeting such stringent accuracy requirements.

Furthermore we must also understand under what conditions these accuracies are achieved. Such conditions include:

- Angle of RTS to works;
- Distance of RTS to works; and
- Speed of moving target.

Thus upon the completion of this project we will have a better understanding of both the dynamic tracking operational accuracies of several instruments as well as better understanding under what conditions an RTS best performs.

## **1.5 Overview of Dissertation**

Following is a brief overview of each chapter contained within this dissertation.

Chapter 2 aims to provide a basis for drawing any conclusions. It does this by providing the following information:

1. Background into advanced technological background into the precise workings of each RTS to be tested.
2. Review and comment on previous testing which has been undertaken.
3. Brief background into the working of the Kalman Filter, which, is to be utilised during the result analysis stage.

Chapter 3 provides detailed information into both the testing regime which has been implemented and the data analysis methodology.

Chapter 4 will provide my testing results, accompanied by some discussion.

Chapter 5 is where conclusions will be drawn and any recommendations will be presented.

## **1.6 Conclusion**

Due to the rapid expansion of RTS's operational limits there has been little testing performed to validate the true accuracy of an RTS whilst operating in the dynamic tracking mode. Thus due to the increased applications for an RTS it has become necessary to undertake comprehensive testing into these instrument accuracies.

In order to understand each individual instrument's operational accuracy we must first understand each instruments mechanical operation. Thus Chapter 2 will provide detailed information on each tested instruments mechanical operation.

## CHAPTER 2

### LITERATURE REVIEW

#### 2.1 Introduction

In order to provide some background into the operations of an RTS, I will first describe in detail the mechanical workings of three current RTS's, two of which will be tested. These three instruments are the Trimble S6, the Leica TPS1200 and the Topcon GPT-8200 (see Figure 2.1).



**Figure 2.1:** Three current RTSs.

The second stage of the literature review will be to examine and discuss all existing literature relating to the testing of RTS. The third and final stage is a description of the Kalman Filter and its application for this project.

## 2.2 Trimble S6

### 2.2.1 Servo Drive

The Trimble S6 incorporates a revolutionary servo/angle system called the MagDrive. The MagDrive is an integrated servo and angle system that utilises a direct drive and frictionless electromagnetic drive technique (*Lemmon & Jung, 2005*). A major benefit of the direct drive system is that it allows the servo drive to be mounted directly to the horizontal and vertical axis, thus eliminating the need for any additional mechanical gearing.

The servo drive itself consists of a holder containing areas of magnets and soft iron. These materials are distributed into two concentric cylindrical compartments that are separated by an air gap. This air gap provides space for a cylindrical motor winding which controls the changing of direction and the fine control of the rotation (refer to Figure 2.2).

Applying a current through the motor winding drives the instrument (refer to Figure 2.3). According to known electromagnetic theory this then provides non-contacting, frictionless motion by using electromagnetic force to rotate the magnet holder (*Lemmon & Jung, 2005*).

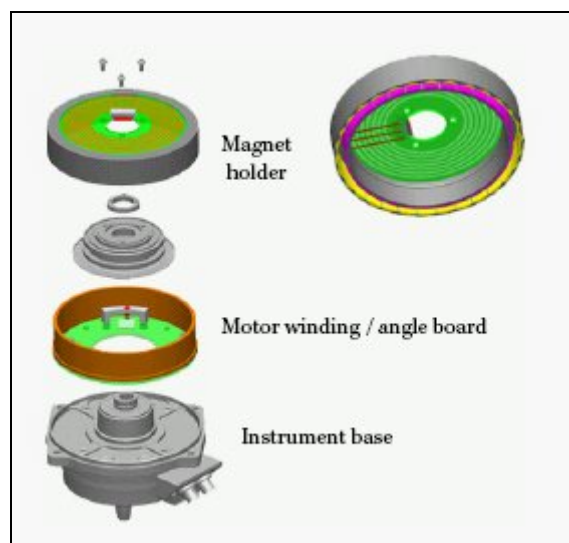


**Figure 2.2:** Integrated angle and servo system.

(Source: *Lemmon & Jung, 2005*)

The servo drive technology contains three different working modes. These include:

1. Driving Mode. Movement is controlled by the tangent screws or system process;
2. Friction Mode. The drive allows the instrument to be turned manually;
3. Holding Mode. The drive works as a clutch to lock the instruments position and prevent movements.

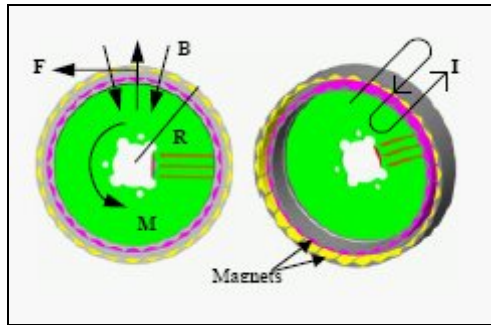


**Figure 2.3:** Servo drive operation.  
(Source: Lemmon & Jung, 2005)

The working modes and design of the direct drive system combine to provide exceptional performance when compared to more conventional systems. Following is a table highlighting the increased performance of the S6.

**Table 2.1:** Comparison of RTS instrument turning speeds.

| Instrument    | Specified max turning speed |
|---------------|-----------------------------|
| Trimble S6    | 115°/sec                    |
| Leica TPS1200 | 45°/sec                     |
| Topcon        | 50°/sec                     |

### 2.2.2 Angle Sensor

The S6 incorporates an optical based sensor unit that is integrated with the servo drive. The angle sensor unit itself consists of glass circles that contain a coarse and a fine code pattern. These code patterns are distributed in two tracks on the glass circles. One track contains an absolute code, whilst the other contains an incremental code. The utilisation of two separate tracks provides a uniform accuracy and resolution around the circle. The tracks are then illuminated via a single laser light source. This then projects onto two Complementary Metal Oxide Semiconductor (CMOS) image sensors. Note that in order to ensure that the absolute encoder is robust and less prone to mounting errors the sensor are positioned on opposite sides of the disk.

The projected image is then analysed using a numerical Fourier phase-detection algorithm. This creates a high-resolution angle from the fine code. The final angle value is then calculated by the mean value of the two CMOS image sensor readings (*Lemmon & Jung, 2003*).

The angle sensor unit is integrated in to the servo drive housing. The encoded glass tracks, laser transmitter, image area detectors and the servo drive windings are all located within the central unit (refer to Figure 2.4). Thus the angle sensor is design to display and store angle data as well as supporting the servo system with fast data for angular calculation.

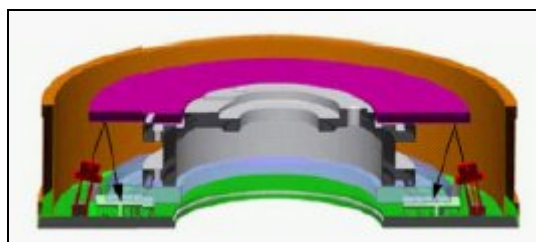


**Figure 2.4:** Cross-section of Angle Sensor Unit.

(Source: *Lemmon & Jung, 2005*)

In addition to determining the angle, the angle measurement system also compensates for the following: (see figure 2.5)

1. Deviation of the plumb axis;
2. Collimation errors;
3. Trunnion axis tilt; and
4. Arithmetic averaging for reducing sighting errors.

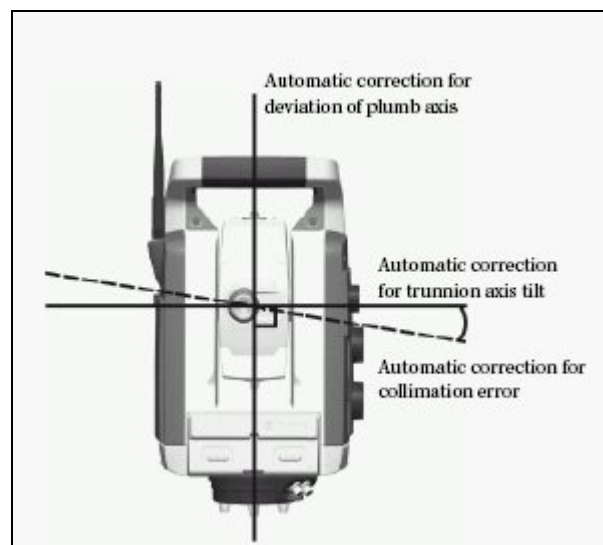


**Figure 2.5:** S6 automatic corrections.

*(Source: Lemmon & Jung, 2005)*

### 2.2.3 Deviation of the plumb axis

In order to automatically correct any deviation of the plumb axis the S6 utilises a light beam that is reflected towards a free liquid surface via an optical lens. A CMOS image sensor is then used to detect the inclination of the light beam in both the measuring direction and perpendicular to this direction and thus the instrument is automatically corrected.



#### **2.2.4 Collimation errors**

The S6 is able to account for collimation errors by performing a pre-measurement collimation test. Angular measurements are observed on both instrument faces to enable the collimation errors (both horizontal and vertical) to be calculated. These values are then stored in the instrument and applied to all subsequent angle measurements. The method is applied during the Autolock (Automatic Targeting) collimation test.

#### **2.2.5 Trunnion axis tilt**

Similar to the process for correcting collimation errors the trunnion axis is automatically corrected by performing a pre-measurement trunnion axis tilt test. Angular measurements are performed on both faces to enable the horizontal tilt axis to be calculated. Again these values are stored and applied to all subsequent horizontal angles.

#### **2.2.6 Arithmetic averaging for reducing sighting errors**

The S6 is able to automatically reduce sighting errors which are caused by misalignment of the instrument or by movement during measurement. This is done via:

1. Using Autolock technology. When Autolock is enabled the instrument will automatically lock to and track the target. Thus reducing manual sighting errors.
2. SurePoint accuracy assurance. When the S6 is manually aimed at a target the servomotors are finely tune to hold the aimed angle. SurePoint ensures that sighting errors due to unintentional small movements of the instrument are eliminated.
3. Automatically averaging angles during distance measurement. When in Standard mode the instrument will take approximately 1.2 seconds to measure distance. Fully synchronized angles and distances are averaged over the measurement period to obtain averaged, highly accurate measurement.

### 2.2.7 Distances

The Trimble S6 offers two forms of Direct reflex (distance) measurement. The first being the DR300+ which utilizes the Time of Flight (Pulsed Laser) method and the second being the DR Standard which utilises the phase shift method.

### 2.2.8 DR300+: Time of Flight Method (TOF)

In this system distance measurement is determined by precisely measuring the time taken by a pulse to return to the instrument. The instrument does this by generating many short infrared or laser pulses that are transmitted through the telescope to the intended target. These pulses then reflect off the target and return to the instrument where electronics determine the round trip time for each light pulse (refer to Figure 2.6). The travel time is then used to compute the distance between the instrument and the target (*Hoglund & Large, 2003*).

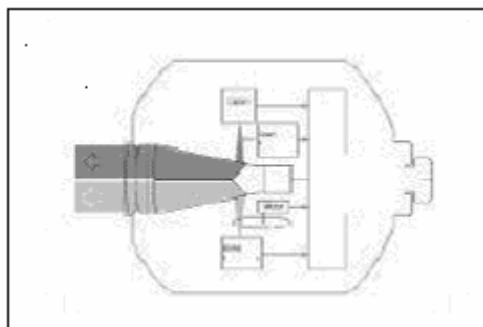


**Figure 2.6:** Optical Principles for Pulsed Laser.

(Source: *Hoglund & Large, 2003*)

Each pulse produces a direct range measurement, thus by emitting thousands of pulses per second a good average value can be achieved relatively quickly. (Typically 20,000 pulsed laser measurements are taken every second)

The accuracy problem that is associated with the TOF method is that it relies on time. This time become very critical when dealing with light as it moves at 299,792,458m/s (Google, 2005).

Therefore in order to achieve an accuracy of 0.003m the time must be able to be measured to  $1 \times 10^{-11}$ .

### 2.2.9 DR Standard

The DR standard is a laser distance unit based on the phase comparison method. The instrument transmits a coaxial modulated optical measuring beam that is either reflected by a prism or scattered by a surface to which the beam is directed. The phase difference between the transmitted light and the reflected received light is detected and used to determine the distance (refer to Figure 2.7) (Hoglund & Large, 2003).

The instrument measures a constant phase offset despite the inevitable variations between the emitted and received signal. Initially the cycle ambiguity prevents the total distance from being calculated. This cycle ambiguity is then resolved by using multiple modulations of the measurement beam wavelength, this provides a unique integer number of cycles. This integer number is then used to accurately determine the target distance.

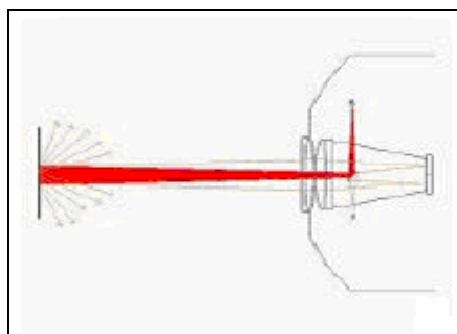


**Figure 2.7:** Optical Principle for Phase Shift EDM.

(Source: Hoglund & Large, 2003)

Note that the S6 with DR Standard technology is not yet available in Australia.

### 2.2.10 Comparison of DR300+ and the DR Standard

**Table 2.2:** Comparison of accuracies of both measurement systems

|            | DR300+     | DR Standard |
|------------|------------|-------------|
| Prism Mode | 3mm + 3ppm | 1mm + 1ppm  |
| DR Mode    | 3mm + 3ppm | 3mm + 2ppm  |

(Source: Hoglund & Large, 2005)

**Table 2.3:** Trimble DR Ranges to Various Target Surfaces

| Surface    | DR300+ | DR Standard |
|------------|--------|-------------|
| Kodak 90%  | >800m  | >240m       |
| Kodak 18%  | >300m  | >120m       |
| Concrete   | >400m  | >100m       |
| Wood       | >400m  | >200m       |
| Light Rock | >300m  | >150m       |
| Dark Rock  | >200m  | >80m        |

(Source: Hoglund & Large, 2005)

From tables 2 and 3 we can see that the DR300+ has a far greater range than the DR Standard whilst in DR mode, however the DR Standard possesses superior accuracy in both the DR and Prism modes.

### 2.2.11 ATS (Advanced Tracking Sensor)

Trimble defines ATS RTS as-

*“..automatically lock on the active target and continuously measures the target’s position and transmits the data to the computer, which then determines the desired elevation and slope for that position.” (Trimble Data Sheet, 2004)*

Trimble has designed its ATS specifically for the high speed, low-latency demands associated with machine control. The ATS in advanced tracking mode has a latency of less than 200ms. This low level of latency, combined with the S6's turning speed enable the ATS to track a machine driving at over 46kph at ranges of less than 30m (*Trimble, 2005*). Furthermore the onboard application software is able to compensate for any errors associated with this data latency. This results in a more accurate location of the target in real time.

The synchronization of data from the angle and distance measurement sensors means that the output data is computed for a single instantaneous location of the moving target (refer to Figure 2.8). This results in an increased level of accuracy for a 3D position.

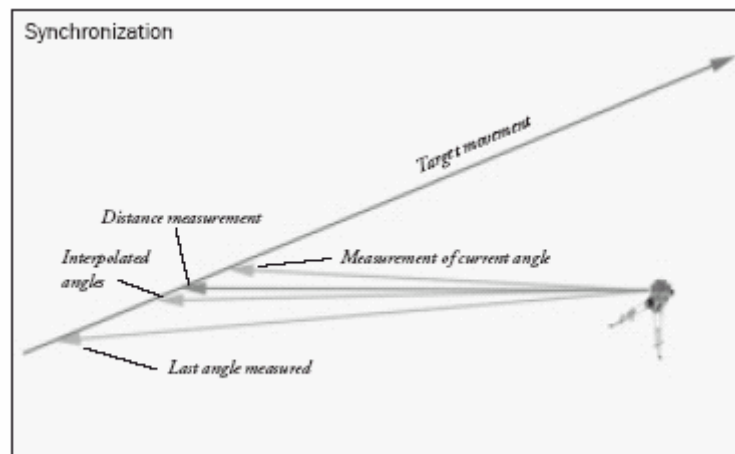


**Figure 2.8:** Diagram of the Synchronization process.

(Source: *Trimble, 2005*)

Trimble also suggests that the ATS has built in “search intelligence”, this enables the instrument to locate the target should contact be temporarily interrupted. It does this by initiating a search grid until the target is found.

The ATS also has programmable target recognition capabilities. This allows for the use of several instruments on the same site without any interference. This is possible because the ATS has Target ID. This means that the ATS can be programmed to recognize one of four possible targets. This provides the freedom to operate four machines or surveys in the same area (refer to Figure 2.9) (*Trimble, 2005*).

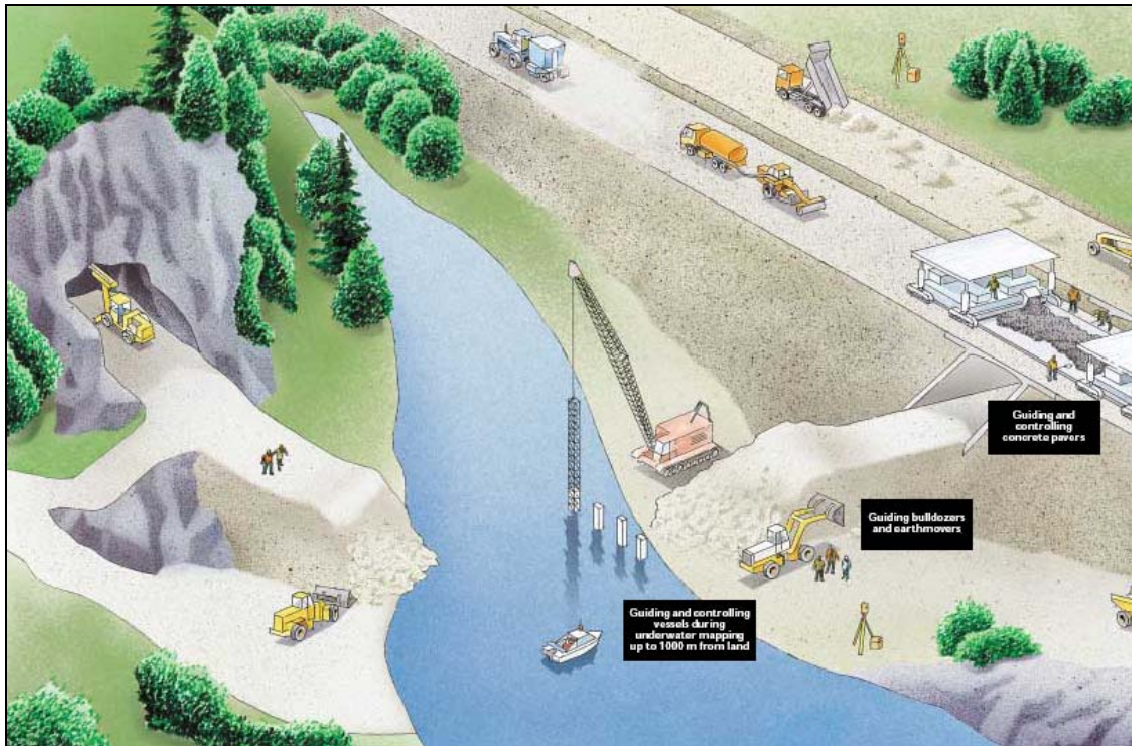


**Figure 2.9:** Diagram showing several RTS's operating on a construction site.

(Source: Geodimeter, 2004)

## 2.3 Leica TPS1200

### 2.3.1 Servo Drive

Unlike the S6 the TPS1200 is mechanically driven by servomotors. These servomotors are used to rotate both the horizontal and vertical axis. The downside of these motors is that they use a lot more power than MagDrive technology and they are only able to rotate at a fraction of the speed. Refer to Table 1 for exact turning speeds.

### 2.3.2 Angles

The TPS1200's angle measurement system consists of a static line-coded glass circle, which is read by a linear CCD array. A special algorithm is then used to determine the

exact position of the code lines on the array and thus determine the precise angle measurement instantly.

The system also contains a dual axis compensator that constantly monitors the two axis of vertical tilt. The compensator consists of an illuminated line pattern on a prism, which is reflected twice by a liquid mirror. This forms the reference horizon. The reflected image of this line pattern is read by a linear CCD array and then used to mathematically determine both of the tilt components. These calculated tilt components are then used to correct all angle measurements in real time (refer to Table 2.4 for specific angle accuracies).

**Table 2.4:** TPS 1200 series angle accuracies (Std Dev).

|                           | TPS 1201                          | TPS 1202 | TPS 1203 | TPS 1205 |
|---------------------------|-----------------------------------|----------|----------|----------|
| <b>Accuracy (Std dev)</b> |                                   |          |          |          |
| Hz, V:                    | 1''                               | 2''      | 3''      | 5''      |
| Display least count:      | 0.1''                             | 0.1''    | 0.1''    | 0.1''    |
| <b>Method</b>             |                                   |          |          |          |
| Working Range:            | 4'                                | 4'       | 4'       | 4'       |
| Setting Accuracy:         | 0.5''                             | 0.5''    | 1.0''    | 1.5''    |
| Method:                   | Centralized dual axis compensator |          |          |          |

(Source: Leica Geosystems, 2005)

### 2.3.3 Distance Measurement

The TPS 1200 series utilizes a phase shift measurement technique (EDM), which operates in both the reflector and reflectorless modes.


The EDM works by transmitting an invisible beam (modulated frequency of 100MHz), this beam is then reflected back by the prism or target. This reflected light is then detected by a sensitive photo receiver and converted into an electrical signal. Once this electrical signal is digitized and accumulated, the distance is then determined via standard phase measurement techniques as employed by the Trimble S6 DR Standard.

### 2.3.4 ATS

The ATS of the TPS 1200 series, which Leica refers to as Automatic Target Recognition ATR/LOCK, is similar to the S6 in that it actively follows the prism as it moves (refer to Table 2.5 for Leica specifications). The TPS 1200 however, also has additional on board software that predicts the reflector movement path, this enables the TPS1200 to continue to track despite obstruction and short interruptions. Should the interruption be too long then the operator must utilize the Power Search function.


Power Search is a function that allows the instrument to find the prism with in seconds no matter how far it has moved. When Power Search is activated the TPS1200 rotates and sends out a laser fan. As soon as this fan strikes the prism the TPS1200 stops rotating (refer to Table 2.6 for Lieca specifications). From here the ATR takes over.

**Table 2.5:** Leica ATR specifications

| Automatic Target Recognition (ATR)  |   |  |
|---|---|--|
|  | <b>Range ATR mode / LOCK mode</b><br>(average atmospheric conditions) | Round prism (GPR1): 1000 m / 800 m<br>360° reflector (GRZ4): 600 m / 500 m<br>Mini prism (GMP101): 500 m / 400 m<br>Reflective tape (60 mm x 60mm): 55 m (175 ft)<br>Shortest measurable distance: 1.5 m / 5 m |
|   | <b>Accuracy / Measurement time</b>                                    | Positioning accuracy: < 2 mm<br>Measurement time: 3 – 4 s  |
|   | <b>Maximum speed (LOCK mode)</b>                                      | Tangential (standard mode): 5 m / s at 20 m, 25 m / s at 100 m<br>Radial (tracking mode): 4 m / s  |
|   | <b>Method</b>   | Digital image processing (laser beam)  |

(Source: Leica, 2005)

**Table 2.6:** Leica PowerSearch specifications

| PowerSearch (PS)  |  |   |
|---|--|---|
|  | <b>Range</b><br>(average atmospheric conditions) | Round prism (GPR1): 200 m<br>360° reflector (GRZ4): 200 m (perfectly aligned to instrument)<br>Mini prism (GMP101): 100 m<br>Shortest distance: 5 m |
|   | <b>Search time</b>                               | Typical search time: < 10 s   |
|   | <b>Maximum speed</b>                             | Rotating speed: 45° / s   |
|   | <b>Method</b>                                    | Digital signal processing (rotating laser fan)  |

(Source: Leica, 2005)



## **2.4 Topcon GPT-8200**

### **2.4.1 Servo Drive**

As is the case with the TPS1200, the GPT-8200 is mechanically driven by servomotors. These servomotors are used to rotate both the horizontal and vertical axis. Again the downside of these motors is that they use a lot more power than MagDrive technology and they are only able to rotate at a fraction of the speed. Refer to Table 1 for exact turning speeds.

### **2.4.2 Distance Measurement**

Similar to the Trimble S6's DR300+, the GPT-8200 determines distance by precisely measuring the time taken by a pulse to return to the instrument. The instrument does this by generating many short infrared or laser pulses which are transmitted through the telescope to the intended target. These pulses then reflect off the target and return to the instrument where electronics determine the round trip time for each light pulse. The travel time is then used to compute the distance between the instrument and the target. Each pulse produces a direct range measurement, thus by emitting thousands of pulses per second a good average value can be achieved relatively quickly. (Typically 20,000 pulsed laser measurements are taken every second)

Although similar to the DR300+, the GPT-8200 does in fact have a much larger range (Table 8). This is due to the increased power of the infrared pulses combined with a second pulse mode, Non-Prism Long Mode. This mode has decreased accuracy and thus can read further.

Table 2.7 lists the GPT-8200 accuracy specifications:

**Table 2.7:** Accuracy specification of the GPT-8200

| Accuracy                           |   |
|------------------------------------|---|
| Prism Mode                         |   |
| Fine Mode                          | $\pm(2\text{mm}+2\text{ppm}\times D^*)\text{m.s.e.}$  |
| Coarse Mode                        | $\pm(10\text{mm}+2\text{ppm}\times D^*)\text{m.s.e.}$ |
| Non-Prism Normal Mode              |   |
| Fine Mode 3 - 25m (9.8 ft - 82 ft) | $\pm(10\text{mm})\text{ m.s.e.}$                      |
| Fine Mode 25m (82 ft)              | $\pm(3\text{mm}+2\text{ppm})\text{ m.s.e.}$           |
| Coarse Mode                        | $\pm(10\text{mm}+2\text{ppm})\text{ m.s.e.}$          |

(Source: Topcon, 2004)

### 2.4.3 ATS

Unlike the S6 and TPS1200, the GPT-8200 does not rely on radio communication between the instrument and the pole. Instead the GPT-8200 utilizes infrared (IR) communication technology. This is achieved by attaching a system, known as the RC-211w “Fast-Trak”, to the prism pole. This unit is then capable of communicating with the instrument via the use of IR (see Figure 2.10). Refer to Table 8 for specific operating ranges.

Similarly, the RC-211w is used by the instrument to locate the prism pole should the pole be obstructed/lost at any time whilst working.

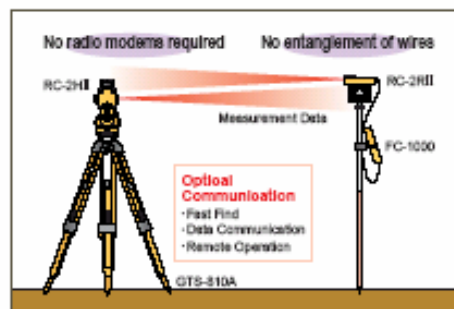


**Figure 2.10:** GPT-8200 communicating via infrared with a RC-211w.

(Source: Topcon, 2004)

## 2.5 Comparison of RTS Specifications

**Table 2.8:** Comparison between the three RTS systems.

|   | <b>Trimble S6</b>   | <b>Leica TPS1200</b>  | <b>Topcon GTP-8200</b>                |
|---|---|---|---------------------------------------|
| Configuration                               | Total Station,<br>Coaxial EDM                                 | Total Station,<br>Coaxial EDM   | Self contained<br>Coaxial Measurement |
| <b>Distance Measurement</b>                 |   |   |                                       |
| Distance Measuring<br>Type                  | Pulse   | Phase shift   | Pulse laser                           |
| Range (Single Prism)                        | 5500m   | >10,000m  | 7000m                                 |
| EDM Accuracy (normal)                       | $\pm 3\text{mm} + 3\text{ppm}$                                | $\pm 5\text{mm} + 2\text{ppm}$  | $\pm 2\text{mm} + 2\text{ppm}$        |
| Measuring Time,<br>single read/tracking     | 1.2sec<br>0.4sec  | 0.8sec<br>0.15sec   | 0.3sec<br>0.3sec                      |
| <b>Theodolite Components</b>                |   |   |                                       |
| Angle Accuracy                              | Varies<br>1", 2", 3" & 5"                                     | 1"  | Varies<br>1", 2", 3" & 5"             |
| Stores Collimation and<br>Index Corrections | Yes   | Yes   | Yes                                   |
| Stores Trunnion Axis<br>Corrections         | Yes   | Yes   | Yes                                   |
| <b>Advanced Features</b>                    |   |   |                                       |
| Target Tracking                             | MultiTrack,<br>Combines Passive<br>with active Target ID      | Passive, automatic<br>targeting & tracking                            | CCD array,<br>standard prism          |
| Robotic Search Control                      | User definable,<br>search window,<br>control from rod,<br>Map | PowerSearch,<br>joystick, user<br>definable, compass,<br>working area | RC-211 Quick-Lock                     |
| Distance at which RTS<br>can be controlled  | 700m  | 800m  | 250m                                  |
| Number of servo speeds                      | MagDrive (5)  | 2   | 7                                     |
| Range to 90% Kodak<br>grey card             | 800m  | 500m  | 1200m                                 |
| Range to 18% Kodak<br>grey card             | 300m  | 300m  | 600m                                  |

(Source: Product Survey, 2005)

## 2.6 Previous Testing Undertaken

Besides the manufactures testing (specifications) there has been very little testing performed in relation to the dynamic accuracy of RTS. Following is a description and brief discussion relating to two previous tests which have been carried out.

The two previous tests carried out in order to “*determine the dynamic accuracy and reliability of RTS’s.*” were carried out by:

- Chua in 2004; and
- Ceryova in 2002.

### 2.6.1 Chua 2004

In order to complete his testing, Chua set out several objectives, these included:

- Simple testing in a fixed circular path with various speeds;
- Complex testing in a higher speed environment;
- Straight line testing;
- Analysis of the various testing results; and
- Comparison to various manufacturers’ specifications.

The instrument Chua chose to perform this testing was the Trimble RTS 5603.

To complete his field testing Chua employed two different testing regimes. These regimes were:

- **Testing of a fixed circular path:** - Chua set the RTS up on a tripod, while the prism was attached to an aluminium bar and set up on a pillar. He used a bar with a known radius and the distance between the RTS and the pillar was fixed. The bar/prism was then rotated in a circular path at a very low speed whilst the RTS stored dynamic measurements directly to a PC.
- **Straight line testing:** - Chua set up a prism on a fixed bench and moved the prism horizontally along the bench.

In order to comprehensively analyse his results Chua input his test results into a CAD package, after this initial analysis Chua determined that it would be necessary to smooth his results using the Kalman Filter. He then used these filtered results to produce final outputs which he then used to draw his conclusions.

From the results of his testing Chua concluded that, “*the reliability of the RTS is greatly related to the speeds of the prism and measurement distances.*” (Chua, 2004)

Furthermore Chua goes on to state that the dynamic accuracy of an RTS is better at longer distances than at shorter distances.

Chua also attributes much of the results deviation to the shape of the prism, and that the tracked reflected reading is not always a true indication of the centre of prism. This consequently results in point positioning errors.

### **2.6.2 Ceryova 2002**

Similar to Chua, Ceryova performed two separate tests. Again these tests were:

1. Fixed Circular Curve; and
2. Straight Line.

Unlike Chua however Ceryova utilized several different types of RTS in order to obtain his results, these instruments included:

- Leica TCA 1800;
- Leica TCRA 1101; and
- Zeiss Elta S10.

In order to complete his field testing Ceryova employed the following testing regimes:

- Fixed circular path: - Ceryova used a simulator for testing sensors of the circular path measurement systems. The main arm would rotate in a horizontal plane and at the end of the arm was a fixed measuring board that would rotate in the opposite direction to the spinning arm. This ensured that the measurement board (and

prism) would always be facing the observer. The platform was rotated through a 0.5m radius at several speeds. The reflector system was mounted to the measurement board and a program that observed the motion managed each RTS. The resulting measurements were then stored to a PC.

- Straight line testing:- for this Ceryova incised a line (with in an accuracy of 0.1mm) into the middle of a metal block. They then observed measurements from three separate stations all with different relationships to this line (i.e. distance and angle).

Linear regression analysis was used by Ceryova to estimate the prism path, parameters and their subsequent accuracy. By comparing the measured and pre-defined paths Ceryova was able to determine the overall accuracy of each RTS.

Ceryova concluded that as the speed of rotation increased the subsequent point deviation also increased. Ceryova suggests that *“measurement of the cinematic target is influenced by a certain systematic influence which is probably a result of the time slide between angular and length measurement.”* (Ceryova et al., 2002)

Ceryova also went onto suggest that by increasing the speed of rotation you are also increasing the mean error in the RTSs automated pointing system.

### 2.6.3 Conclusion

There are some distinct similarities between the results obtained by Chua and Ceryova. Both parties concluded that the overall accuracy of an RTS is dependent on two main factors:

1. The speed of the moving target: and
2. The distance from the RTS to the target.

Furthermore both concluded that the dynamic accuracy of an RTS is improved as the target distance is increased.

## 2.7 The Kalman Filter

The Kalman Filter was first designed by Rudolf Kalman in 1960, and has since become a fundamental component in most navigation systems (Levy, 2002). The filter employs a statistical approach to weight every new measurement relative to previously gathered information in order to provide a current estimation of the system variables. The filter also determines the statistical uncertainties associated with these estimates. This provides an analytical tool for quality assessment of each new position.

Due to the filter's approach to the statistical review and analysis of point position, the filter was well received by surveyors although the filter's practical applications did require some additional fine-tuning.

### 2.7.1 Kalman Filter Description

The Kalman Filter is a multi-input and multi-output of digital filter that can optimally estimate; in real time, the states of a system based on its noisy outputs (Figure 2.11). The Kalman Filter is able to estimate the desired position by filtering the noisy input measurements. These position estimates are statistically optimal in that they minimize the mean-square error (Levy, 2002).

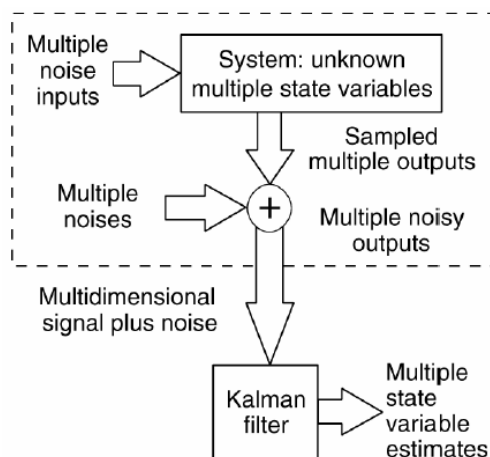


**Figure 2.11:** The purpose of Kalman Filter is to estimate the values of variables describing the state of a system from a multidimensional signal contaminated by noise.

(Source: Levy, 2002)

## 2.8 Conclusion

From the above literature the three following conclusions can be draw:

1. The Kalman Filter is a necessary analysis tool for the filtering of outliers in the test results;
2. Due to the different mechanical operations of these three instruments we can expect that each instrument will have a different accuracy; and
3. Previous research highlights that conditions do in fact play a role in the overall operational accuracy of an RTS.

Chapter 3 provides the specific testing and data analysis regime which has been utilized in order to test the above conclusions and to ultimately determine each instruments dynamic accuracy.



## CHAPTER 3

### RESEARCH APPROACH

#### 3.1 Introduction

As previously described, the aim of this project is to establish the dynamic accuracy and reliability of robotic total stations when used in the dynamic tracking mode. In order to achieve the objectives associated with fulfilling this aim the following steps will need to be performed:-

Field-testing:

- Fixed circular path testing at various speeds; and
- Extended straight line testing at various speeds.

Data Analysis

- Comprehensive analysis of the various test results;
- Comparison between my test results and the manufacturers' specifications.

As described by the literature review in Chapter 2, previous testing performed by both Ceryova et al., 2002, and Chua, 2004 demonstrated that the dynamic accuracy of the RTS can be determined by performing both circular path and straight line testing

##### 3.1.1 Project Planning

A five-stage plan has been implemented in order undertake this project:

1. Primary Research: This initial stage involves performing a literature review of all articles, books, journals, magazines or any other appropriate source to gather an understanding of both the workings of the current RTSs, along with their manufacturers specified and previously tested accuracies and reliability.

2. **Data Collection and Testing:** This stage involves the testing of RTSs in both a fixed circular path and straight line sense. This testing is to be performed at several target distances and at several target speeds.
3. **Analysis:** The data obtained during stage 2 of this process will be edited, plotted, reviewed and reports produced using Terramodel. These reports will then be presented in graphical form.
4. **Comparison of Systems and Discussions:** Reports and graphs are to be analysed for validity, significance and subsequent use within the body of the project.
5. **Conclusion:** Reflect on the data which has been analysed and draw conclusion as to the impact of various factors upon the accuracy and reliability of the RTSs.

## **3.2 Research Method**

### **3.2.1 Literature Contribution to Research Method**

The literature review (Chapter 2) has provided a basis for understanding RTS and thus enables me to tailor my testing as to achieve the best possible results. From the literature review, the following aspects must be taken into consideration:

- (a) Each instrument has a different distance measurement speed and associated distance accuracy (Product Survey, 2005);
- (b) Each instrument utilises a different system of instrument rotation. These differences mean that each instrument rotates at a different rate;
- (c) Accuracy of the results are closely associated with the speeds of the moving target (Ceryova et al., 2002);

- (d) Shorter observation ranges have larger standard deviation ( $\sigma$ ) compared to longer distances (Retscher, 2002);
- (e) Circular path testing and straight line testing are the key components in determining the dynamic accuracy of the RTSs (Kopacik, 1998); and
- (f) Measurements are not always taken to the centre of the target, this is caused by the shape of the target (Chua, 2004).

### 3.2.2 Data Collection and Testing

#### 3.2.2.1 Equipment Utilised

Two instruments have been utilised throughout this project. These instruments are:

- Leica TPS1205; and
- Trimble S6.



**Figure 3.1:** Leica TPS1205



**Figure 3.2:** Trimble S6

### **3.2.2.2 Components of an RTS**

There are four main components associated with an operational RTS system, these include:

1. Robotic Total Station (RTS) itself;
2. 360° Prism (target);
3. Detachable/remote keypad; and
4. Radio communication.

Refer to Figure 3.3 for a graphical representation of each component.

### **3.2.2.3 Operation of an RTS System**

The RTS operates by first taking a measurement to the target. This measurement is then available on the instrument face, simultaneously; this measurement information is also transmitted through the use of a radio link to the external remote keypad (ie detachable face or RCU). The remote keypad then sends a message back to the RTS informing the RTS what is to be done with this measurement (ie store or disregard the measurement). Once the measurement has been taken and the target begins to move, the instrument's ATS takes over. The ATS allows the instrument to actively track the moving target. Measurements can either be made automatically by the instrument to the moving target, or the target can be stationary whilst the measurement is taken.

Please note that whatever is displayed on the instrument face is also displayed at the remote keypad. The remote keypad has full control of the instrument and anything that can be performed at the instrument itself can be performed through the use of the remote keypad.

Figure 3.3 below is a basic graphical representation of how an RTS operates.

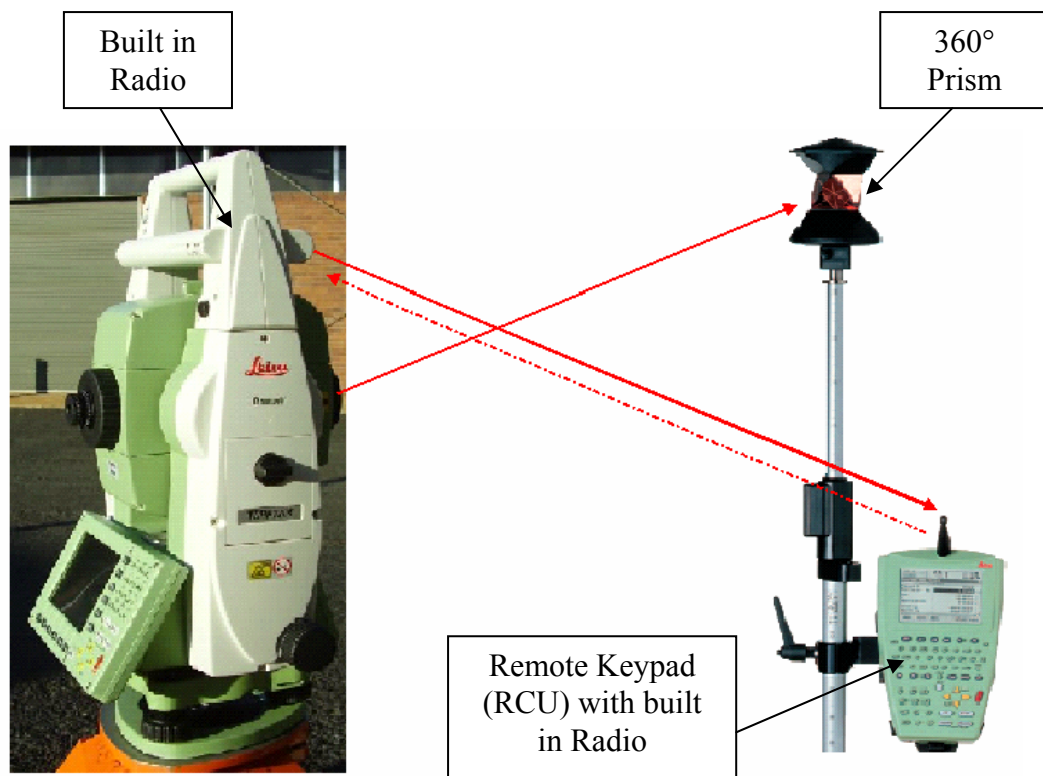


**Figure 3.3:** Operation and Components of an RTS.

#### 3.2.2.4 Field Testing

In order to determine the dynamic accuracy and reliability of the RTSs two types of testing was undertaken, these testing regimes included:

1. Fixed circular path; and
2. Extended straight line testing.

All testing has been carried out at the campus of Toowoomba campus of the *University of Southern Queensland (USQ)*.

### Fixed Circular Path Testing

This testing involved attaching a 360° prism to a metal bar. This bar was then fixed to a concrete pillar in a manner that enabled the bar to be rotated through 360°. The RTS was then set up on an adjacent pillar. The target was then rotated about the pillar whilst the RTS continuously read and stored measurements to the prism.



**Figure 3.4:** Circular Path target assembly.

This testing was performed under several conditions. These conditions included:

- Three separate target rotation speeds; and
- Three different RTS – target distances.

Note that each instrument was only tested using that manufacturers supplied target assembly (360° prism), and that the testing was carried out during the day time.

Table 3.1 illustrates the exact circular path testing regime, whilst tables 3.2 and 3.3 describe the specifics of each test.

**Table 3.1:** Circular Path testing undertaken

|               | <b>Target Location</b> | <b>Target Movement Speed</b> |
|---------------|------------------------|------------------------------|
| <b>Test 1</b> | Pillar 1               | Speed 1                      |
| <b>Test 2</b> | Pillar 1               | Speed 2                      |
| <b>Test 3</b> | Pillar 1               | Speed 3                      |
| <b>Test 4</b> | Pillar 2               | Speed 1                      |
| <b>Test 5</b> | Pillar 2               | Speed 2                      |
| <b>Test 6</b> | Pillar 2               | Speed 3                      |
| <b>Test 7</b> | Pillar 3               | Speed 1                      |
| <b>Test 8</b> | Pillar 3               | Speed 2                      |
| <b>Test 9</b> | Pillar 3               | Speed 3                      |

**Table 3.2:** Approximate distance of target from the RTS

|                 | <b>Approximate Distance to RTS</b> |
|-----------------|------------------------------------|
| <b>Pillar 1</b> | 4.3m                               |
| <b>Pillar 2</b> | 57.9m                              |
| <b>Pillar 3</b> | 115.8                              |

**Table 3.3:** Approximate target movement speeds

|                | <b>Approximate Target Movement Speeds</b> |
|----------------|---|
| <b>Speed 1</b> | 0.17m/s                                   |
| <b>Speed 2</b> | 0.4m/s                                    |
| <b>Speed 3</b> | 0.7m/s                                    |

### Extended Straight Line Testing

The straight line testing involved fixing a rail system of approximately 10m in length to the side of an existing building. This rail system was set out with a total station to be both straight and level. A 360° prism was then attached to a runner which ran inside the rail system. This rail allowed us to create a pre-determined and consistent target motion. The RTS was then set up adjacent to this rail system and continuously stored measurements to the prism as it is moved through the rail system. This process was then repeated using both the Leica and Trimble instruments.

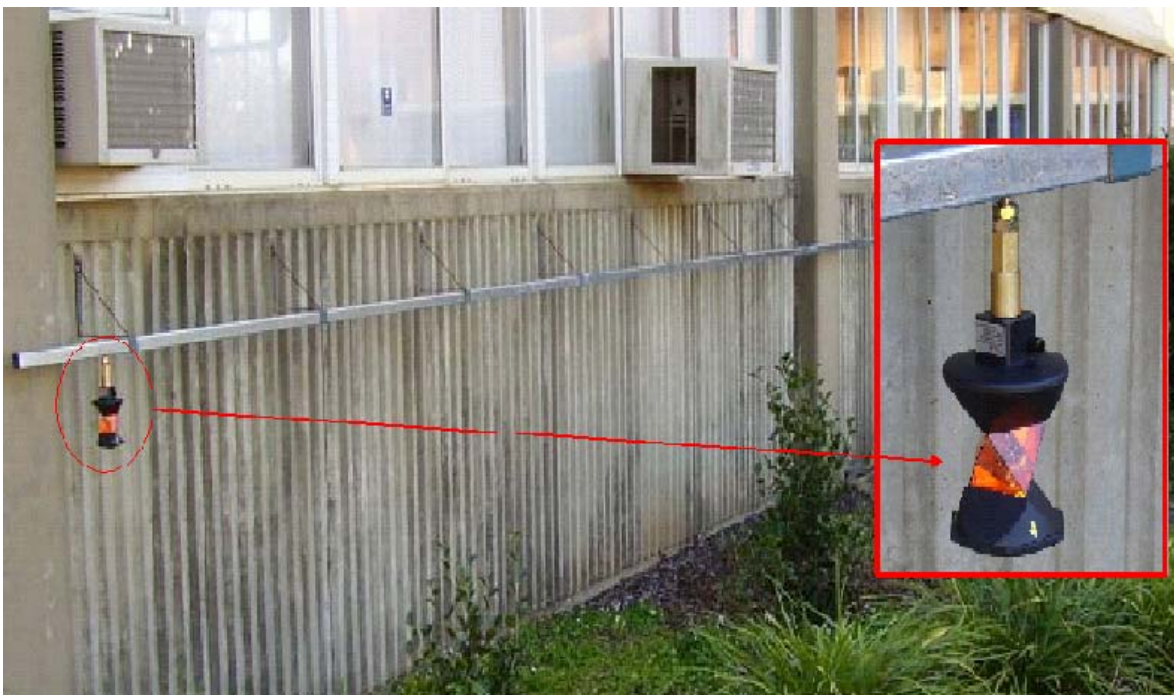


**Figure 3.5:** Straight line rail and target assembly.

Again the testing was performed under several conditions. These conditions again included:

- Three separate target movement speeds; and
- Two different RTS to target ranges.

Note that each instrument was only tested using that manufacturer's supplied target assembly (360° prism), and that the testing was carried out during the night time.



The Table 3.4 illustrates the straight-line testing regime, whilst tables 3.5 and 3.6 describe the specifics of each test.

**Table 3.4:** Straight-line testing undertaken

|               | <b>RTS<br/>Position</b> | <b>Target Movement<br/>Speed</b> |
|---------------|-------------------------|----------------------------------|
| <b>Test 1</b> | Stn 1                   | Speed 1                          |
| <b>Test 2</b> | Stn 1                   | Speed 2                          |
| <b>Test 3</b> | Stn 1                   | Speed 3                          |
| <b>Test 4</b> | Stn 2                   | Speed 1                          |
| <b>Test 5</b> | Stn 2                   | Speed 2                          |
| <b>Test 6</b> | Stn 2                   | Speed 3                          |

**Table 3.5:** Approximate distance from RTS to target

|                  | <b>Approximate<br/>Distance to West End</b> | <b>Approximate Distance<br/>to East End</b> |
|------------------|---|---|
| <b>Station 1</b> | 16.8m                                       | 21.4m                                       |
| <b>Station 2</b> | 55.3m                                       | 58.1m                                       |

**Table 3.6:** Approximate speed of moving target

|                | <b>Approximate Target<br/>Movement Speeds</b> |
|----------------|---|
| <b>Speed 1</b> | 0.35m/s                                       |
| <b>Speed 2</b> | 0.55m/s                                       |
| <b>Speed 3</b> | 1.1m/s  |

### **3.2.3 Data Analysis and Discussion**

#### **3.2.3.1 Data Transfer**

All test measurement data obtained in the field was automatically stored to the internal memory of the RTS systems. This data was then transferred to a PC. This transfer process was different for each RTS.

The Leica TPS1205 data transfer is performed via a PC card. The data was formatted by the instrument into a file which contained, Point Number, Easting, Northing, Height and Time. This card was then simply plugged into the PC and the required data cut and pasted to the hard drive. This data was then imported into Terramodel via the: Import – ASCII Points command.

Data transfer on the Trimble S6 is a little more complex. Either the RTS or the detachable face linked to a docking station must be connected to the PC via a USB cable. The PC must then use the ActiveSync program to allow the PC to communicate with the detachable face. The data can then simply be cut and pasted from the face to the PC. Similar to the Leica, the S6 is capable of outputting multiple formats. For this application I have chosen to output the .sdr format. The data was then imported into Terramodel via the: Import - .sdr format command.

#### **3.2.3.2 Software Utilised**

Whilst undertaking the analysis of the test data, two main software packages were utilised:

1. Terramodel; and
2. Microsoft Excel.

Terramodel was used for the transfer of the raw instrument data into a spatial format. This spatial data was then used to produce chainage and offset reports within Terramodel. These chainage and offset reports were produced by:

- (a) Inputting the true alignment of the target;
- (b) Producing the chainage and offset report of all measured points in relation to the input true alignment.

The chainage and offset reports were then imported into Microsoft Excel which was used to statistically analyse this report data as well as to generate the graphs used in the analysis of the data.

### 3.2.3.3 Analysis of Results

Figure 3.6 illustrates the exact process which was followed during the analysis and evaluation of the test results, from the initial transferring of the Raw data to the final drawing of conclusions.

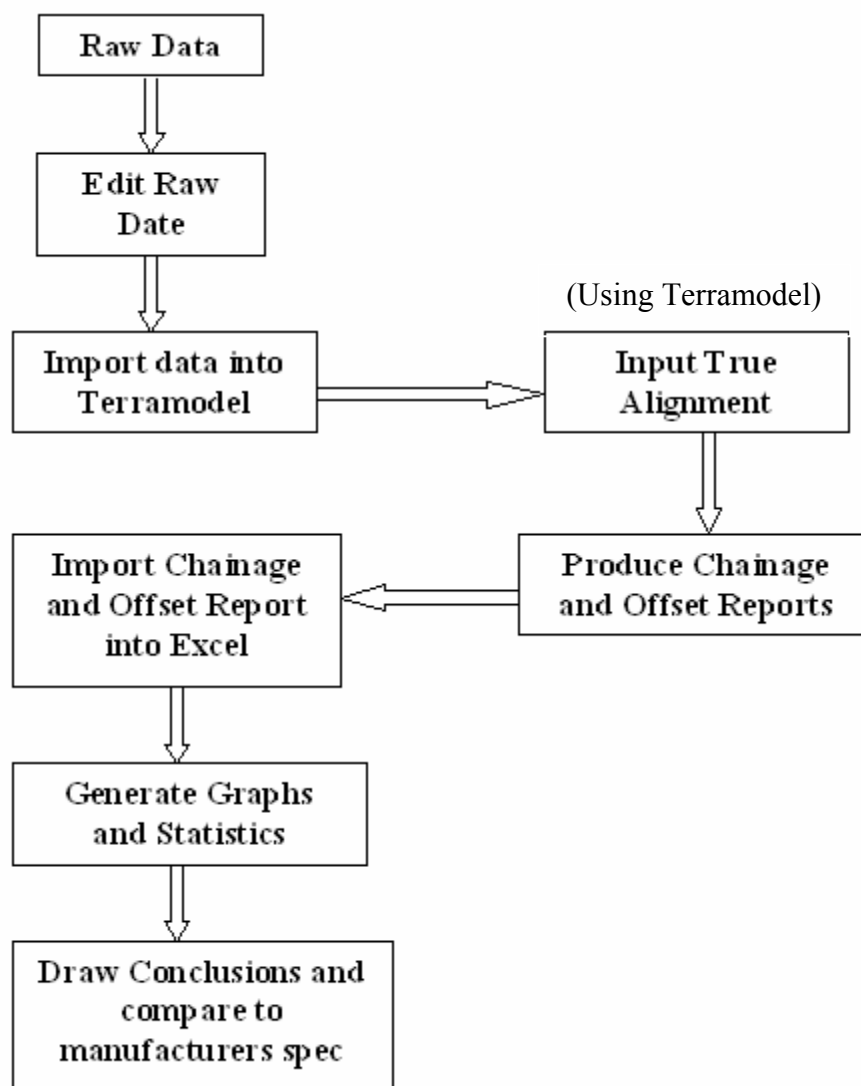


Figure 3.6: Analysis Process

### **3.3 Conclusion**

All testing described in this chapter has been completed successfully and the results will be examined and discussed in the next chapter. As described previously, two types of instruments have been used throughout this project. I had envisaged using a third instrument, the Topcon GTP-8200 however, due to problems sourcing the instrument combined with time constraints this was not possible.

Furthermore, additional testing of the instruments using a different manufacturers 360° prism may also be beneficial in the future as this to could contribute to the overall performance of an RTS.

Additional position testing may also have been beneficial. This testing could have included elevated station positions and different angles to the target. Again however time constraints restricted these possibilities.

However, the overall analysis of the test results as set out by the research method was completed without any major problems.

The next chapter will analyse and discuss the obtained test results in detail.

## CHAPTER 4

### RESULTS AND DISCUSSION

#### 4.1 Introduction

The operational efficiency of an RTS is critical on any task requiring the continuous tracking and recording of measurements. This efficiency then determines what tasks are capable of being performed by the RTS within acceptable limits. Such efficiency issues relate to:

- Distance measurement time; and
- Point processing time.

Both of which influence the accuracy and reliability capabilities of the RTS in real time applications.

RTSs have been available for more than 10 years now and are widely used for machine guidance, however little information is known about their operational capabilities. Therefore, this chapter will discuss my various test results and compare them to the stated manufacturer's specifications in order to determine each RTSs real-time operational accuracy and reliability. As described in the previous chapter both circular path and straight-line testing has been undertaken in order to determine the final accuracy and reliability of these instruments.

Furthermore, in determining the accuracy and reliability of RTSs the following instruments and instrument recording times were utilized throughout the testing:

1. Leica TPS 1205 at a recording time of 0.1 seconds;
2. Leica TPS 1205 at a recording time of 0.5 seconds; and
3. Trimble S6 at a recording time of 1.0 seconds.

During the analysis of the test data, several statistical values were calculated, these included:

- Standard Deviation ( $\sigma$ );
- Range; and
- Average tracking speed (in degrees / second).

These values were calculated using Microsoft excel software and will be discussed in more detail later in this chapter.

Prior to the analysis of any test data, several processes were undertaken, these included;

1. Transforming all test data into the same format;
2. Eliminating non-vital data, caused by stationary readings;
3. Assessing the quality of the test data; and
4. Refining the test data.

These processes were performed in order to ensure that the final analysed test data was a true representation of the RTSs capabilities.

Once the test data had been refined via the above stated process, the analysis of the test data then commenced. The exact analysis method will be discussed in detail later in this chapter.

## 4.2 Analysis of Results

The following process was used to analyse the test data within Microsoft excel:

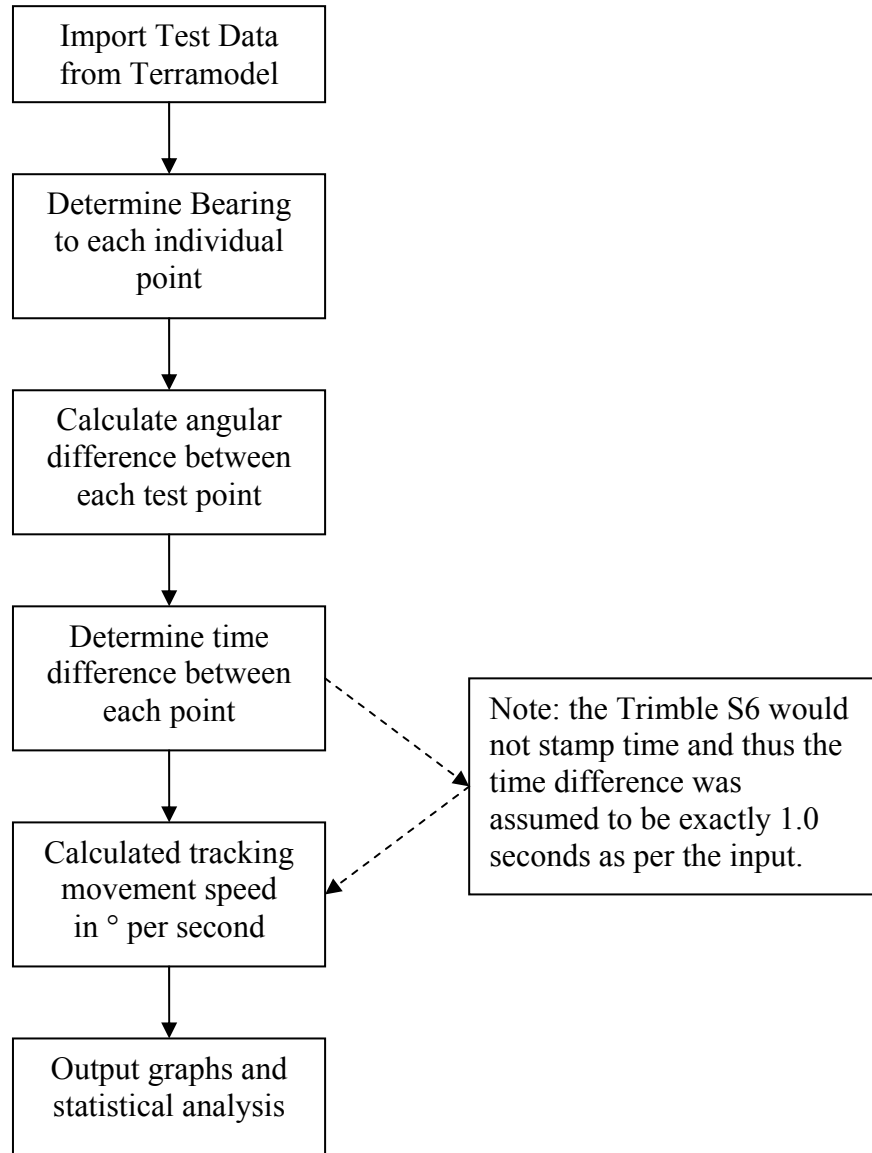


**Figure 4.1:** Data analysis process with in Microsoft excel

### 4.3 Circular Path Test Results

In order to analyse the circular test results, the following regime was utilised in order to determine the true alignment for all instruments and testing:

- i. Import point data into Terramodel;
- ii. Create the centre point of the circle by utilising the best-fit circle command in Terramodel. This command uses all the points within a defined window to produce a line of best fit, in this case an arc/circle;
- iii. Circle of best fit was created by the data captured at Speed 1. This is because the data captured at speed 1 is the most accurate and also has the largest number of points. This centre point was then reproduced in the other testing speeds to produce the predefined circular path; and
- iv. Chainage and offset reports were produced based on this circle of best fit.

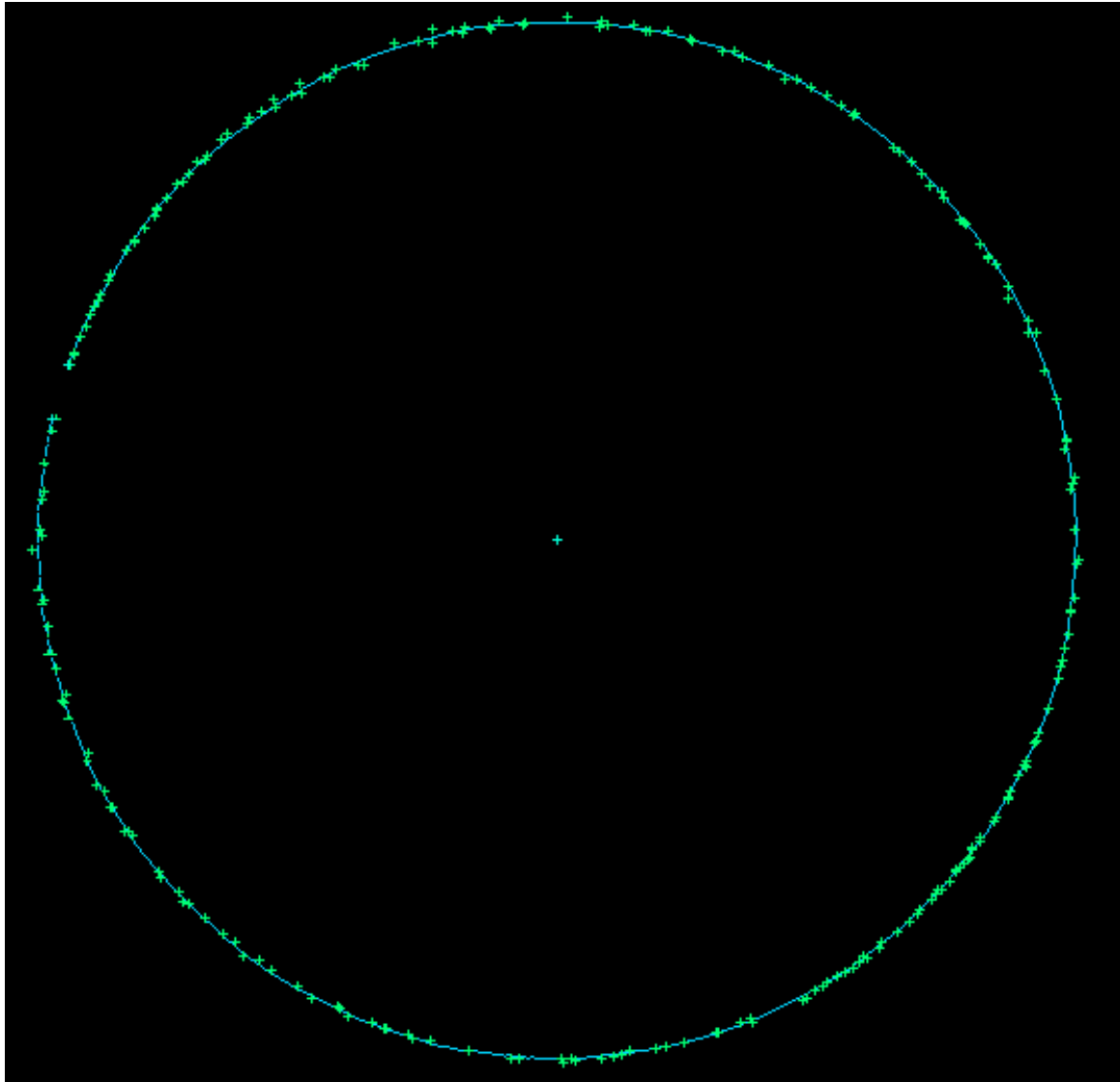
Note that in all cases once the circle of best fit has been produced two check measurements were performed in order to ensure the circles accuracy. These two tests were:

1. Measure the radius of the best fit circle to ensure that it is the same as the known radius of the circle; and
2. The measurement from the new created centre point to the RTS was measured to ensure that it was the same as the known distance from the RTS to the centre point.



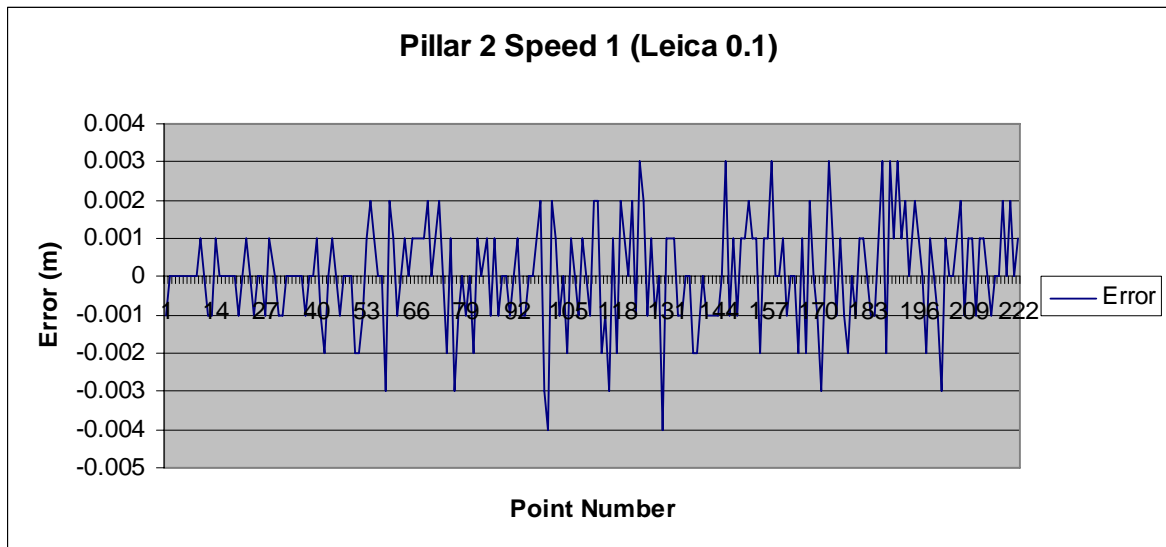
### 4.3.1 Leica TPS 1205 at 0.1 second record time.

Figure 4.2 shows the realised RTS measurements on the fixed circular path. The solid line represents the pre-defined true alignment of the circular path as determined by the process detailed above, while the crosses scattered about that line represent the measured/stored test points.



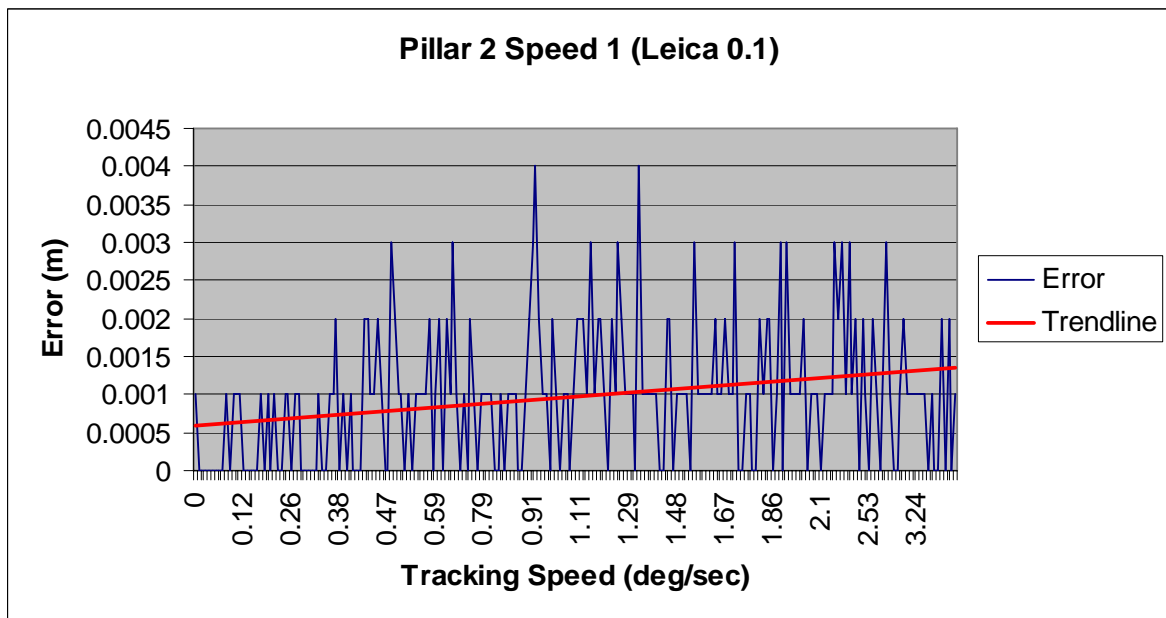
**Figure 4.2:** Circular Path test results for the Leica TPS 1205 at 0.1 second record time.

Figure 4.3 illustrates the error associated with each specific point captured during testing. It highlights that there is no systematic error present as the data ranging between  $-0.004$  and  $0.003$ m.



**Figure 4.3:** Offset error associated with each point captured by the Leica TPS1205.

Figure 4.4 illustrates the error associated with different angular movement speeds. The graph clearly illustrates that as the tracking speed of the instrument is increased the accuracy of the points captured decreases, although it does not appear to be significant at this stage.

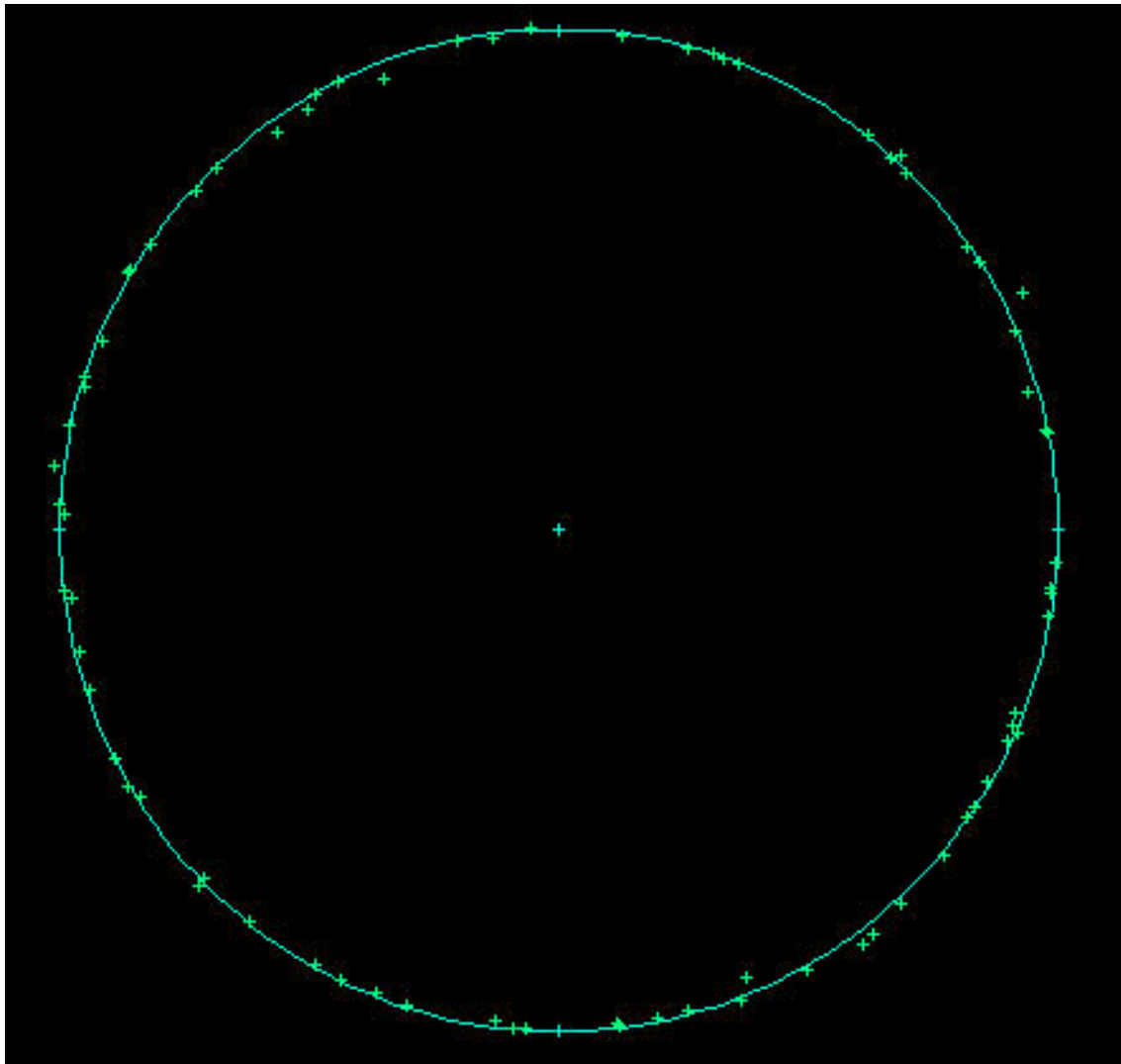


**Figure 4.4:** Error associated with angular movement speeds to Pillar 1.

Please note that the above graphs are for illustration purposes only, for the full test results please refer to Appendix B.

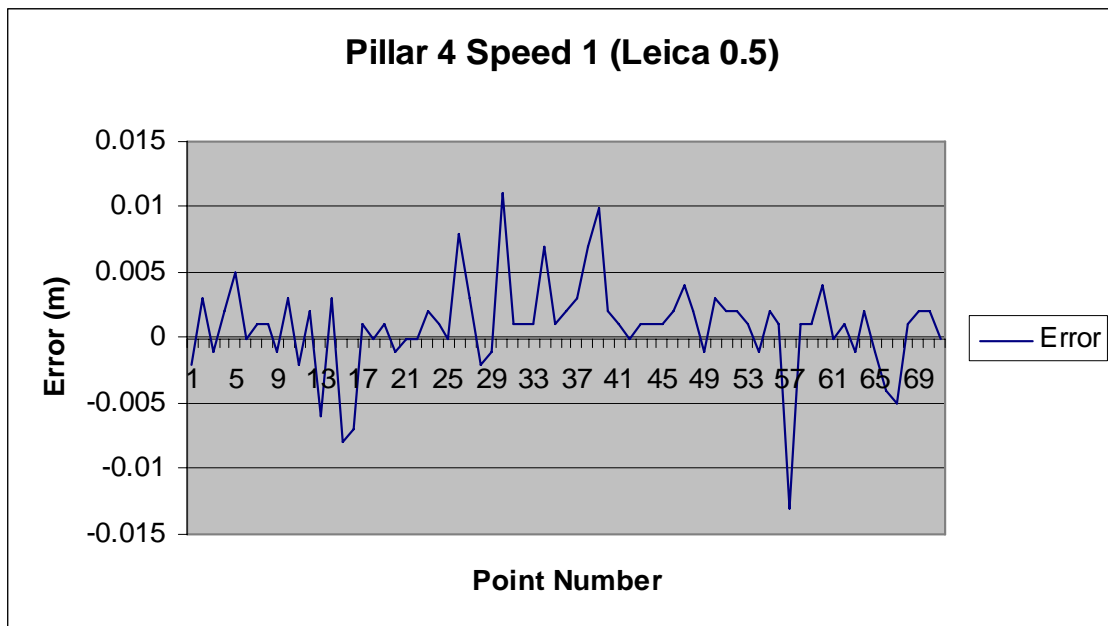
### 4.3.2 Leica TPS 1205 at 0.5 second record time.

Figure 4.5 shows the realised RTS measurements on the fixed circular path. The solid line represents the pre-defined true alignment of the circular path as determined by the process detailed in Chapter 4.3, while the crosses scattered about that line represent the measured/stored test points.



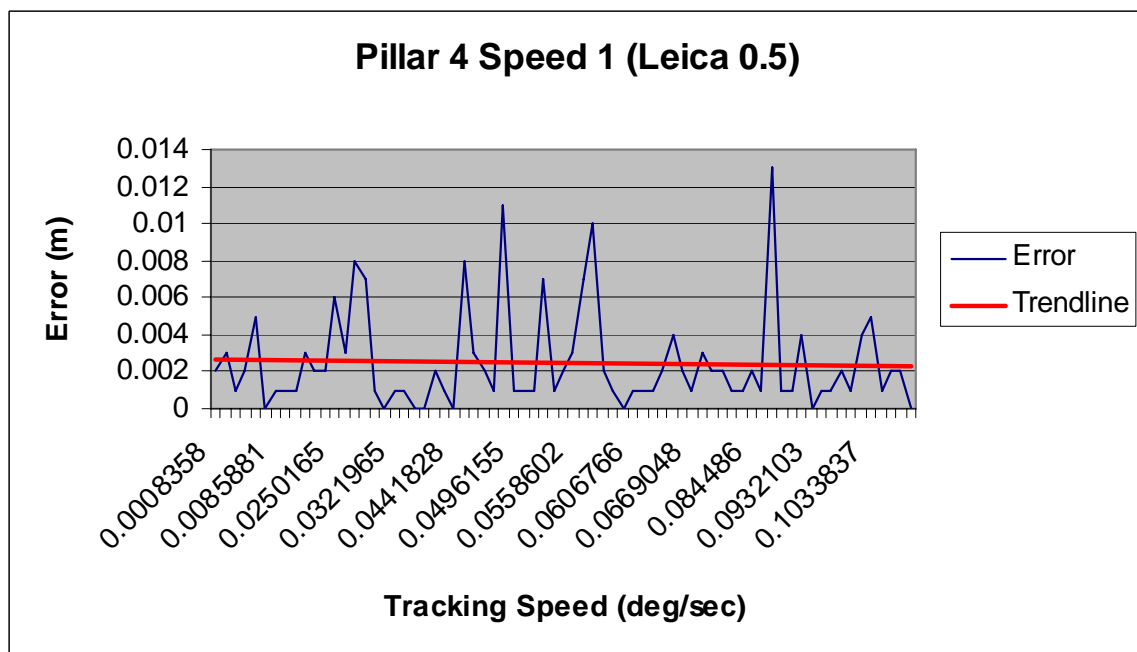
**Figure 4.5:** Circular Path test results for the Leica TPS 1205 at 0.5 second record time.

Figure 4.6 illustrates the error associated with each specific point captured during testing. Again, no systematic errors are present, with the accuracy ranging between the values of -0.013 and 0.011m



**Figure 4.6:** Offset error associated with each point captured by the Leica TPS1205.

Figure 4.7 illustrates the error associated with different tracking angular movement speeds. This graph illustrates that point error remains relatively constant when angular movement speeds are very low.



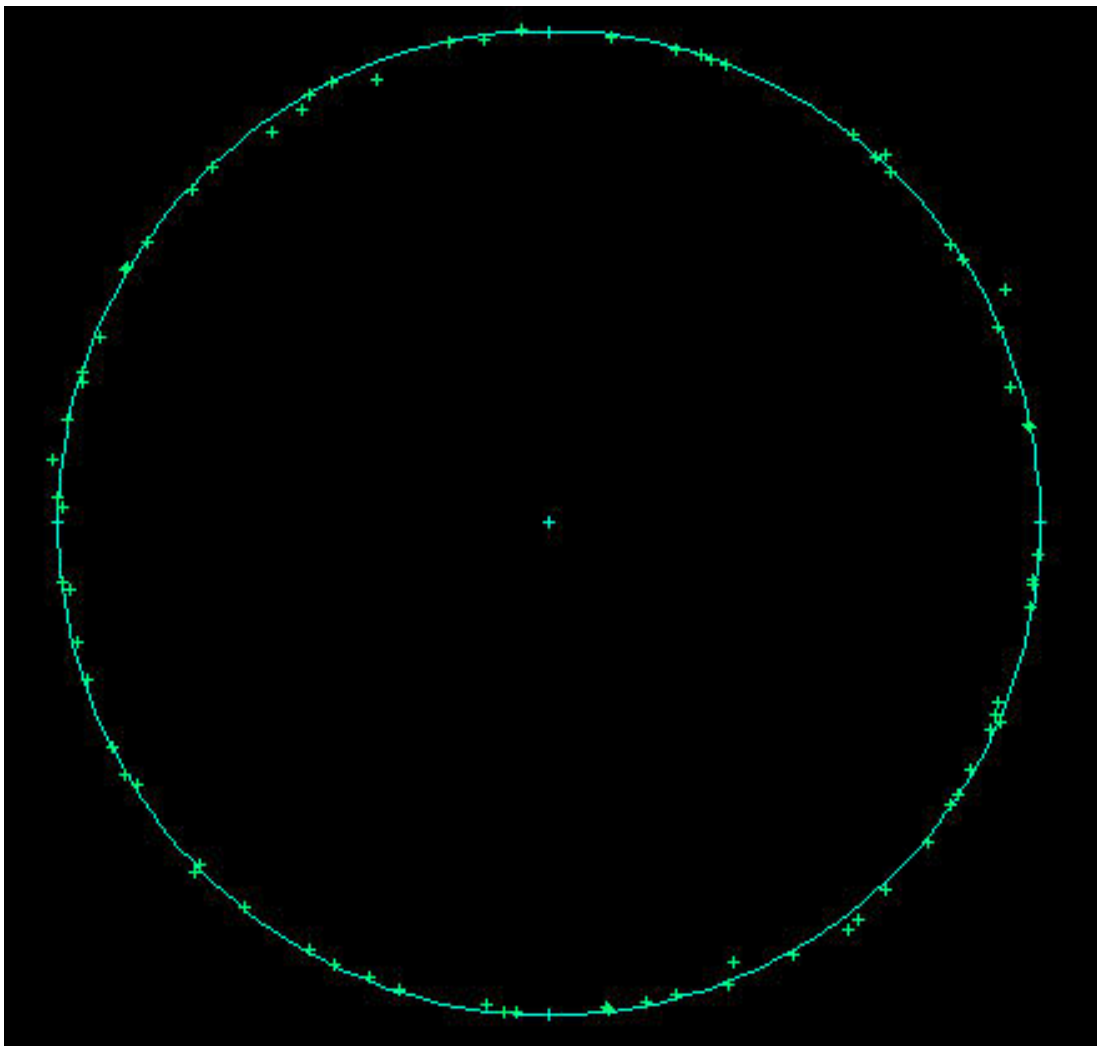
**Figure 4.7:** Error associated with angular movement speeds to Pillar 4.

Please again that the above graphs are for illustration purposes only, for full test results please refer to Appendix C.

### 4.3.3 Trimble S6 at 1.0 second record time.

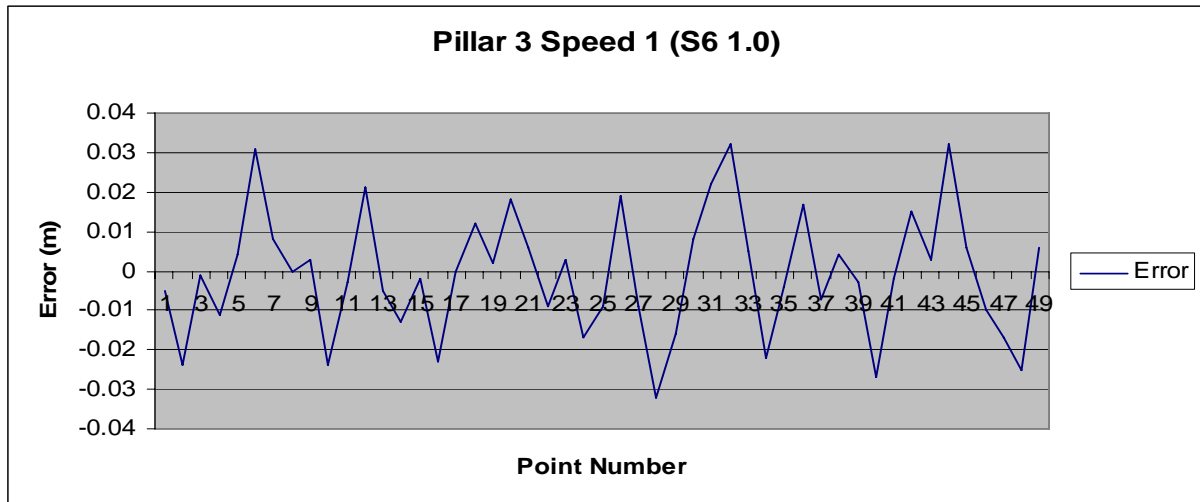
Please note that for the testing of the Trimble S6, the time difference between point measurements was set to 1.0 seconds. As the Trimble was however unable to attach a time to each point the absolute time difference between point measurements was assumed to be 1.0 seconds.

Figure 4.8 shows the realised RTS measurements on the fixed circular path. The solid line represents the pre-defined true alignment of the circular path as determined by the process detailed in Chapter 4.3, while the crosses scattered about that line represent the measured/stored test points.



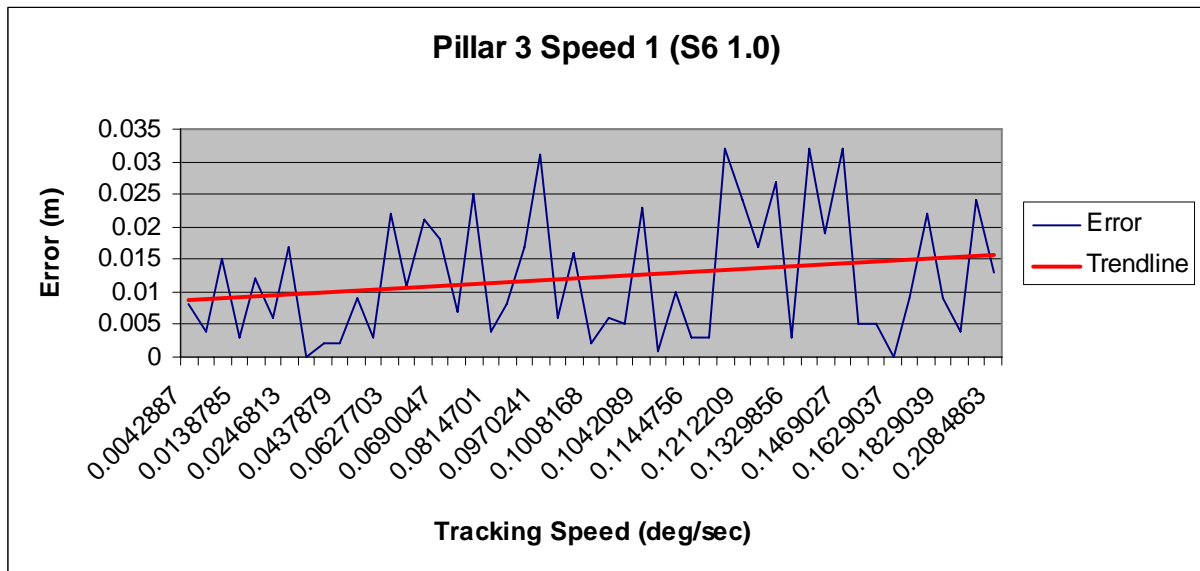
**Figure 4.8:** Circular Path test results for the Trimble S6 at 1.0 second record time.

Figure 4.9 illustrates the error associated with each specific point captured during testing, similar to the Leica testing no systematic error appear to be present and the data ranges between -.032 and 0.032.



**Figure 4.9:** Offset error associated with each point captured by the Trimble S6.

Figure 4.10 illustrates the error associated with different angular movement speeds. This instrument is beginning to show a more significant relationship between accuracy and angular movement speed.



**Figure 4.10:** Error associated with angular movement speeds to Pillar 3.

Please note that the above graphs are for illustration purposes only, for the full test results please refer to Appendix D.

## 4.4 Straight-Line Test Results

In order to analyse the straight-line test results, the following regime was utilised in order to determine the true alignment for all instruments and testing:

- i. Import point data into Terramodel;
- ii. Create the predefined alignment of the rail by utilising the best-fit line command in Terramodel. This command uses all the points within a defined window to produce a line of best fit, in this case a straight-line;
- iii. Line of best fit was created by the data captured at Speed 1. This is because the data captured at speed 1 is the most accurate and also has the largest number of points, this line was then reproduced for the next speeds; and
- iv. Chainage and offset reports were produced based on this line of best fit.

Note that in all cases once the line of best fit has been produced the following check measurement was performed in order to ensure each line's accuracy. This test was:

- Producing a line of best fit for each test, this line was then tested against that created by the data captured at Speed 1 to ensure that the same alignment was created.

#### 4.4.1 Leica TPS 1205 at 0.1 second record time.

Figure 4.11 shows the realised RTS measurements on the fixed straight-line testing. The solid line represents the pre-defined true alignment as determined by the process detailed above, while the crosses scattered about that line represent the measured/stored test points.

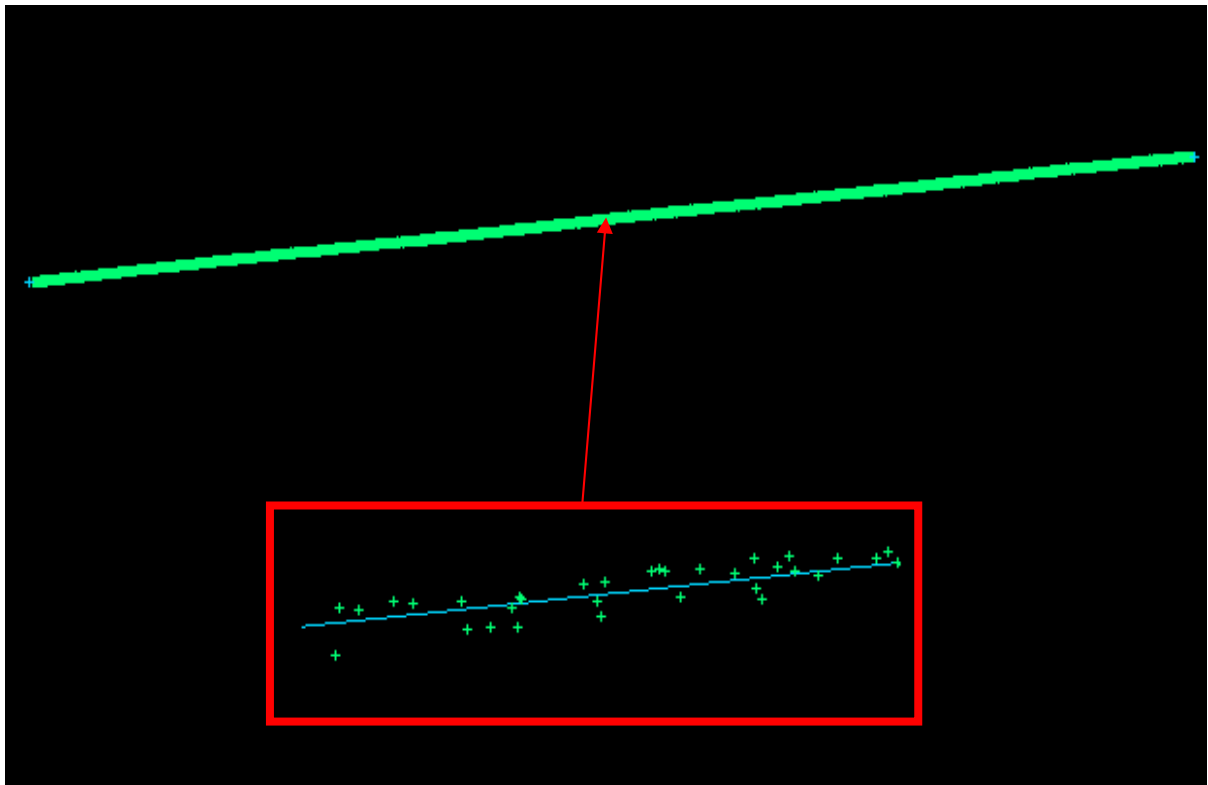


**Figure 4.11:** Straight-line test results for the Leica TPS 1205 at 0.1 second record time.

Figure 4.12 illustrates the error associated with each specific point captured during testing. There does not appear to be any systematic error present with the data ranging between -0.01 and 0.01m.



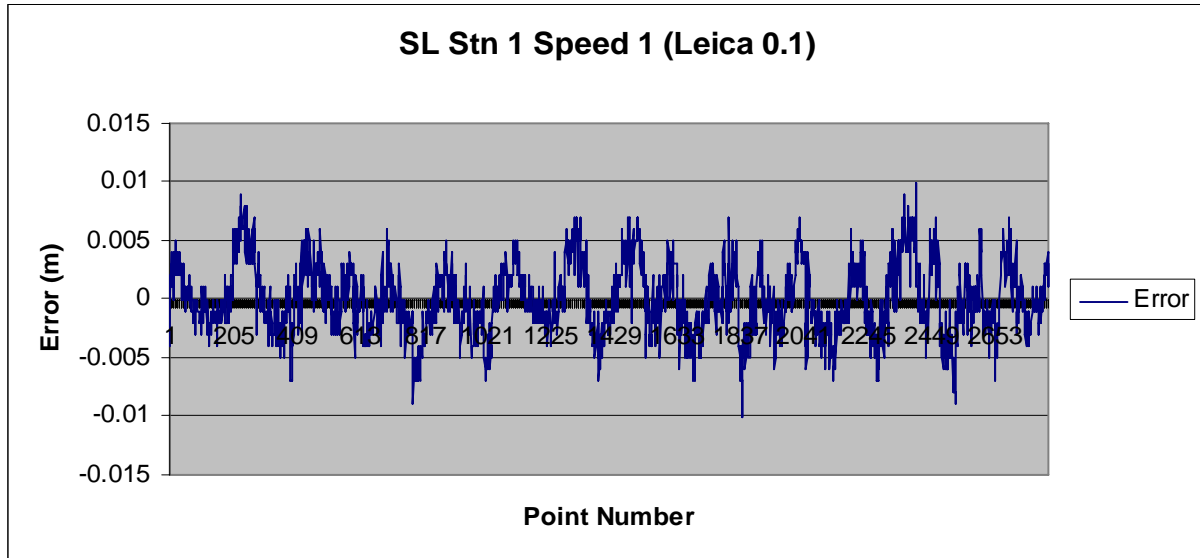


**Figure 4.12:** Offset error associated with each point captured by the Leica TPS1205.

Figure 4.13 illustrates the error associated with different angular movement speeds. It illustrates a similar trend to the circular path testing, that is, as angular movement speed is increased the accuracy decreases. This decrease in accuracy however is only small.

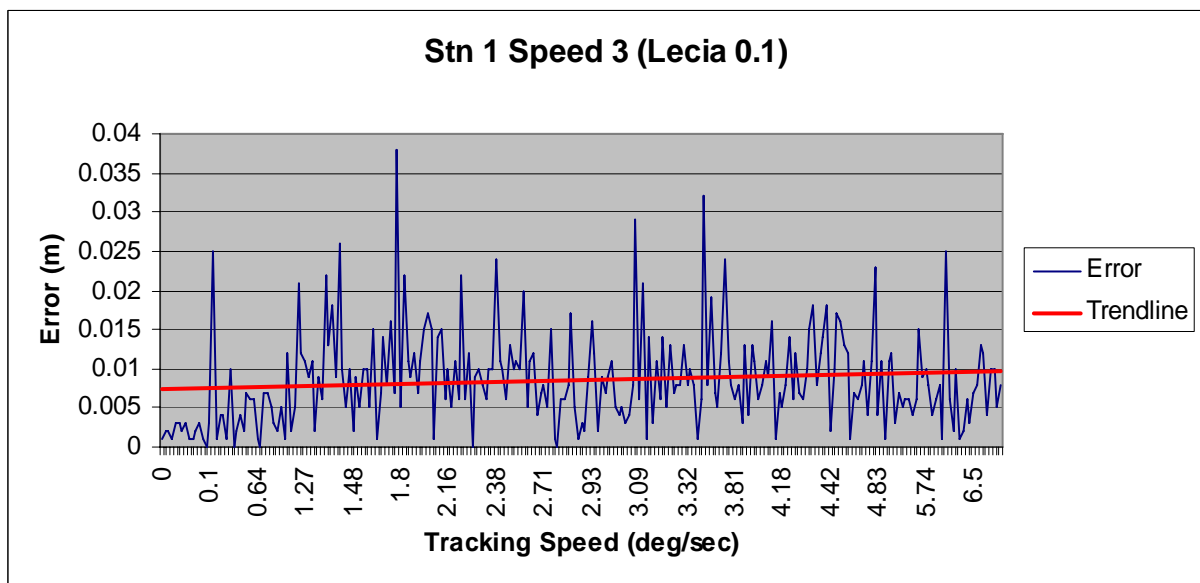
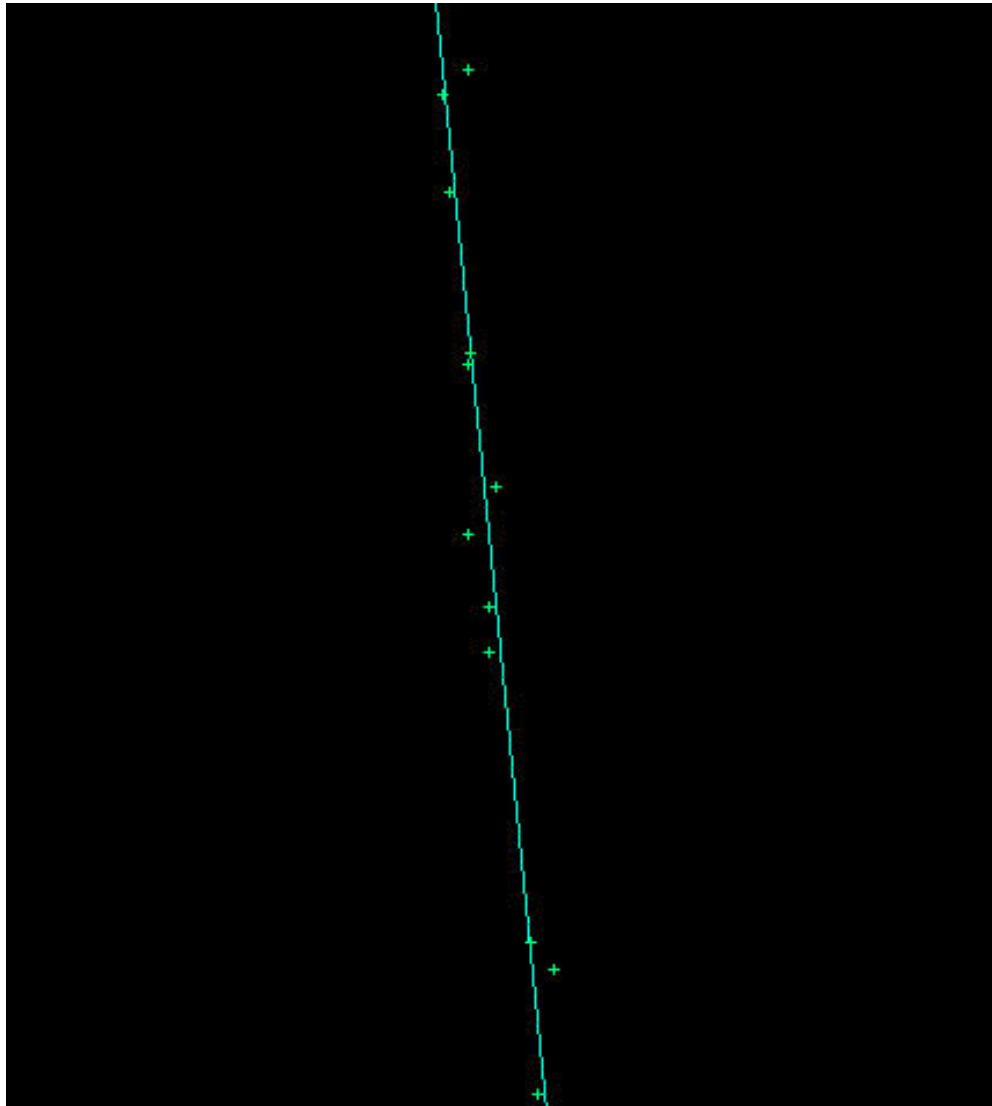


**Figure 4.13:** Error associated with angular movement speeds from Stn 1.

Please note that the above graphs are for illustration purposes only, for full test results please refer to Appendix E.

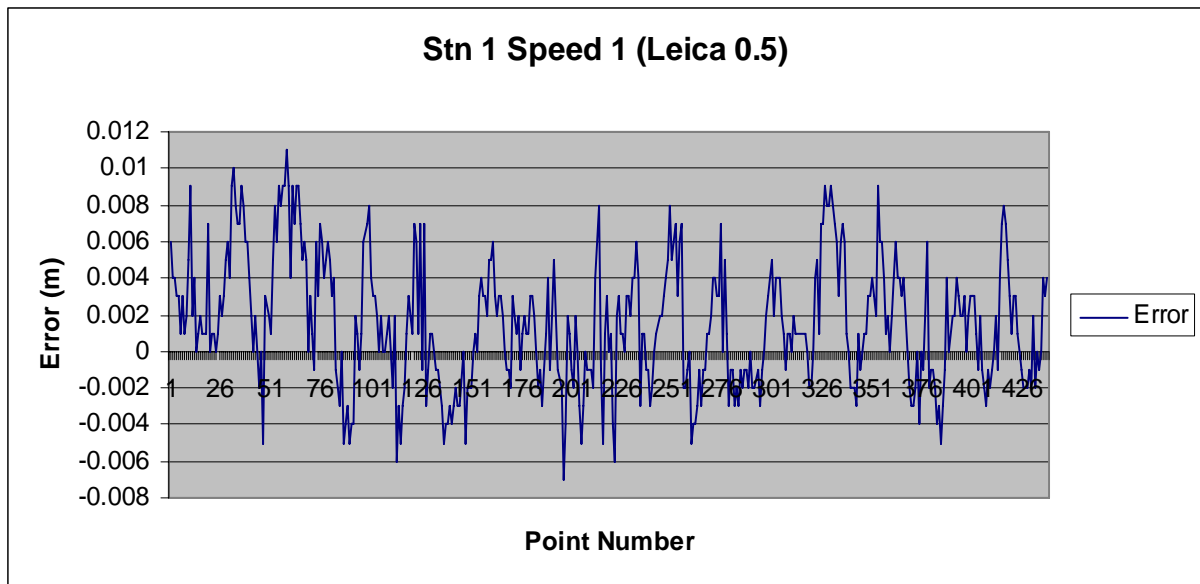
#### 4.4.2 Leica TPS 1205 at 0.5 second record time.

Figure 4.14 shows the realised RTS measurements on the straight-line. The solid line represents the pre-defined true alignment as determined by the process defined in Chapter 4.4, while the crosses scattered about that line represent the measured/stored test points.



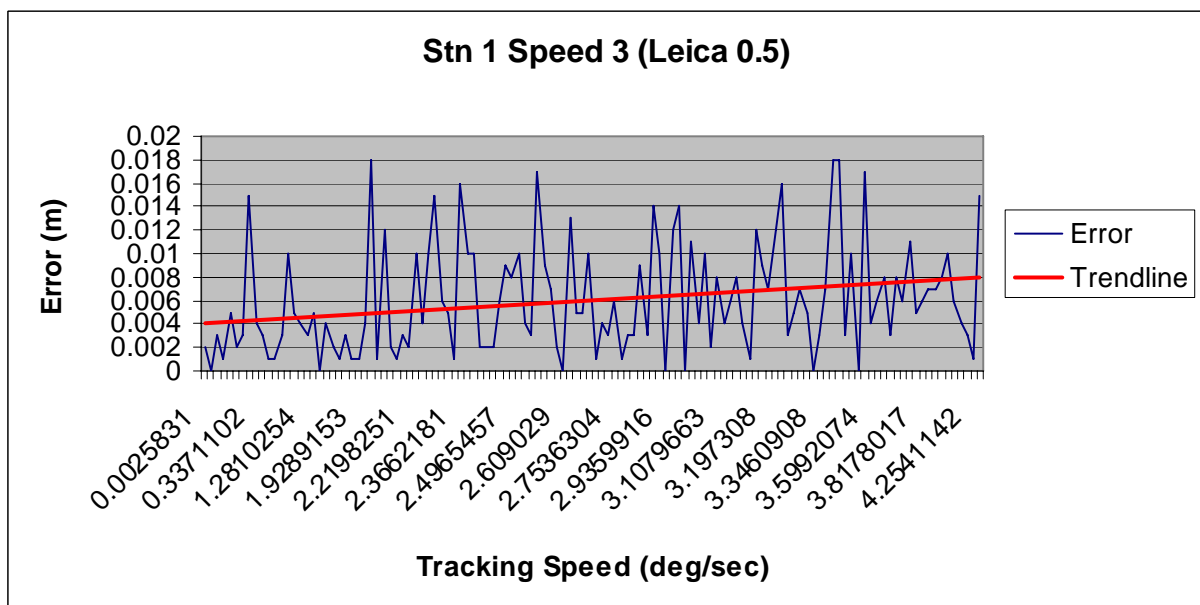
**Figure 4.14:** Portion of Circular Path test results for the Leica TPS 1205 at 0.5 second record time.

Figure 4.15 illustrates the error associated with each specific point captured during testing. There is no systematic error with the data ranging between -0.007 and 0.011m.



**Figure 4.15:** Offset error associated with each point captured by the Leica TPS1205.

Figure 4.16 illustrates the error associated with different angular movement speeds. Similar to previous testing, as the tracking speed is increased the associated point accuracy decreases.



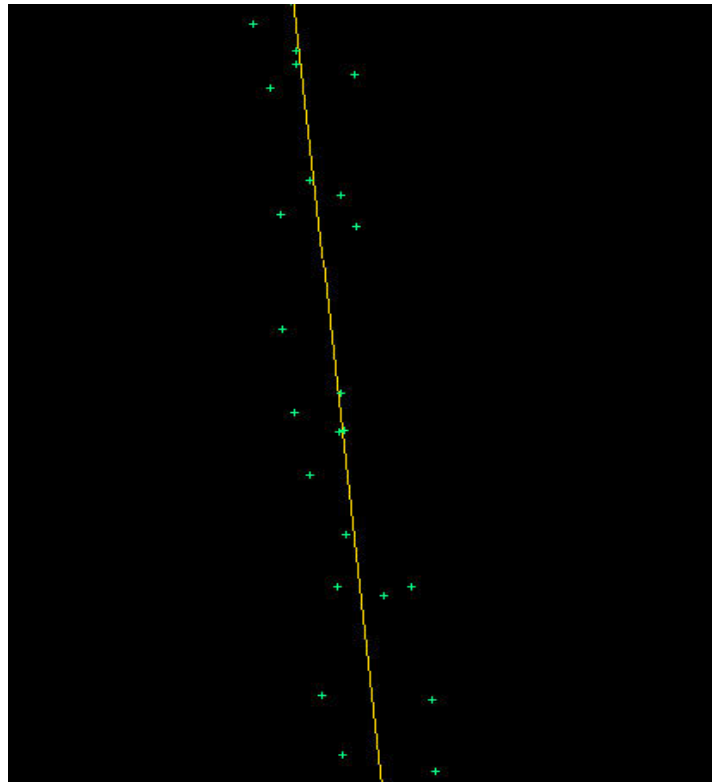
**Figure 4.16:** Error associated with angular movement speeds from Stn 1.

Please note that the above graphs are for illustration purposes only, for full test results please refer to Appendix F.

#### 4.4.3 Trimble S6 at 1.0 second record time.

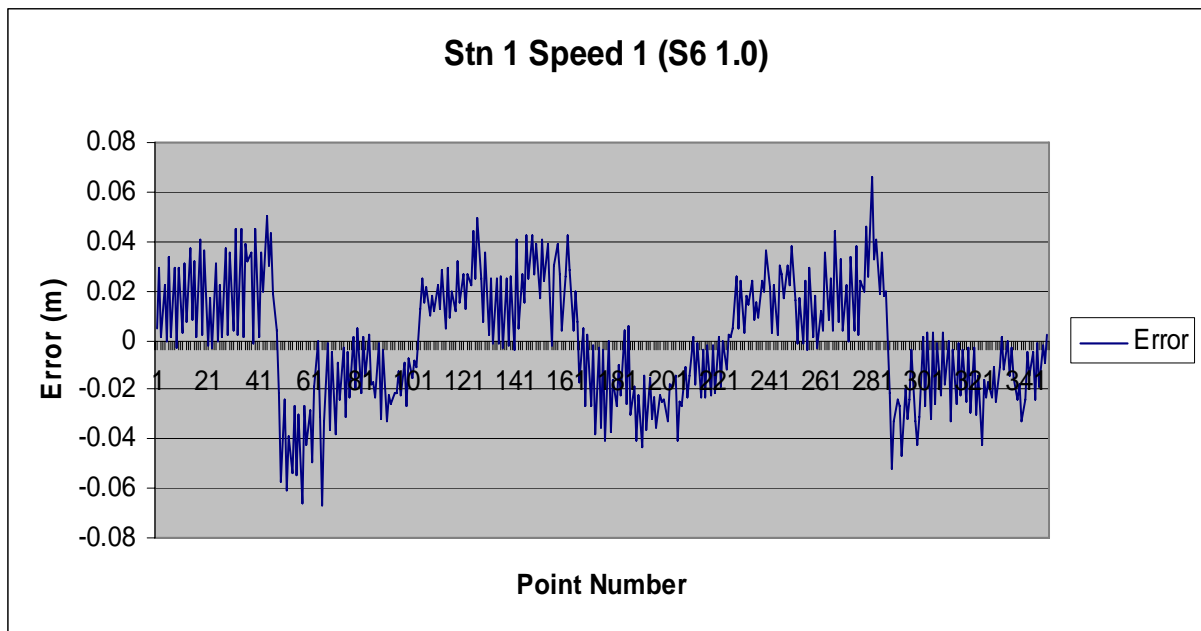
As with the circular path testing please note that for the testing of the Trimble S6, the time difference between point measurements was set to 1.0 seconds. As the Trimble was however unable to attach a time to each point the absolute time difference between point measurements was assumed to be 1.0 seconds.

Figure 4.17 shows the realized RTS measurements on the straight-line. The solid line represents the pre-defined true alignment as determined by the process detailed in Chapter 4.4, while the crosses scattered about that line represent the measured/stored test points.



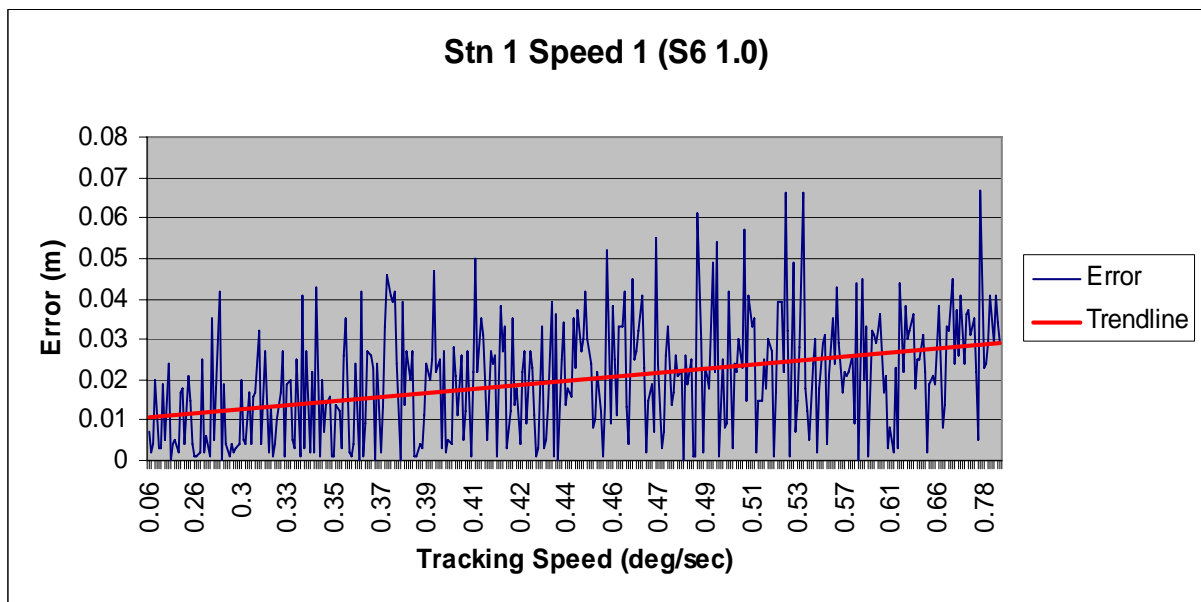
**Figure 4.17:** Portion of Straight-line test results for the Trimble S6 at 1.0 second record time.

Figure 4.18 illustrates the error associated with each specific point captured during testing. There are no systematic errors present with the data ranging between -0.063 and 0.064m. However the S6 results contain three distinct sharp drops from a positive error to a negative error. This relates to the direction in which the target is being moved through the rail system. The drop occurs when the target goes from moving away from the RTS to moving towards the RTS.



**Figure 4.18:** Offset error associated with each point captured by the Trimble S6.

Figure 4.19 illustrates the error associated with different angular movement speeds. Again as the angular movement speed is increased the accuracy decreases. This trend is far more evident with the S6 results when compared to the Leica instrument.



**Figure 4.19:** Error associated with angular movement speeds from Stn 1.

Please note that the above graphs are for illustration purposes only, for full test results please refer to Appendix G.

## 4.5 Discussion

Before analysing these test results each manufacturer's specifications must be noted.

These specification figures are:

- Leica TPS1205:  $5\text{mm} \pm 2\text{ppm}$  whilst in tracking mode. This figure was then converted to a 95% confidence level prior to any comparison (approximately 0.01m).
- Trimble S6:  $10\text{mm} \pm 2\text{ppm}$  whilst in tracking mode. This figure was then converted to a 95% confidence level prior to any comparison (approximately 0.02m).

### 4.5.1 Circular Path results summary

Table 4.1 is a table summarising the circular path results obtained by the Leica working at 0.1 seconds. It identifies that as distance and speed increase, the relative point accuracy and reliability decreases.

**Table 4.1:** Circular Path results summary for the Leica TPS 1205 working at 0.1 seconds.

| Pillar | Speed | Std Dev | Range | Av Speed<br>(deg/sec) | Average<br>Distance | Above<br>Man<br>Spec | %<br>Above<br>Man<br>Spec |
|--------|-------|---------|-------|-----------------------|---------------------|----------------------|---------------------------|
| 2      | 1     | 0.0013  | 0.007 | 1.3163                | 4.9                 | 0                    | 0                         |
| 2      | 2     | 0.0032  | 0.019 | 2.8072                | 4.9                 | 3                    | 1.2                       |
| 2      | 3     | 0.0067  | 0.041 | 5.1976                | 4.9                 | 2                    | 2.9                       |
| 3      | 1     | 0.0027  | 0.027 | 0.0923                | 57.9                | 8                    | 2.2                       |
| 3      | 2     | 0.0038  | 0.025 | 0.261                 | 57.9                | 4                    | 3.3                       |
| 3      | 3     | 0.0058  | 0.032 | 0.4608                | 57.9                | 7                    | 9.2                       |
| 4      | 1     | 0.0035  | 0.034 | 0.0508                | 115.9               | 8                    | 3.1                       |
| 4      | 2     | 0.0053  | 0.035 | 0.1351                | 115.9               | 9                    | 7.6                       |
| 4      | 3     | 0.008   | 0.049 | 0.2348                | 115.9               | 14                   | 18.9                      |

Table 4.2 summarises the circular path results obtained by the Leica working at 0.5 seconds. These results again identify that as distance and speed increase, the relative point accuracy and reliability decreases.

**Table 4.2:** Circular Path results summary for the Leica TPS 1205 working at 0.5 seconds.

| Pillar | Speed | Std Dev | Range | Av Speed<br>(deg/sec) | Average<br>Distance | Above<br>Man<br>spec | %<br>Above<br>Man<br>Spec |
|--------|-------|---------|-------|-----------------------|---------------------|----------------------|---------------------------|
| 2      | 1     | 0.0011  | 0.005 | 0.8315                | 4.9                 | 0                    | 0                         |
| 2      | 2     | 0.0025  | 0.008 | 2.4964                | 4.9                 | 0                    | 0                         |
| 2      | 3     | 0.005   | 0.016 | 4.4967                | 4.9                 | 1                    | 6.7                       |
| 3      | 1     | 0.0029  | 0.023 | 0.108                 | 57.9                | 1                    | 1.4                       |
| 3      | 2     | 0.0034  | 0.014 | 0.2888                | 57.9                | 0                    | 0                         |
| 3      | 3     | 0.0043  | 0.019 | 0.4055                | 57.9                | 1                    | 4.5                       |
| 4      | 1     | 0.0036  | 0.024 | 0.0555                | 115.9               | 3                    | 4.2                       |
| 4      | 2     | 0.0034  | 0.013 | 0.1432                | 115.9               | 0                    | 0                         |
| 4      | 3     | 0.0085  | 0.028 | 0.2129                | 115.9               | 6                    | 30                        |

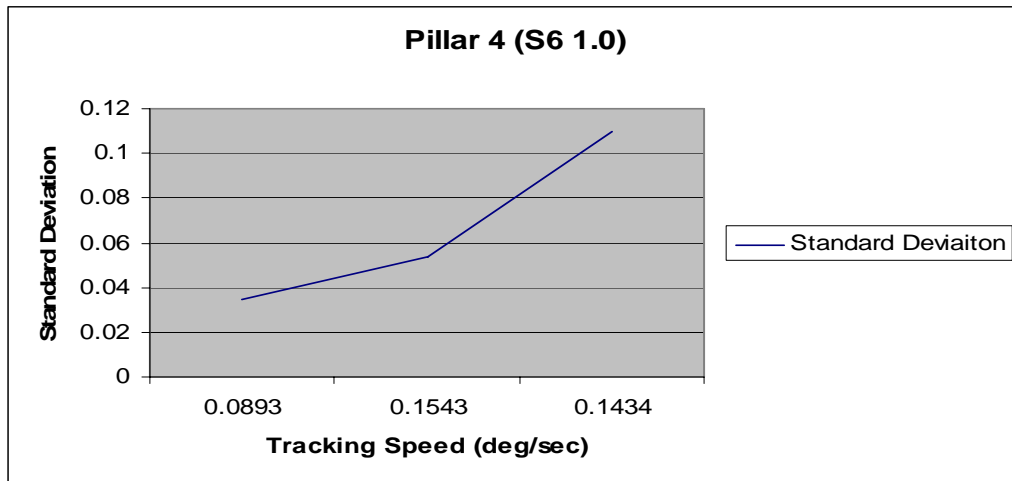
Table 4.3 summarises the circular path results obtained by the Trimble working at 1.0 seconds. These results identify a slightly different trend to those of the Leica instrument. The Trimble results show that accuracy and reliability increase as the distance is increased from short - medium ranges before decreases as the range extends from medium - long.

**Table 4.3:** Circular Path results summary for the Trimble S6 working at 1.0 seconds.

| Pillar | Speed | Std Dev | Range | Av Speed<br>(deg/sec) | Average<br>Distance | Above<br>Man<br>spec | %<br>Above<br>Man<br>Spec |
|--------|-------|---------|-------|-----------------------|---------------------|----------------------|---------------------------|
| 2      | 1     | 0.0231  | 0.083 | 1.3319                | 4.9                 | 8                    | 17.39                     |
| 2      | 2     | 0.0679  | 0.253 | 3.3951                | 4.9                 | 10                   | 43.4                      |
| 2      | 3     | 0.0663  | 0.244 | 5.0077                | 4.9                 | 7                    | 30.4                      |
| 3      | 1     | 0.0156  | 0.064 | 0.0975                | 57.9                | 5                    | 10.2                      |
| 3      | 2     | 0.0441  | 0.178 | 0.2995                | 57.9                | 7                    | 38.9                      |
| 3      | 3     | 0.106   | 0.387 | 0.3835                | 57.9                | 6                    | 46.2                      |
| 4      | 1     | 0.0347  | 0.142 | 0.0893                | 115.9               | 6                    | 21.4                      |
| 4      | 2     | 0.0541  | 0.233 | 0.1543                | 115.9               | 7                    | 36.8                      |
| 4      | 3     | 0.1098  | 0.362 | 0.1434                | 115.9               | 8                    | 57.1                      |

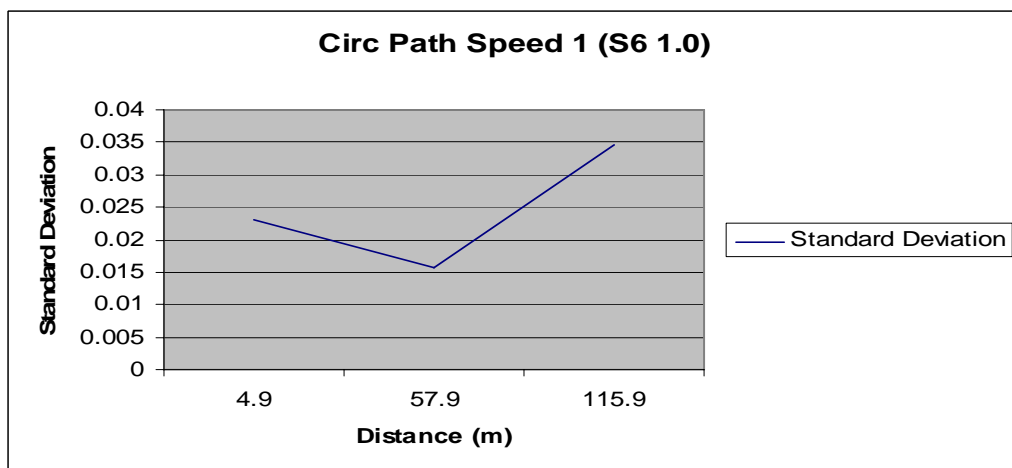
Note that the manufacturer's specifications for the Trimble S6 are significantly higher than those stated by Leica. Trimble quotes  $10\text{mm} \pm 2\text{ppm}$  whilst the Leica quotes  $5\text{mm} \pm 2\text{ppm}$ .

Figure 4.20 illustrates the relationship between standard deviation (accuracy) and angular movement speed (tracking speed). It clearly indicates that as the tracking speed is increased, point accuracy decreases.



**Figure 4.20:** Standard Deviation vs Tracking Speed, Pillar 4.

Figure 4.21 illustrates the relationship between standard deviation (accuracy) and the distance from RTS to target. It clearly indicates that accuracy increases as range is increased from short – medium distances; then the accuracy decreases as range is extended from medium – long.



**Figure 4.21:** Standard Deviation vs Distance, Speed 1.

Note that Figures 4.20 and 4.21 are for illustration purposes only, for full analysis results please refer to Appendices B, C and D.



#### 4.5.2 Straight-line results summary

Table 4.4 summarises the straight-line results obtained by the Leica working at 0.1 seconds. The tables shows that as the distance from RTS to target is extended from short to medium range, both the accuracy and reliability increases.

**Table 4.4:** Results summary for the Leica TPS 1205 working at 0.1 seconds.

| Stn | Speed | Std Dev | Range | Av Speed<br>(deg/sec) | Average<br>Distance | Above<br>Man<br>spec | %<br>Above<br>Man<br>Spec |
|-----|-------|---------|-------|-----------------------|---------------------|----------------------|---------------------------|
| 1   | 1     | 0.0029  | 0.02  | 0.354                 | 18.8                | 2                    | 0.01                      |
| 1   | 2     | 0.0044  | 0.028 | 1.3245                | 18.8                | 16                   | 2.2                       |
| 1   | 3     | 0.0103  | 0.063 | 2.9772                | 18.8                | 76                   | 30.7                      |
| 2   | 1     | 0.0028  | 0.018 | 0.1676                | 56.5                | 0                    | 0                         |
| 2   | 2     | 0.0043  | 0.023 | 0.632                 | 56.5                | 10                   | 2.4                       |
| 2   | 3     | 0.0055  | 0.033 | 1.029                 | 56.5                | 15                   | 6.8                       |

Table 4.5 summarises the results obtained by the Leica working at 0.5 seconds. Similar to the results obtained working at 0.1 seconds again the table shows that as the distance from RTS to target is extended from short to medium range, both the accuracy and reliability increases.

**Table 4.5:** Results summary for the Leica TPS 1205 working at 0.5 seconds.

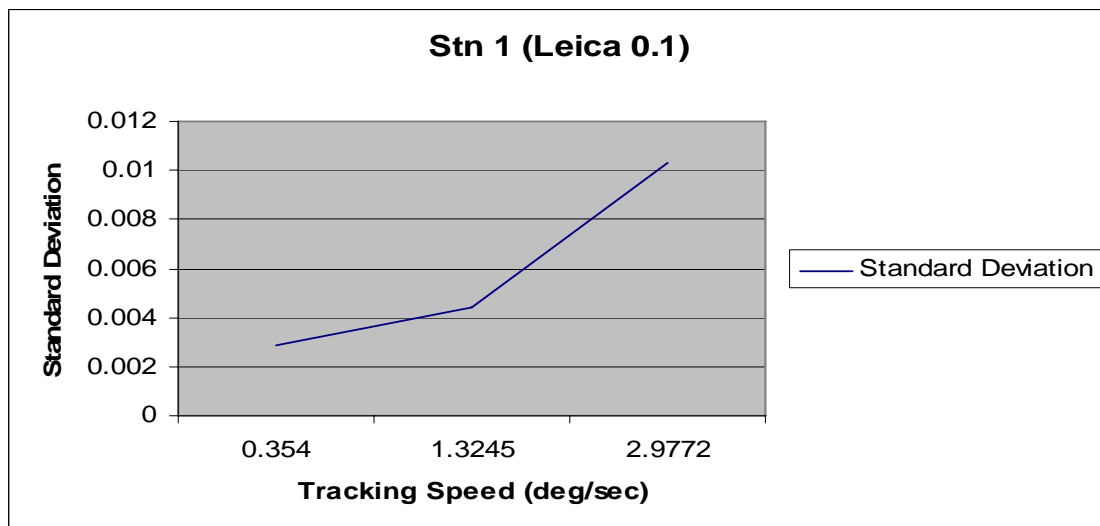
| Stn | Speed | Std Dev | Range | Av Speed<br>(deg/sec) | Average<br>Distance | Above<br>Man<br>spec | % Above<br>Man<br>Spec |
|-----|-------|---------|-------|-----------------------|---------------------|----------------------|------------------------|
| 1   | 1     | 0.0035  | 0.018 | 0.6143                | 18.8                | 2                    | 0.5                    |
| 1   | 2     | 0.005   | 0.027 | 1.5071                | 18.8                | 8                    | 5.1                    |
| 1   | 3     | 0.0075  | 0.036 | 2.5452                | 18.8                | 6                    | 21.5                   |
| 2   | 1     | 0.0033  | 0.024 | 0.1894                | 56.5                | 3                    | 0.8                    |
| 2   | 2     | 0.0043  | 0.022 | 0.4809                | 56.5                | 5                    | 3.2                    |
| 2   | 3     | 0.006   | 0.026 | 1.1346                | 56.5                | 8                    | 12                     |

Table 4.6 summarises the results obtained by the Trimble working at 1.0 seconds. Similar to the results obtained by the Leica testing these results again shows that as the distance from RTS to target is extended from short to medium range, both the accuracy and reliability increases.

**Table 4.6:** Results summary for the Trimble S6 working at 1.0 seconds.

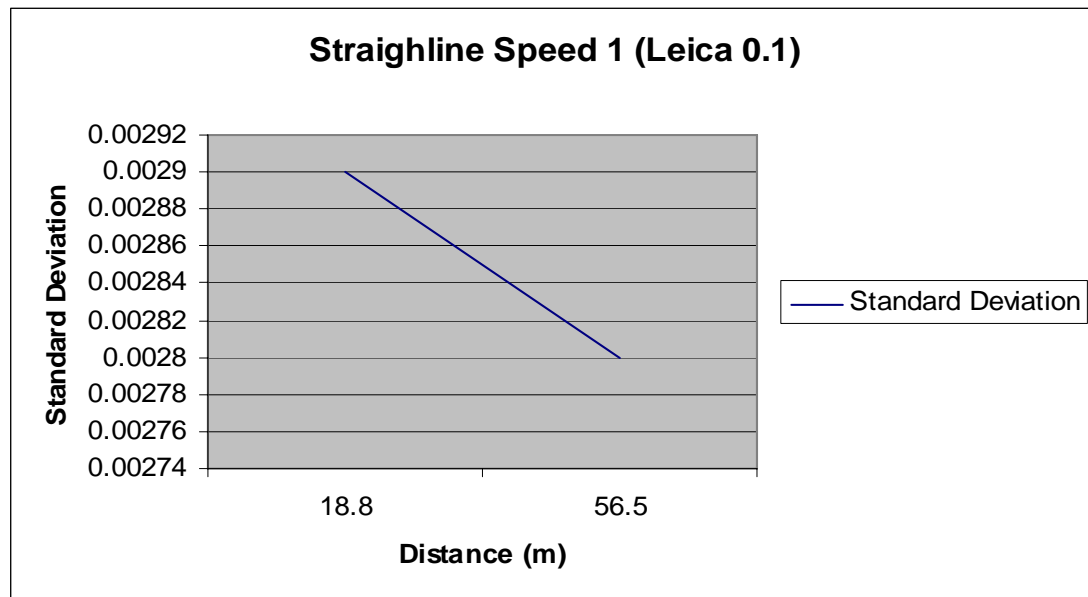
| Stn | Speed | Std Dev | Range | Av Speed (deg/sec) | Average Distance | Above Man spec | % Above Man Spec |
|-----|-------|---------|-------|--------------------|------------------|----------------|------------------|
| 1   | 1     | 0.0247  | 0.133 | 0.4553             | 18.8             | 93             | 26.6             |
| 1   | 2     | 0.0717  | 0.305 | 1.3232             | 18.8             | 63             | 39.4             |
| 1   | 3     | 0.1391  | 0.601 | 2.617              | 18.8             | 36             | 35.6             |
| 2   | 1     | 0.018   | 0.09  | 0.1624             | 56.5             | 49             | 14.8             |
| 2   | 2     | 0.0518  | 0.203 | 0.49               | 56.5             | 51             | 35.7             |
| 2   | 3     | 0.0997  | 0.385 | 1.019              | 56.5             | 27             | 38.0             |

Figure 4.22 is a graphical representation of the relationship between the change in standard deviation and a change in tracking speed. It demonstrates again that as angular movement speed (tracking speed) increases, point accuracy (standard deviation) decreases.



**Figure 4.22:** Standard deviation –vs- Instrument tracking speed.

Figure 4.23 illustrates the relationship between standard deviation and target distance. Similar to the circular path testing, the results indicate that point accuracy (standard deviation) increases as RTS – target range increases from short to medium distances.



**Figure 4.23:** Standard deviation –vs- RTS – target distance.

Note that Figures 4.22 and 4.23 are for illustration purposes only, for full analysis results please refer to Appendices B, C and D.

### 4.5.3 Accuracy

From the presented test results it is clear that there are two main factors which influence the overall accuracy of an RTS. These are:

1. Instrument Tracking Speed (angular movement per second):
  - As the instrument tracking speed is increased, the associated point accuracy is decreased.
2. Achieved accuracy is related directly to the RTS – target distance:
  - Accuracy increases as the RTS – target distance is increased from short (<20m) to mid distances (50m); and
  - Accuracy decreases as the RTS – target distance is increased from mid (50m) to long (>100) range.

Furthermore, the Trimble S6 is far less accurate under all testing regimes than the Leica TPS1205.

#### 4.5.4 Reliability

Similar to results found during the accuracy analysis it is again clear that the reliability of each system is related to two factors. Again these factors are:

1. Instrument Tracking Speed (angular movement per second):
  - As the instrument tracking speed is increased, the associated point reliability is decreased.
2. Reliability is related directly to the RTS – target distance:
  - Accuracy decreases as the RTS – target distance is increased.

Similar to the accuracy findings, the Trimble S6 is far less reliable under all testing regimes than the Leica TPS1205.

#### 4.6 Conclusion

Based on the above test results, it can be concluded that both the accuracy and reliability of an RTS system are greatly influenced by two factors:

1. The instrument tracking speed (target movement speed); and
2. The distance from the RTS to the target.

Furthermore it can also be concluded that both the accuracy and reliability of a given instrument is further influenced by the speed at which an instrument is capable of reading distance measurements. This is evident by the fact that the Leica instrument is far more accurate and reliable than the Trimble instrument. This can be attributed to the fact that the Leica instrument is quoted to read distances in generally  $< 0.15$  seconds, this is opposed to the Trimble instrument which is quoted to read distances in around 0.4 seconds. This significant difference in distance measurement time increases the point latency present within the instrument quite significantly. As a result, the Trimble is far less accurate and reliable when compared to the Leica.

## CHAPTER 5

### CONCLUSIONS AND RECOMMENDATIONS

#### 5.1 Recommendations

Due to time constraints the full operational capabilities of the S6 were unable to be determined. This meant that I was unable to extract exact time measurements to each point, and to reduce the record time below 1 second. Should either of these factors be possible my results may have varied slightly.

This project was limited to testing RTS's on a level surface. This project does therefore not take into consideration the accuracy and reliability of these instruments when a third dimension or Z value is added. For real-world machine guidance applications it is this Z value which is usually the most critical. Thus, further testing should be performed in order to determine the accuracy and reliability of this Z value whilst operating in dynamic mode.

Due to limitations on where the rail system for the straight-line testing could be fitted I was unable to test the straight-line at distances greater than 60. Thus I was unable to establish if a decrease in accuracy occurred beyond this point as was the case in the circular path testing. Thus this should be tested in the future.

The rail system which was constructed could have been improved by fitting another rail under the existing rail. This would have held the target from both the top and bottom and subsequently produced a more stable target. Should any additional testing be required, I would recommend that this be fitted.

In my opinion, my work on this project has proven that the Leica TPS1205 is a far superior instrument than the Trimble S6 for application such as machine guidance. This is attributed to instruments extremely fast distance measurement time when compared to the Trimble S6. I have also shown that there is a high degree of correlation between point accuracy/reliability and operational conditions (eg Speed, distance).

## 5.2 Conclusions

Nowadays, the major application of 3D machine guidance systems is found in the agricultural, construction and mining industries for the guidance of heavy machinery such as dozers, graders, excavators, scraper, tractors, harvesters, etc.

For most of these applications the current accuracy and reliability of the RTS is quite acceptable however, for the guidance of road and paving machines the high precision height component is still very challenging for the current 3D machine guidance systems.

The ability of the current systems to comply with these stringent accuracy requirements is limited by several factors which have been highlighted throughout the proceeding report.

These factors include:

- The distance between the RTS and the target;
- The instrument tracking speed (speed of moving target); and
- The instruments distance measurement speed.

The analysis indicates that the best accuracy results are achieved when the instrument is approximately 50m from the target and the target speed is kept <0.5 meters per second (1.8km/hr).

The accuracies achieved by the Leica TPS1205 under these conditions would comply with the majority of construction accuracy requirements. The reliability of the instrument is also extremely good under these conditions with only approximately 2% of the test data falling outside the manufacturer's specification of  $5\text{mm} \pm 2\text{ppm}$  or 0.01 at 95% confidence. Upon moving outside these conditions the results however are less encouraging. By performing any condition change (distance, speed) results in a loss of accuracy and reliability. The reliability of the instrument should the above conditions be altered ranges between 2% and 30% above manufacturer's specifications. These figures would not be acceptable on a construction site.

The accuracy and reliability of the Trimble S6 instrument are however a lot less encouraging than those achieved by the Leica. The Trimble similar to the Leica performed

best over a range of approximately 50m however the speed was lower at around 0.17m/s. Even under these conditions, the Trimble still produced 10% of the data above the supplied manufacturer's specification. It must also be noted the manufacturer's specification for this instrument is  $10\text{mm} \pm 2\text{ppm}$  or 0.02 at 95% confidence. This specification is twice the size of that supplied by the Leica instrument. Move outside the ideal conditions and the Trimble instruments reliability ranges between 14% and 57% and produces very significant outliers. Over a range of 18m, with a tracking speed of 3°/second the Trimble has a data range of 0.6m. Such an error is far too large for any construction type application.

The difference in operational accuracy between the Leica and Trimble instrument, can be attributed to a difference in distance measurement time. Leica suggests that the TPS1205 is capable of measuring distances in tracking mode is generally  $<0.15$  seconds. This is opposed to the S6 which only measures at around 0.4 seconds. This fact effectively increase the latency of the S6 instrument by 0.25 seconds compared that of the Leica. 0.25 seconds creates significant error when recording a target moving at a reasonable speed.

In conclusion, the author believes that latency caused by distance time measurement is the most critical factor associated with an RTS's performance in terms of its accuracy and reliability. Slower measurement times relate to a decrease in data accuracy and reliability. Furthermore, latency is still a major issue effecting the overall accuracy and reliability of all RTS systems. This latency increases as RTS – target distance is increased beyond 50m, this suggests that there is some time delay associated with longer range distance processing and subsequent point storing. Should Leica be able to reduce this processing time further, their instrument would be very effective for accurate machine guidance.

## References

---

Günther Retscher (1998), *Evaluation concepts for applications of multi-sensor systems*. Paper presented at the XXI International Congress FIG'98, 19-26 July 1998, Brighton, UK.

Günther Retscher (2000), *Trajectory Determination for Machine Guidance Systems*. Paper presented at the KIS2001 Symposium, 5-9<sup>th</sup> June 2001, Banff, Canada. Available: <http://info.tuwien.ac.at/ingeo/pub/papers/kis.pdf> [2004, March 2004].

Günther Retscher (2002), *Multi-Sensor Systems for Machine Guidance and Control*. Vienna: Vienna University of Technology.

Heribert Kahmen and Günther Retscher (2000), *Precise 3-D Navigation of Construction Machine Platforms*. Papers presented at the 2nd International Workshop on Mobile Mapping Technology, 21-23 April 1999, Bangkok, Thailand, pp. 5A.2.1-5A.2.5.

Hoglund, R, Large, P, 2003, *Direct Reflex EDM Technology for the Surveyor and Civil Engineer*, Trimble Intergrated Surveying Group. Westminster, Colorado, USA.

Leica (2005), *Leica TPS1200 Series, High Performance Total Station*, Leica Geosystems, Heerbrugg, Switzerland. Available: <http://www.leica-geosystems.com> [2005, May 2005].

Leica (2005), *Leica TPS1200 Series, Technical Data*, Leica Geosystems, Heerbrugg, Switzerland. Available: <http://www.leica-geosystems.com> [2005, May 2005].

Lemmon, T, Jung, R (2005), *Trimble S6 with Magdrive Servo Technology*, Available <http://www.trimble.com>, April 2004.

Product survey (2005), *2005 Total Station Survey*, Available [www.pobonline.com](http://www.pobonline.com) May 2005.

Queensland Government, (1999), *Laser Safety*, Available <http://www.whs.qld.gov.au/safetylink/plant>, May 2005.



Spatial Sciences Institute (SSI), (2003), *Provisional Code of Ethics*, Available <http://www.spatialsciences.org.au/join/>, April 2004.

Topcon (2004), *GPT-8200 Series, Reflectorless Robotic Total Station*, Topcon, Livermore, CA. Available: <http://www.topconsurvey.com> [2005, May 2005].

Topcon (2004), *GPT-8200 Series, Advanced Robotic Total Station*, Topcon, Livermore, CA. Available: <http://www.topcon.com> [2005, May 2005].

Trimble (2004), *Trimble ATS-Technical Notes*, Trimble Navigation Ltd., Dayton, Ohio, USA. Available: <http://www.trimble.com/ats.html> [2004, March 2005].

Trimble, (2005), *Trimble ATS*, Available <http://www.trimble.com>, May 2005.

Trimble, (2005), *Trimble S6 Total Station – Datasheet*, Available [www.trimble.com](http://www.trimble.com), May 2005.

University of Southern Queensland, (2004), *Automated Surveying Systems*, University of Southern Queensland, Australia.

# **Appendix A**

## Project Specification

**University of Southern Queensland  
Faculty of Engineering and Surveying**

**ENG 4111 / 4112 Research Project**

**PROJECT SPECIFICATION**

**FOR:** DENNIS GARGET

**TOPIC:** TESTING ROBOTIC TOTAL STATIONS FOR DYNAMIC TRACKING

**SUPERVISOR:** Mr. Kevin McDougal

**SPONSORSHIP:** Faculty of Engineering and Surveying

**PROJECT AIM:** This project aims to test a number of Robotic Total Stations in order to evaluate their dynamic accuracy. Robotic Total Stations are currently being used for dynamic measurement applications, however, little information is available on their accuracy and reliability.

**PROGRAMME:** Issue A, 13<sup>th</sup> April 2005

1. Research information on manufacturers' specifications for the various types of Robotic Total Stations to be tested.
2. Design a field measurement programme for the testing of several different types of Robotic Total Stations in dynamic tracking.
3. Analyse field data obtained and provide relevant adjustments for the preliminary report.
4. Analyse field data with an aid from relevant surveying software such as LisCAD or Terramodel.
5. Compare obtained results with relevant manufacturers' specifications.
6. Compare obtained results against the previous research results. (Carried out by Chun Siong Chua)

AGREED: \_\_\_\_\_ (Student) \_\_\_\_\_ (Supervisor)

Dated: \_\_\_\_ / \_\_\_\_ / \_\_\_\_

## **Appendix B**

### Circular Path Test Results for Leica TPS1205 at a recording speed of 0.1 seconds

Part A – Error vs Point Number

Part B – Absolute Error vs Tracking Speed

Part C – Standard Deviation vs Tracking Speed

Part D – Standard Deviation vs Distance

**Part A – Error vs Point Number**

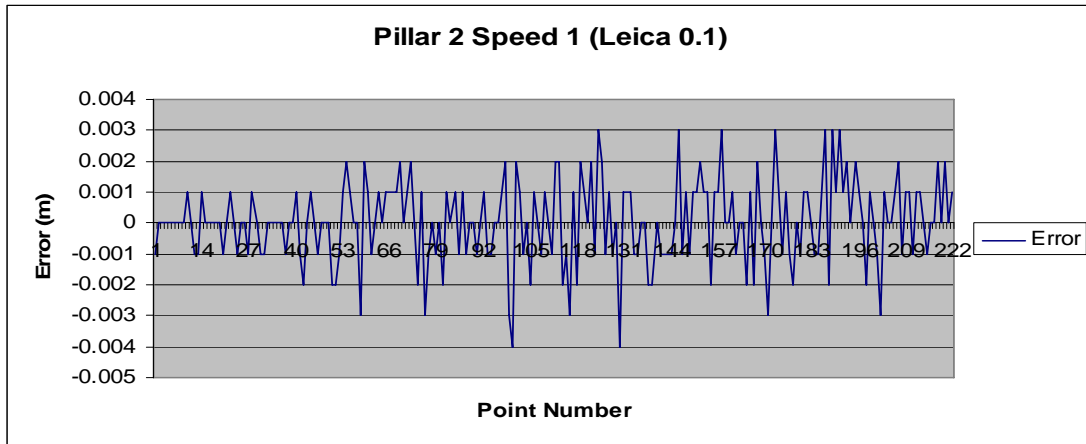


**Figure B.1:** Error vs Point Number graph, Pillar 2 Speed 1.

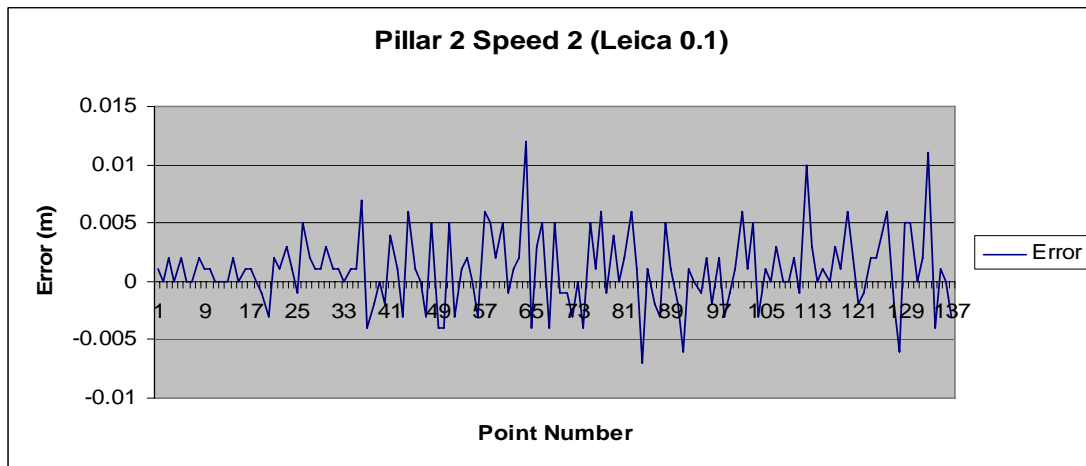


**Figure B.2:** Error vs Point Number graph, Pillar 2 Speed 2.

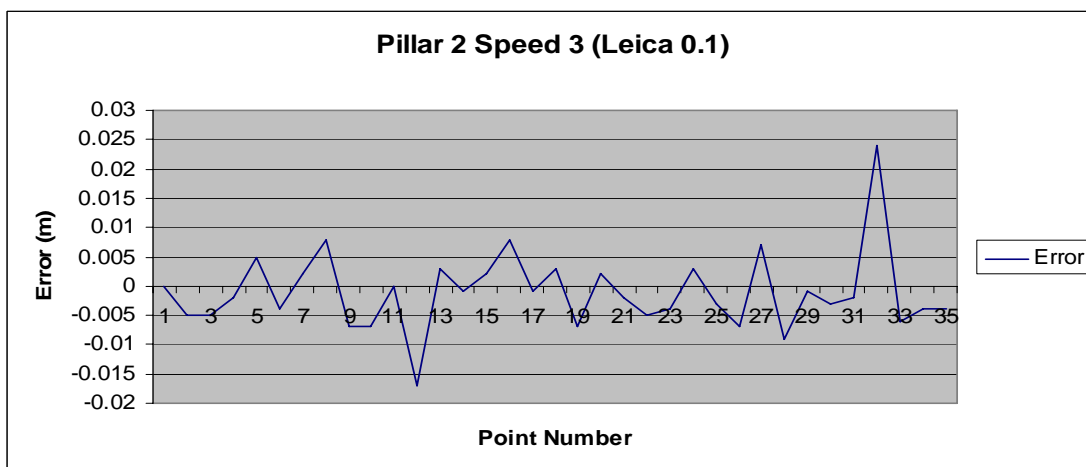


**Figure B.3:** Error vs Point Number graph, Pillar 2 Speed 3.

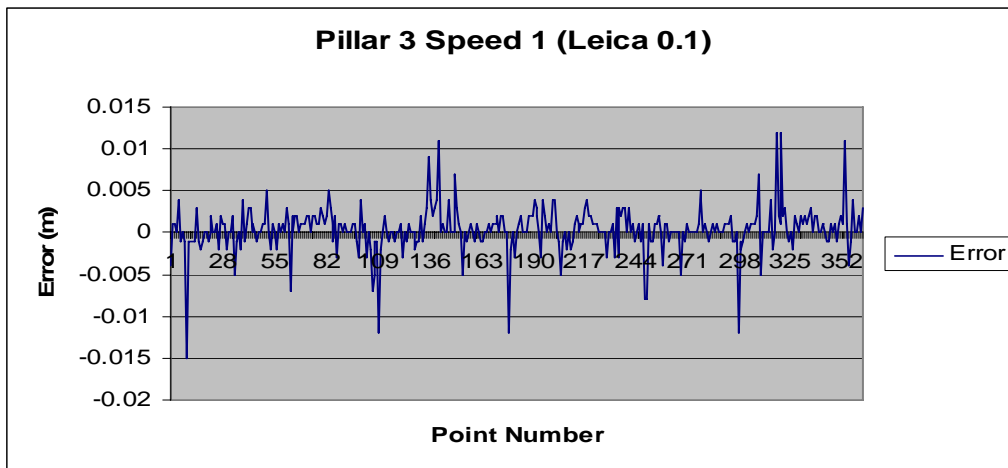


**Figure B.4:** Error vs Point Number graph, Pillar 3 Speed 1.

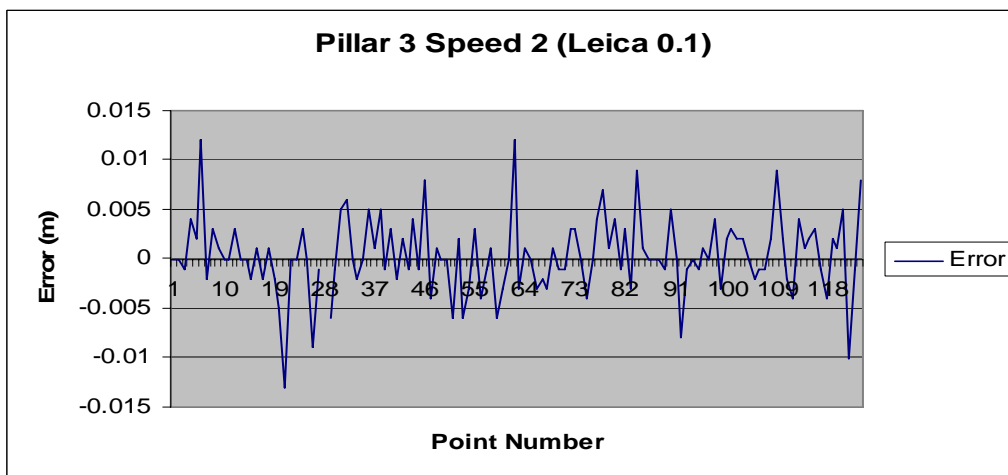


**Figure B.5:** Error vs Point Number graph, Pillar 3 Speed 2.

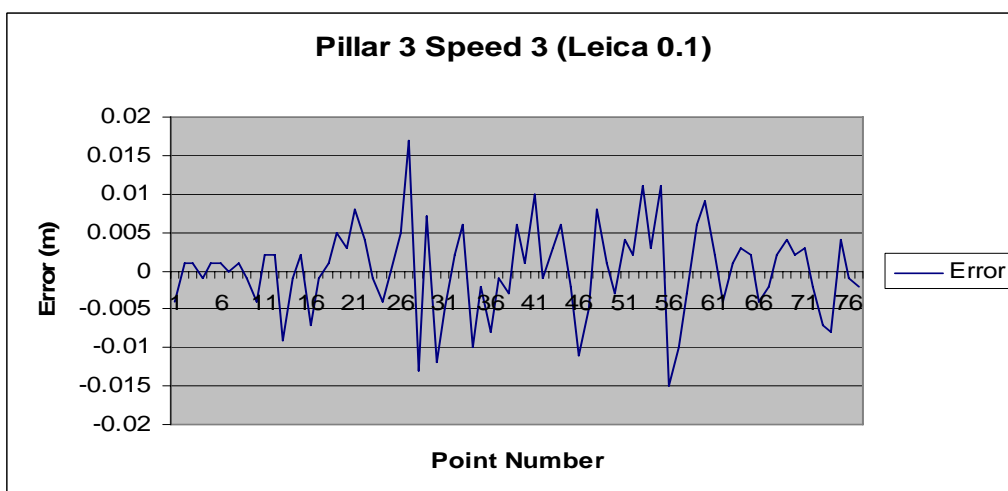


**Figure B.6:** Error vs Point Number graph, Pillar 3 Speed 3.

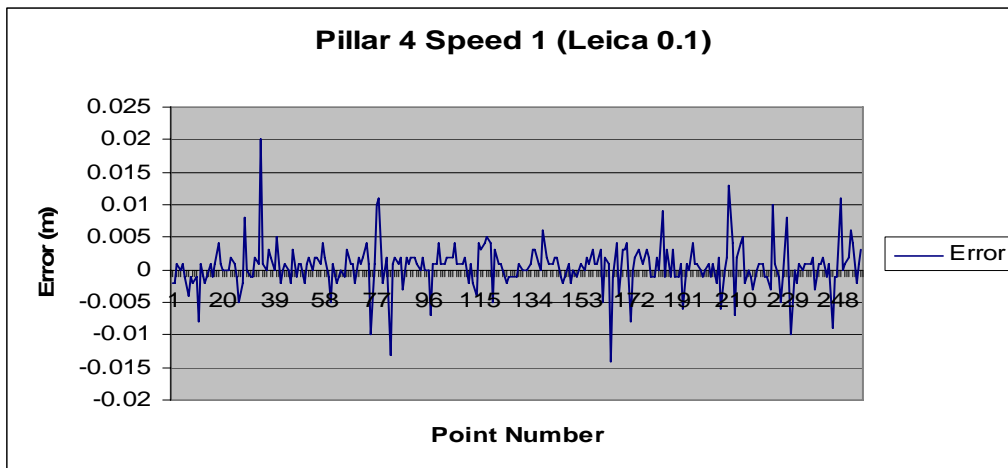


**Figure B.7:** Error vs Point Number graph, Pillar 4 Speed 1.

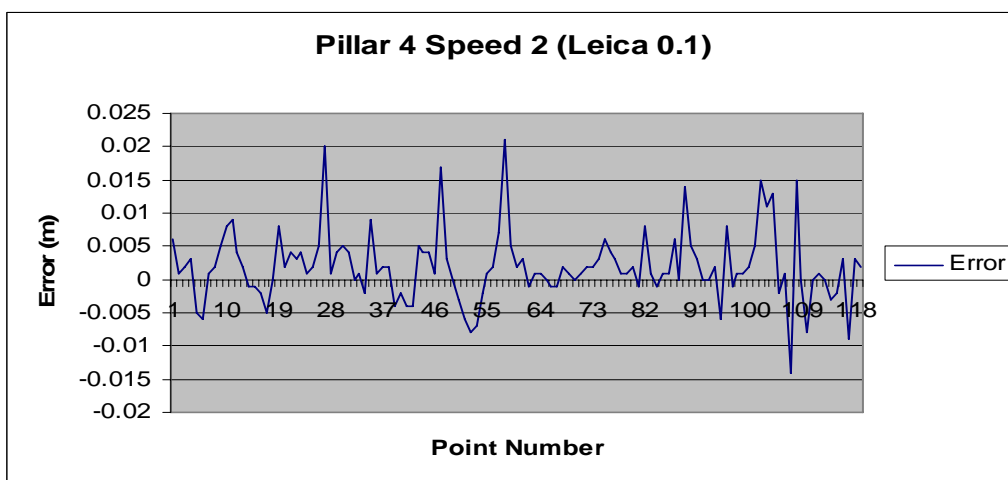


**Figure B.8:** Error vs Point Number graph, Pillar 4 Speed 2.

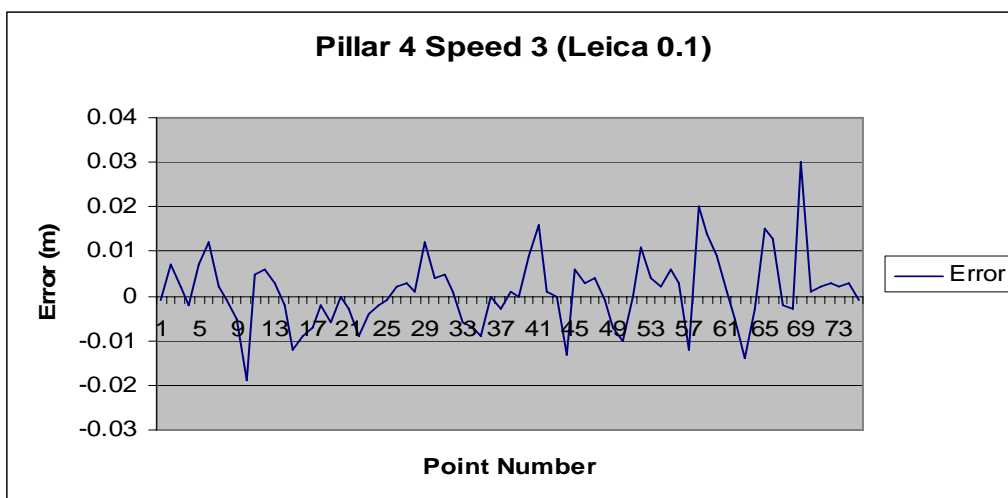


**Figure B.9:** Error vs Point Number graph, Pillar 4 Speed 3.

**Part B – Absolute Error vs Tracking Speed**

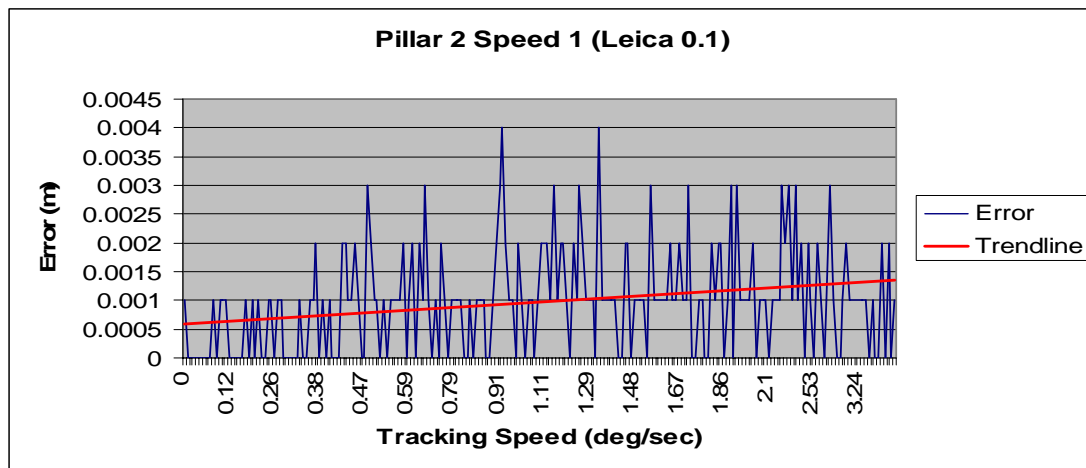


**Figure B.10:** Error vs Tracking Speed graph, Pillar 2 Speed 1.

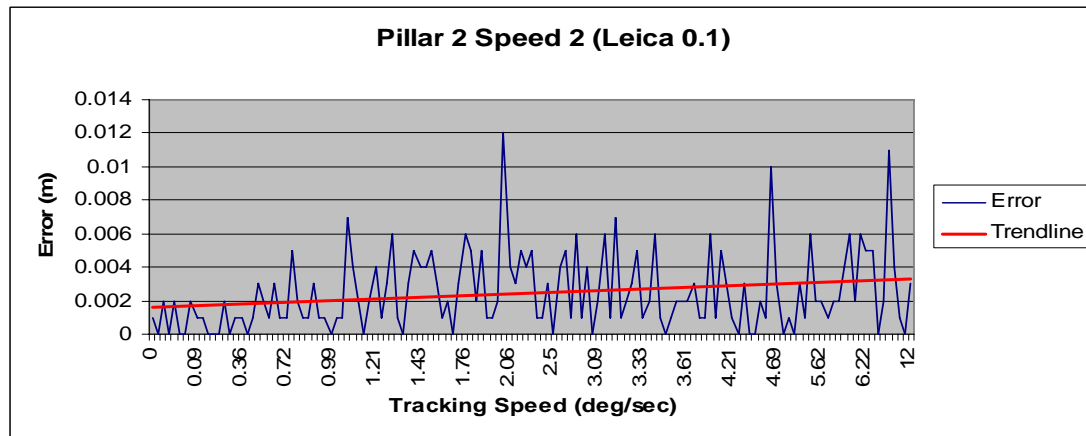


**Figure B.11:** Error vs Tracking Speed graph, Pillar 2 Speed 2.

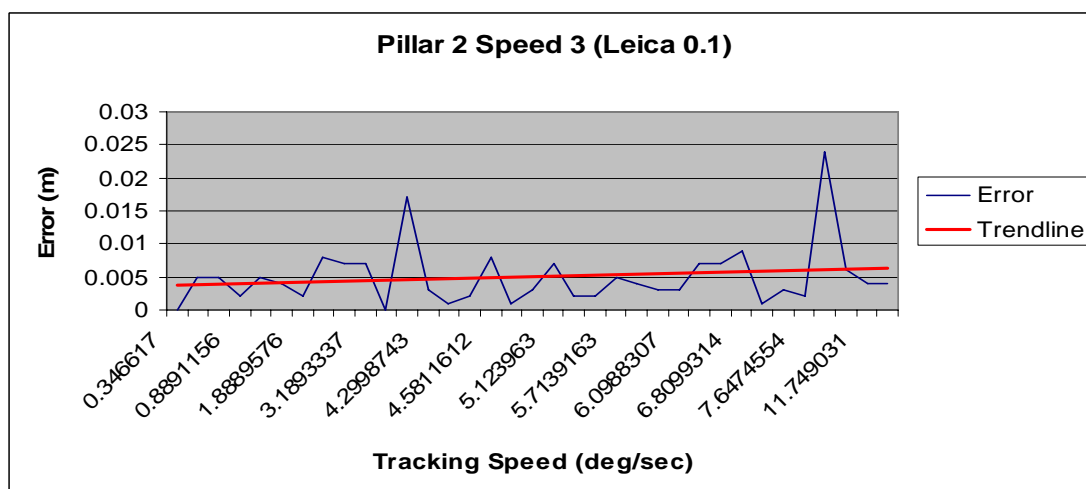


**Figure B.12:** Error vs Tracking Speed graph, Pillar 2 Speed 3.



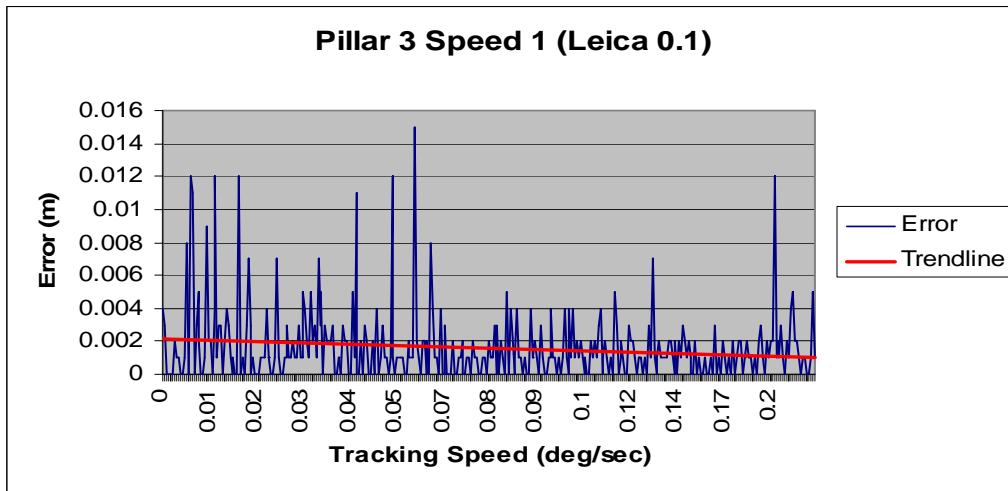


Figure B.13: Error vs Tracking Speed graph, Pillar 3 Speed 1.

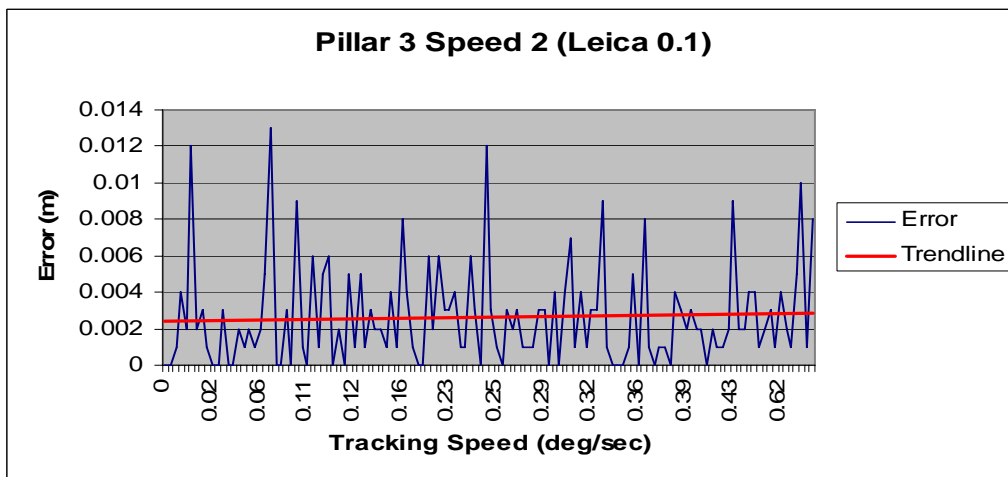


Figure B.14: Error vs Tracking Speed graph, Pillar 3 Speed 2.

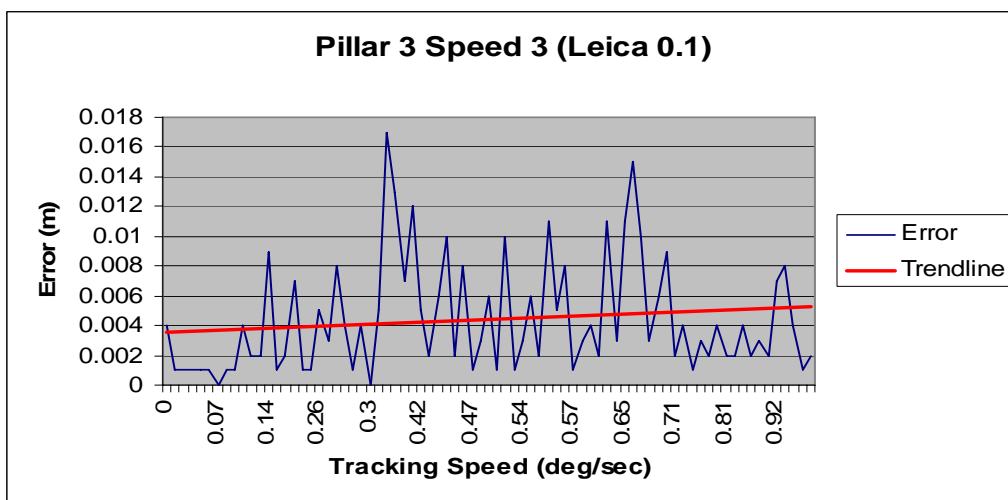


Figure B.15: Error vs Tracking Speed graph, Pillar 3 Speed 3.

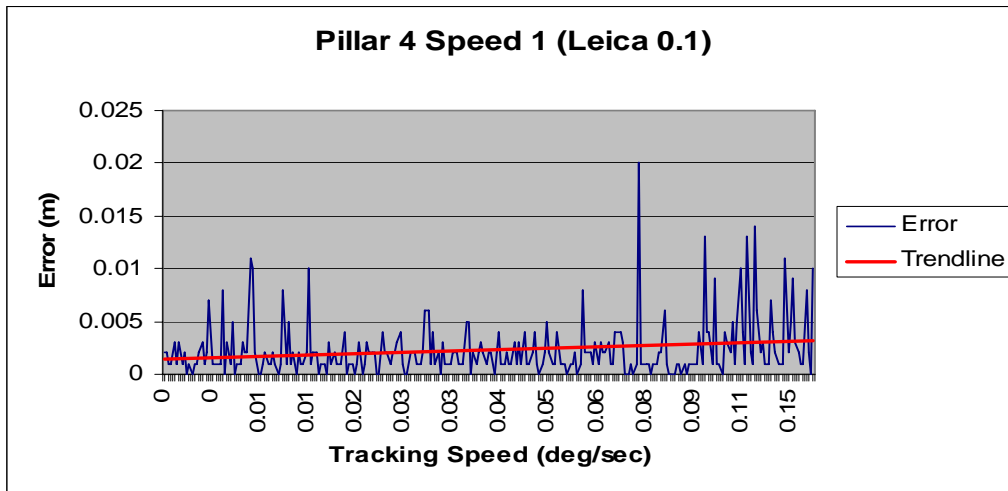


Figure B.16: Error vs Tracking Speed graph, Pillar 4 Speed 1.

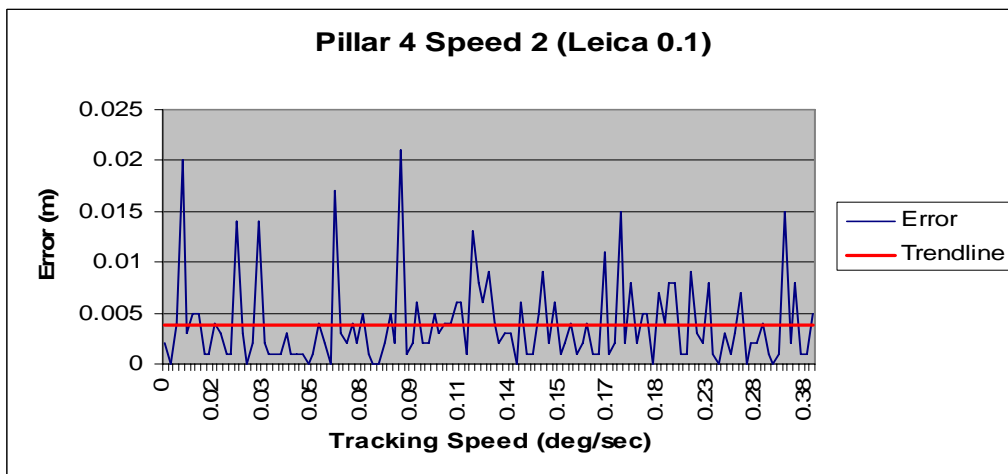


Figure B.17: Error vs Tracking Speed graph, Pillar 4 Speed 2.

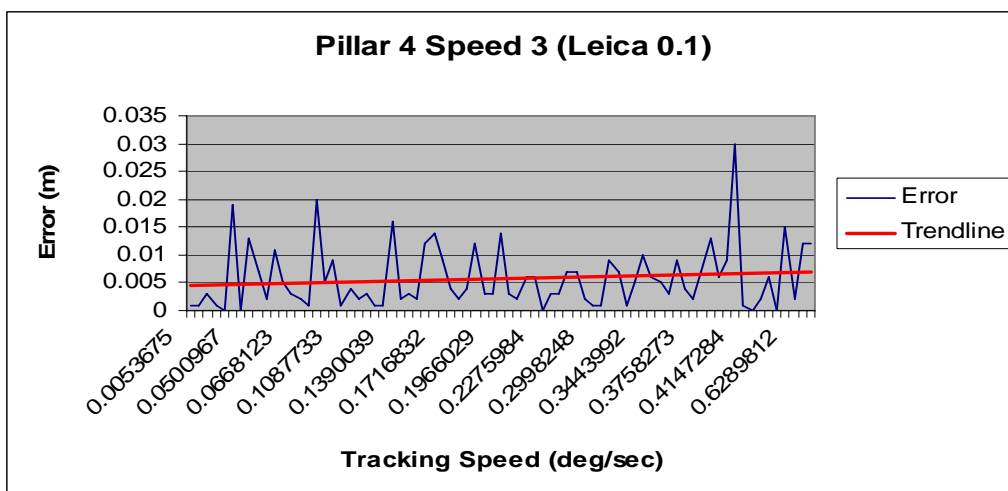
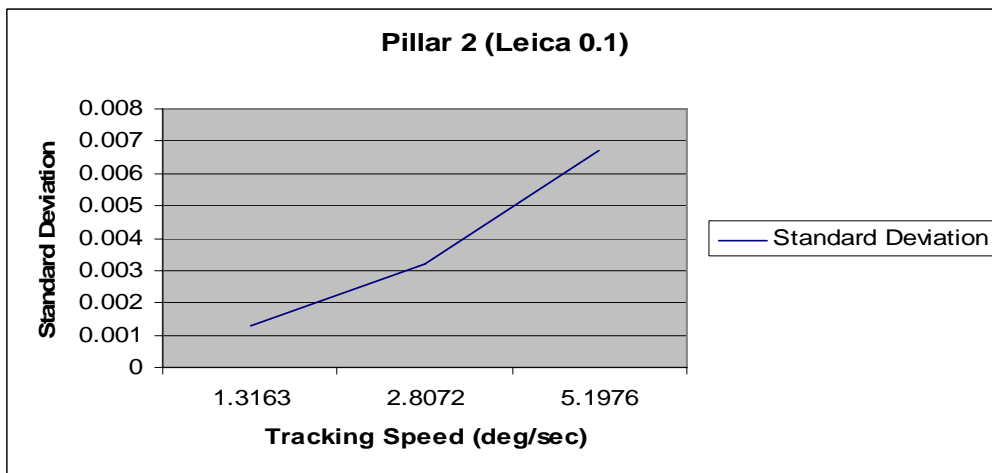
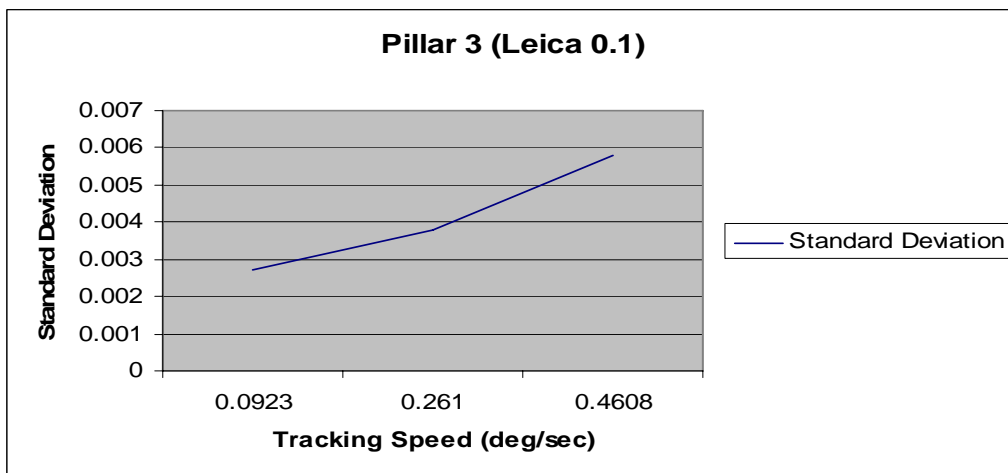


Figure B.18: Error vs Tracking Speed graph, Pillar 4 Speed 3.

**Part C – Standard Deviation vs Tracking Speed**



**Figure B.19:** Standard Deviation vs Tracking Speed graph, Pillar 2.



**Figure B.20:** Standard Deviation vs Tracking Speed graph, Pillar 3.

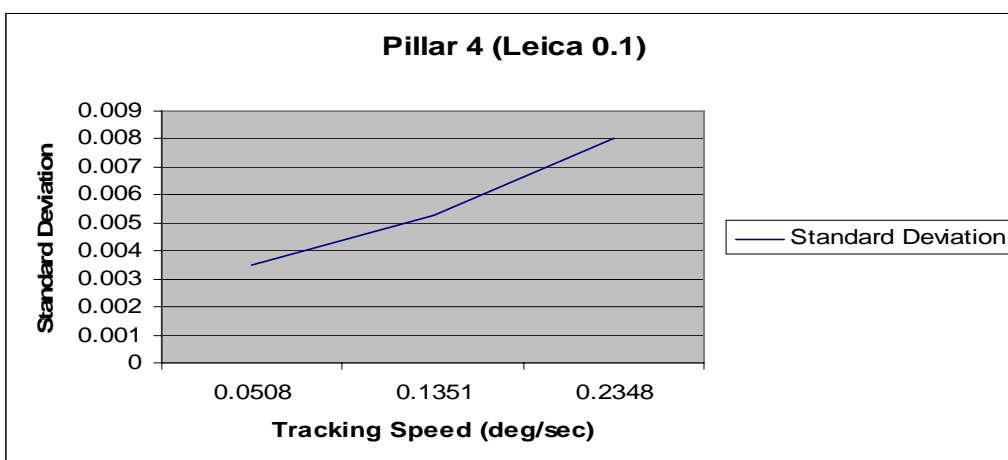


**Figure B.21:** Standard Deviation vs Tracking Speed graph, Pillar 4.

**Part D – Standard Deviation vs Distance**

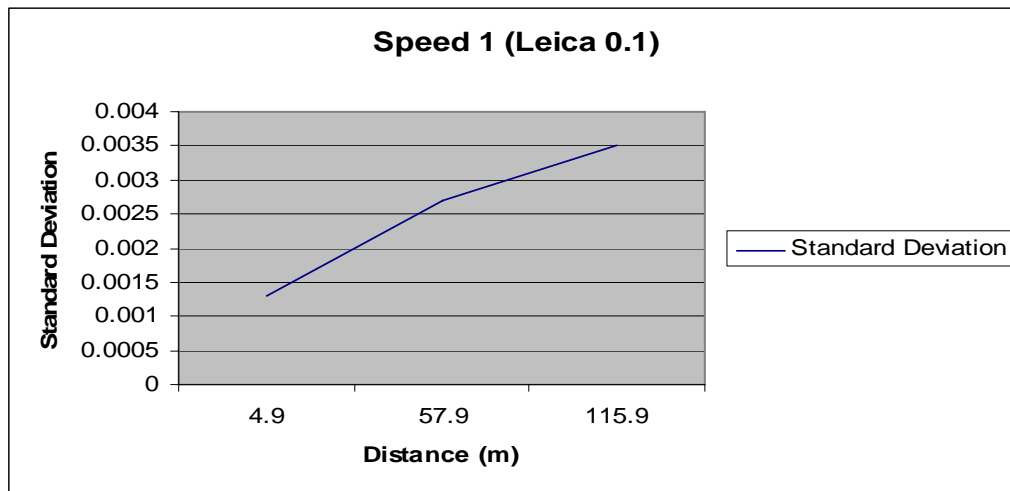


**Figure B.22:** Standard Deviation vs Distance graph, Speed 1.

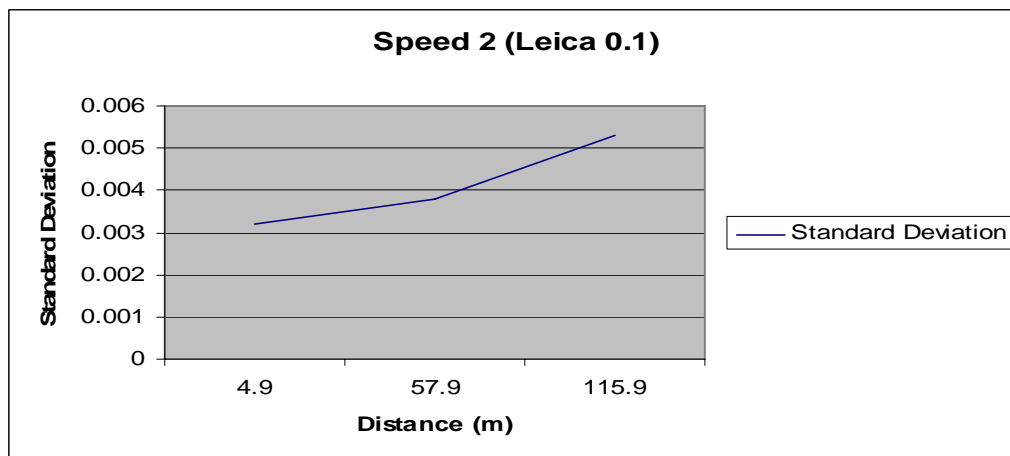


**Figure B.23:** Standard Deviation vs Distance graph, Speed 2.

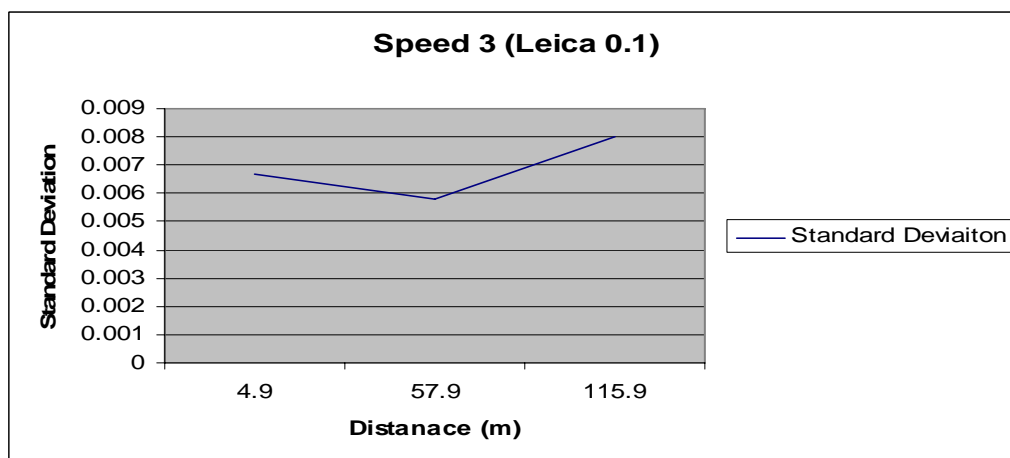


**Figure B.24:** Standard Deviation vs Distance graph, Speed 3.

## **Appendix C**

### Circular Path Test Results for Leica TPS1205 at a recording speed of 0.5 seconds

Part A – Error vs Point Number

Part B – Absolute Error vs Tracking Speed

Part C – Standard Deviation vs Tracking Speed

Part D – Standard Deviation vs Distance

**Part A – Error vs Point Number**

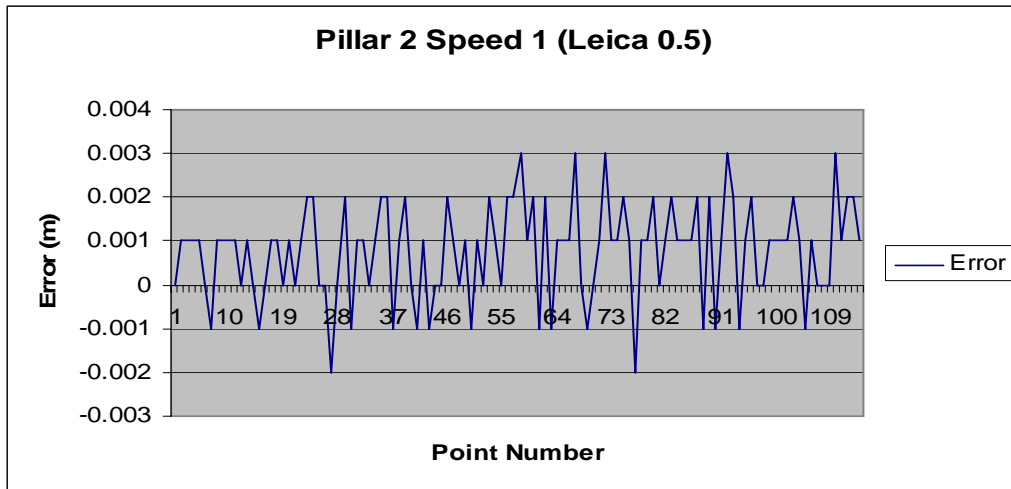


**Figure C.1:** Error vs Point Number graph, Pillar 2 Speed 1.

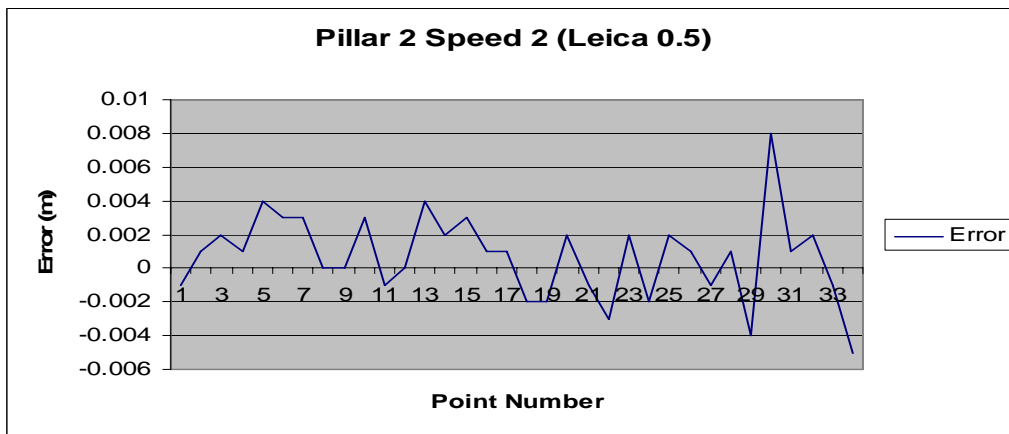


**Figure C.2:** Error vs Point Number graph, Pillar 2 Speed 2.

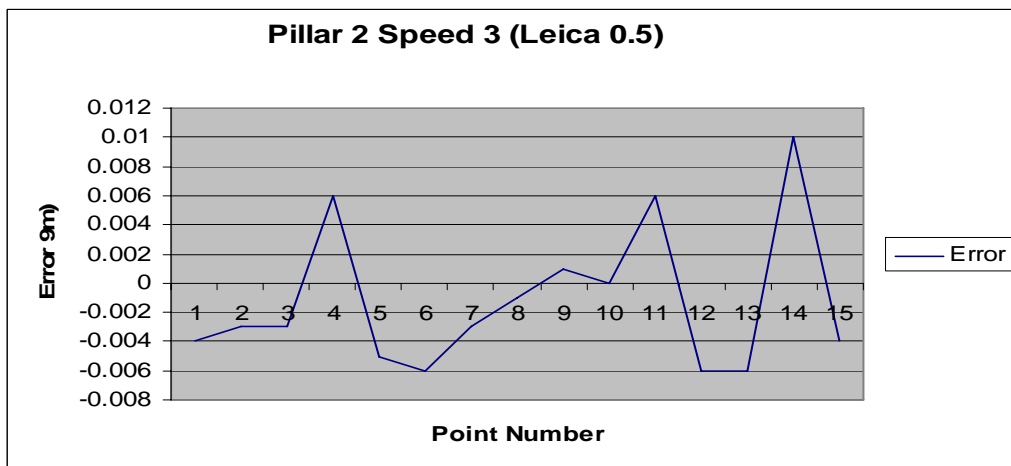


**Figure C.3:** Error vs Point Number graph, Pillar 2 Speed 3.

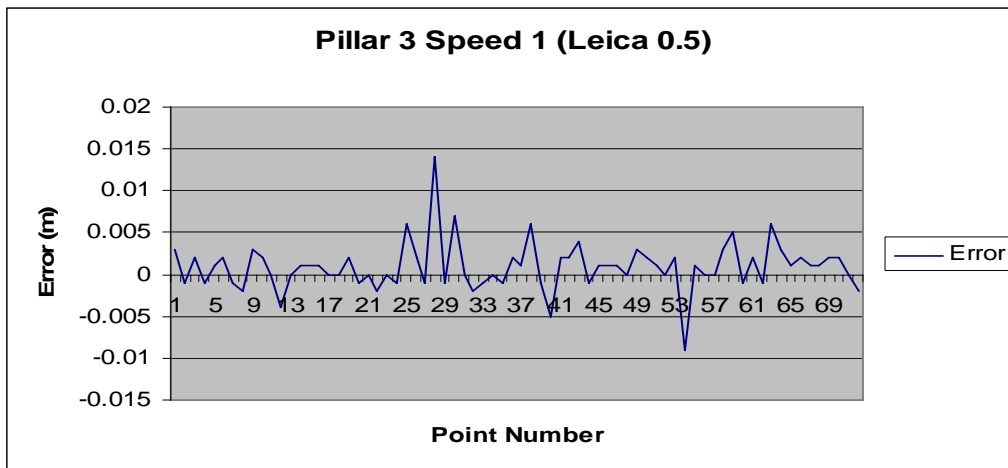


**Figure C.4:** Error vs Point Number graph, Pillar 3 Speed 1.

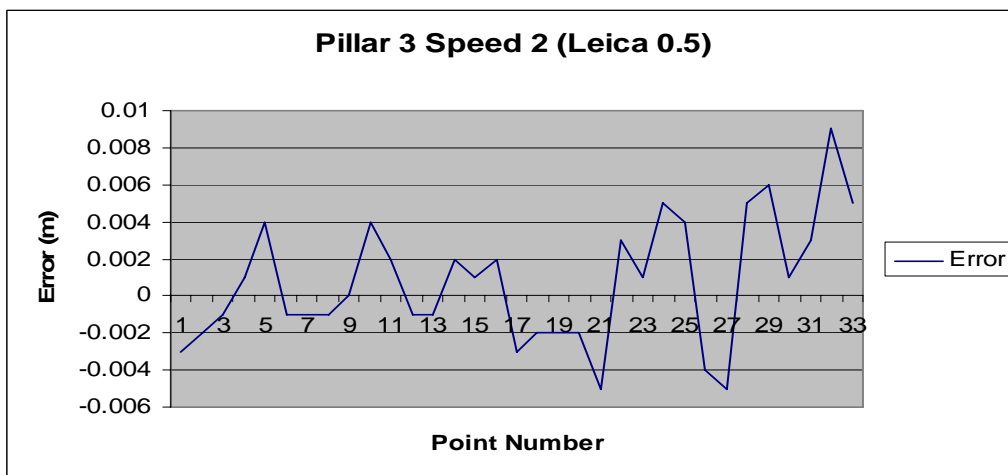


**Figure C.5:** Error vs Point Number graph, Pillar 3 Speed 2.

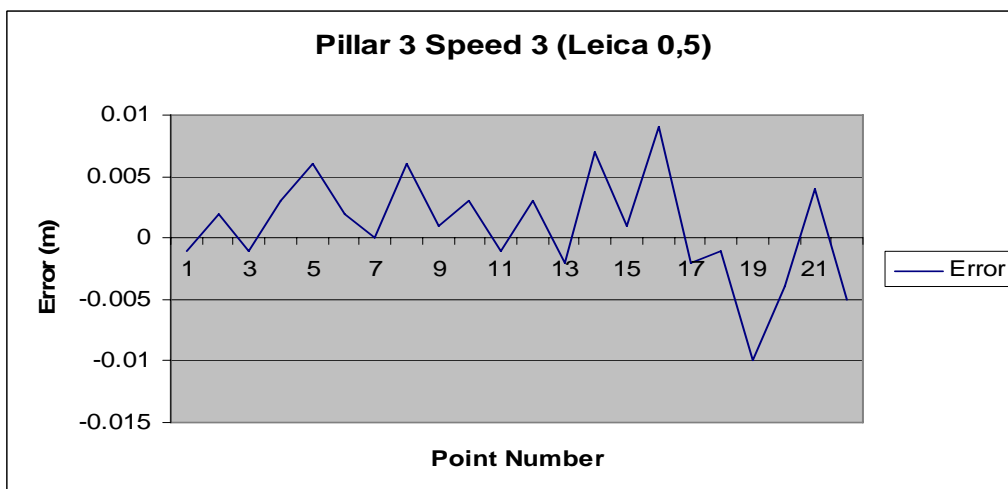


**Figure C.6:** Error vs Point Number graph, Pillar 3 Speed 3.

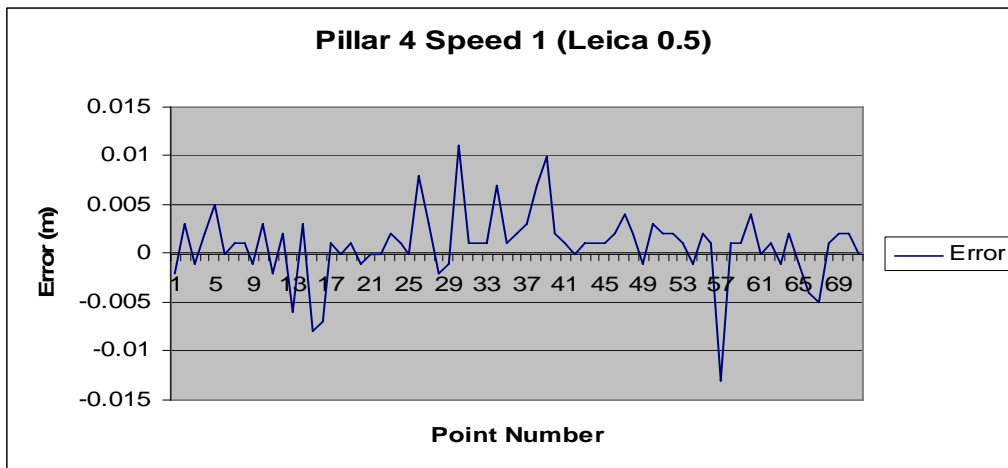


**Figure C.7:** Error vs Point Number graph, Pillar 4 Speed 1.

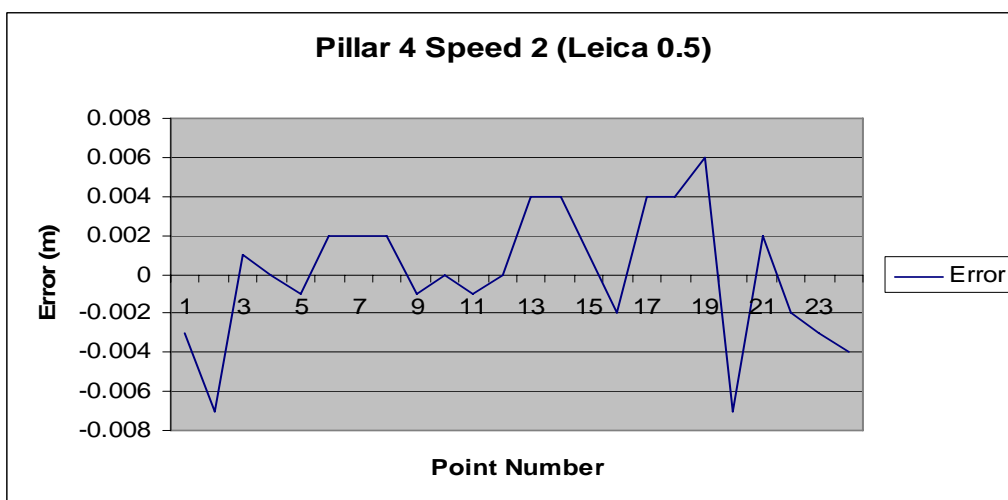


**Figure C.8:** Error vs Point Number graph, Pillar 4 Speed 2.

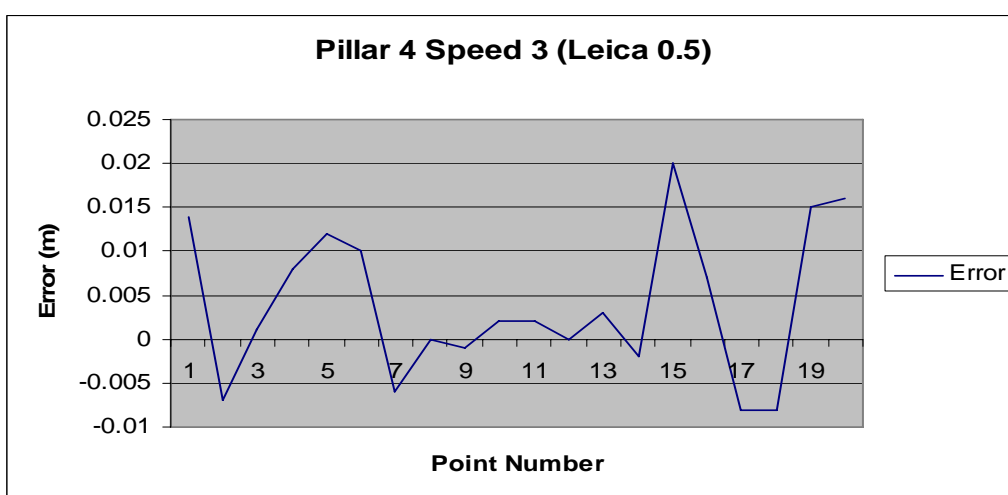


**Figure C.9:** Error vs Point Number graph, Pillar 4 Speed 3.



**Part B – Absolute Error vs Tracking Speed**

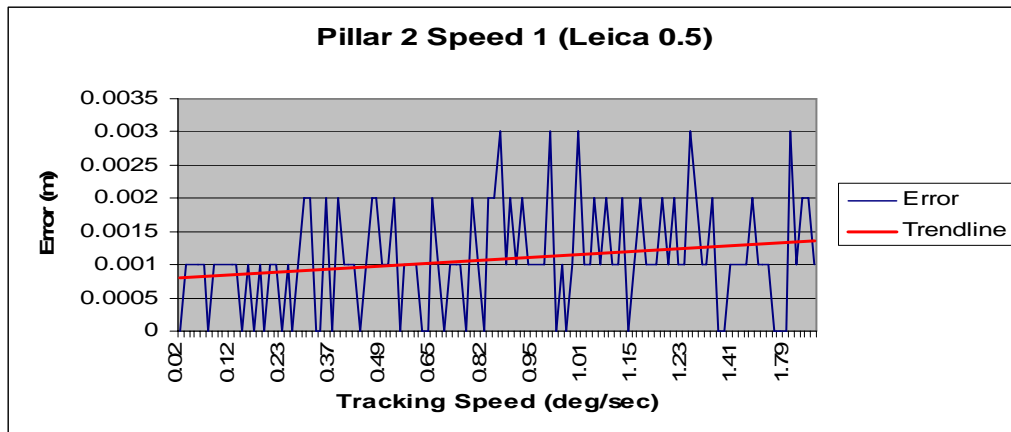


**Figure C.10:** Error vs Tracking Speed graph, Pillar 2 Speed 1.

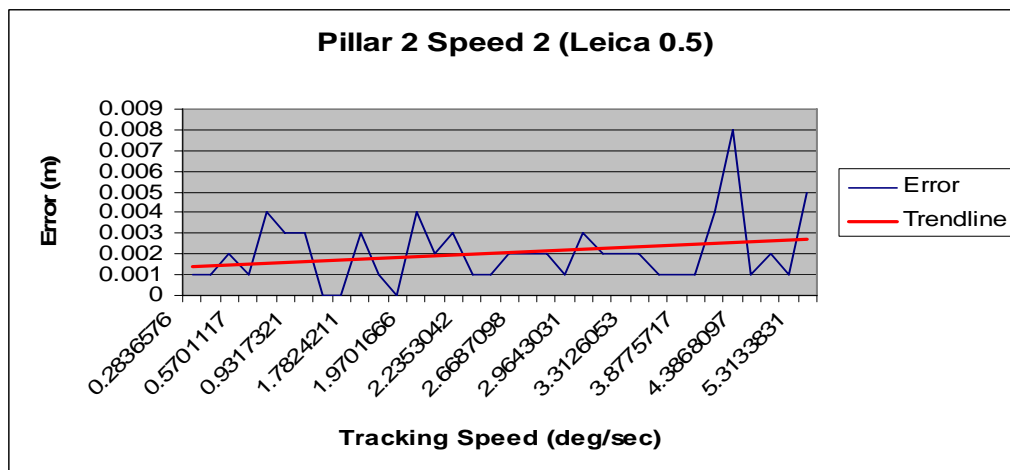


**Figure C.11:** Error vs Tracking Speed graph, Pillar 2 Speed 2.

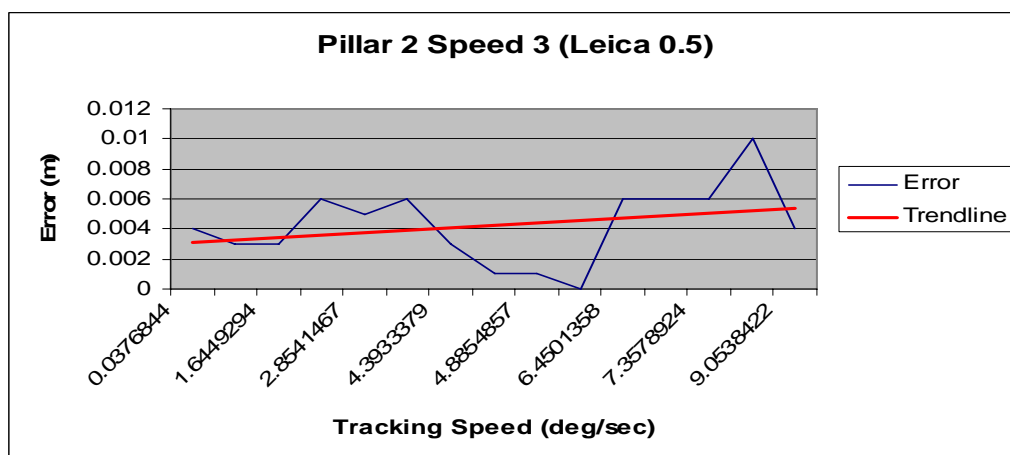


**Figure C.12:** Error vs Tracking Speed graph, Pillar 2 Speed 3.

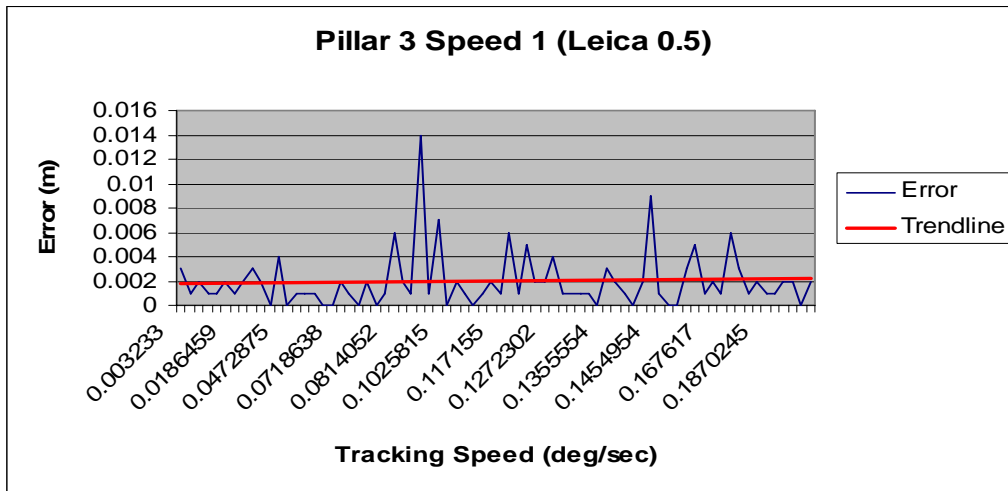


Figure C.13: Error vs Tracking Speed graph, Pillar 3 Speed 1.

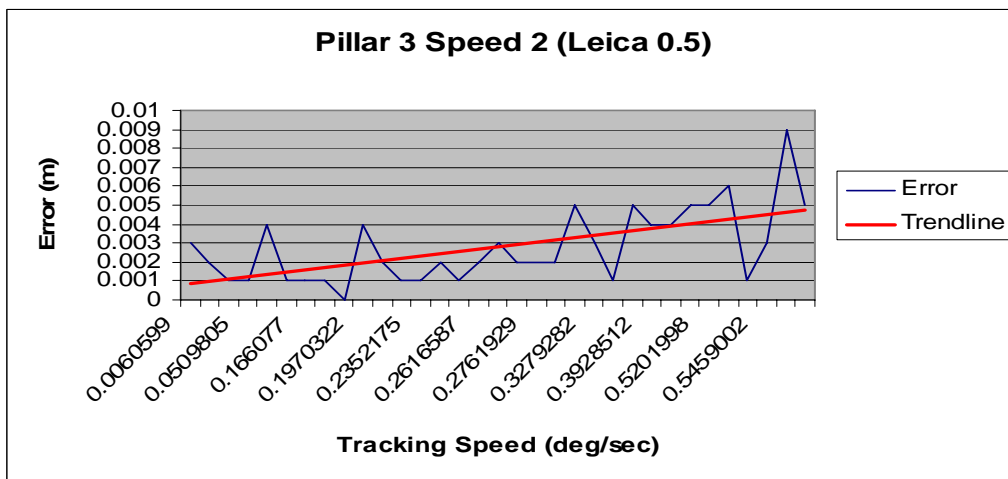


Figure C.14: Error vs Tracking Speed graph, Pillar 3 Speed 2.

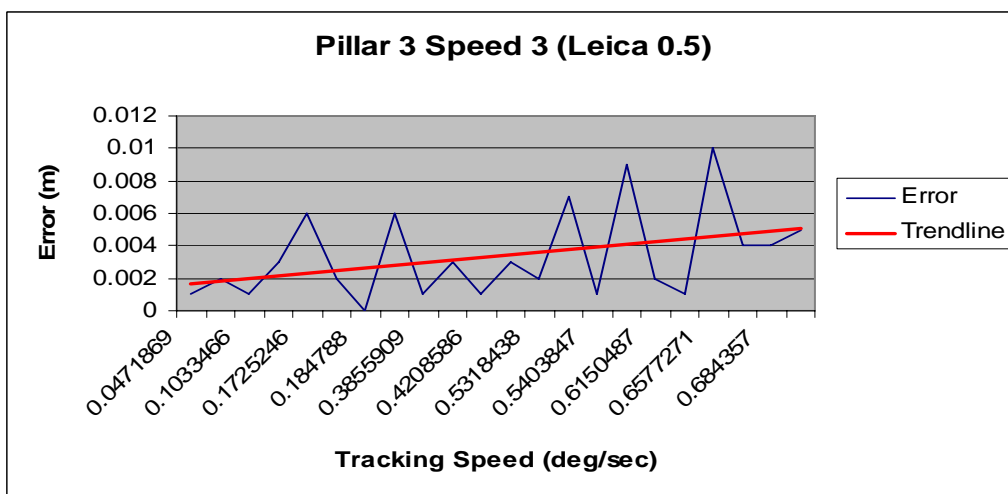


Figure C.15: Error vs Tracking Speed graph, Pillar 3 Speed 3.

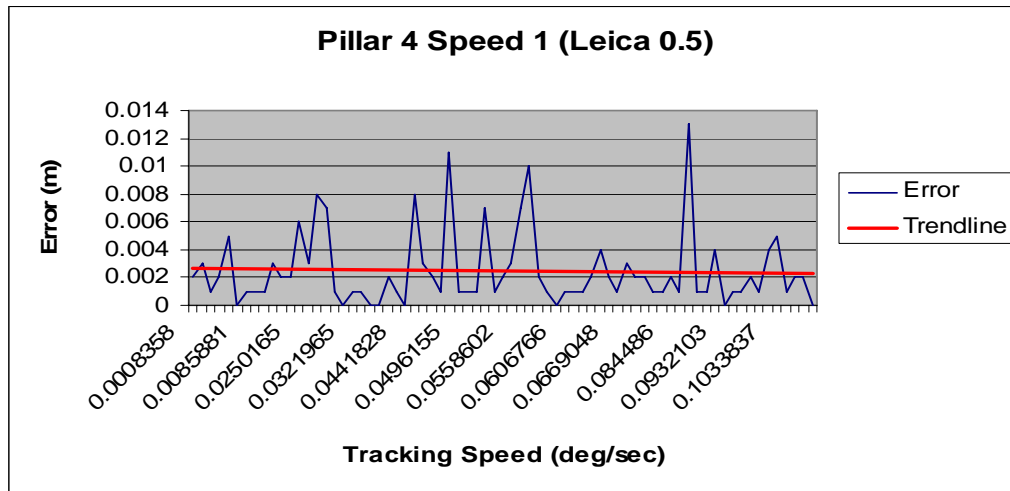


Figure C.16: Error vs Tracking Speed graph, Pillar 4 Speed 1.

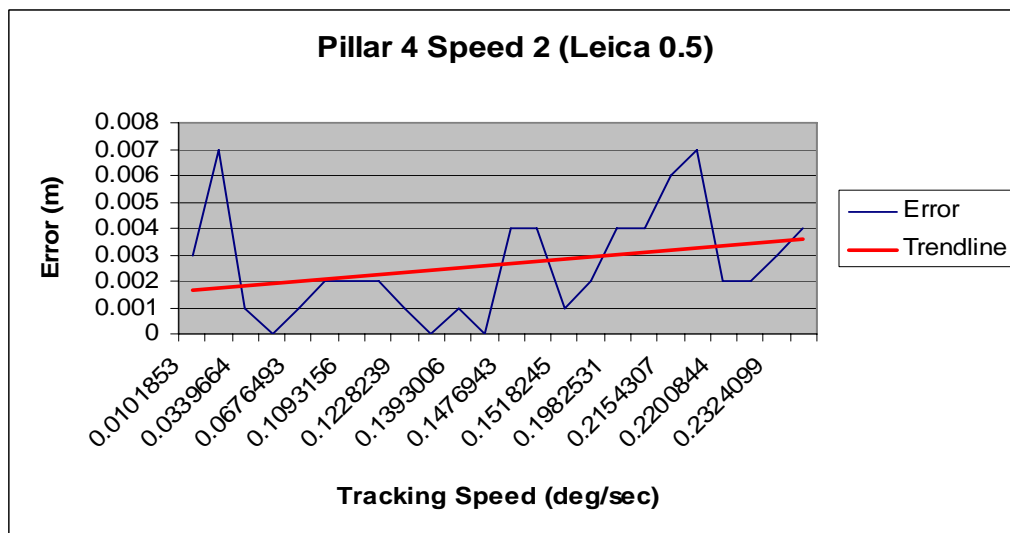


Figure C.17: Error vs Tracking Speed graph, Pillar 4 Speed 2.

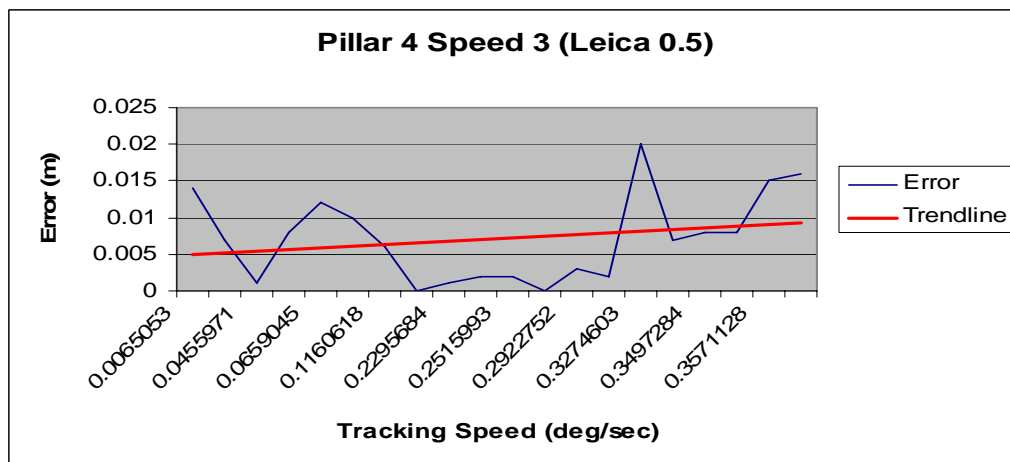
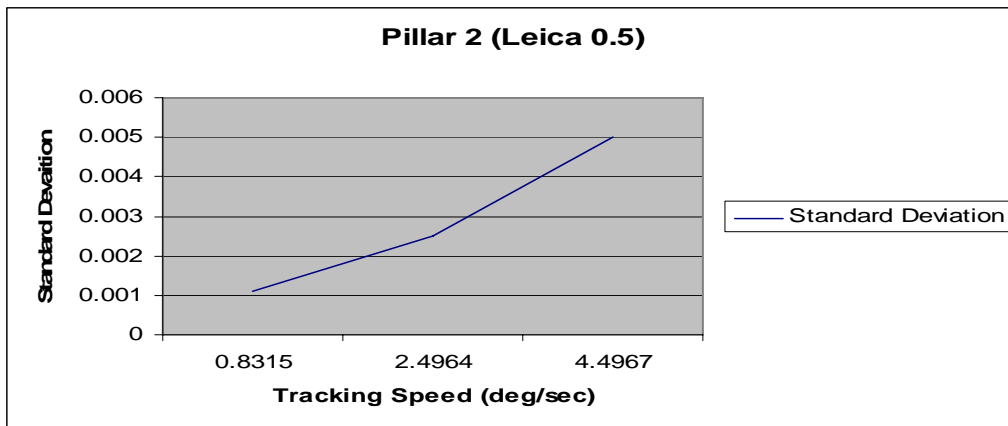
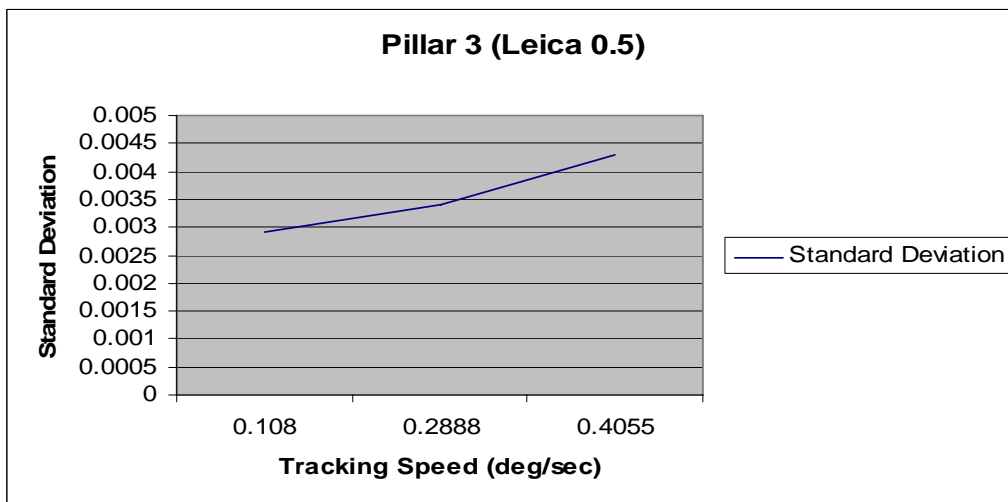


Figure C.18: Error vs Tracking Speed graph, Pillar 4 Speed 3.

**Part C – Standard Deviation vs Tracking Speed**



**Figure C.19:** Standard Deviation vs Tracking Speed graph, Pillar 2.



**Figure C.20:** Standard Deviation vs Tracking Speed graph, Pillar 3.

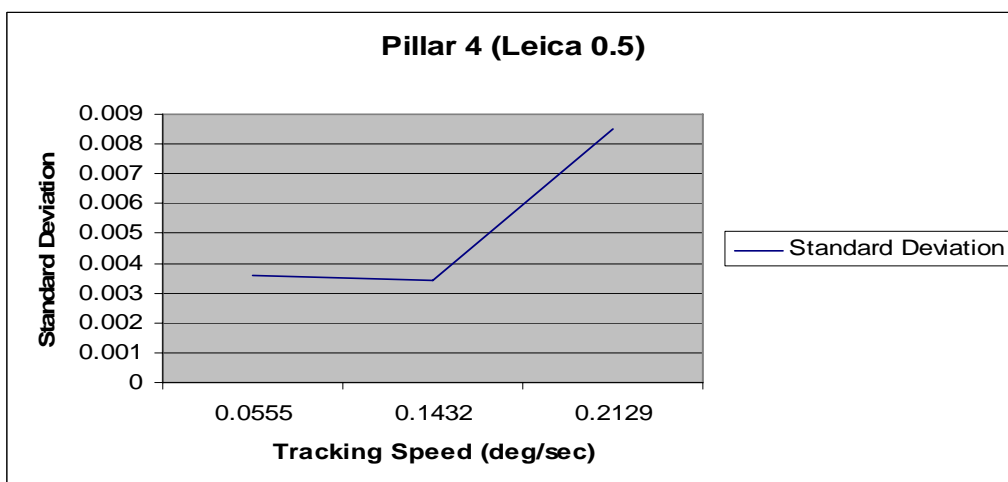


**Figure C.21:** Standard Deviation vs Tracking Speed graph, Pillar 4.

**Part D – Standard Deviation vs Distance**

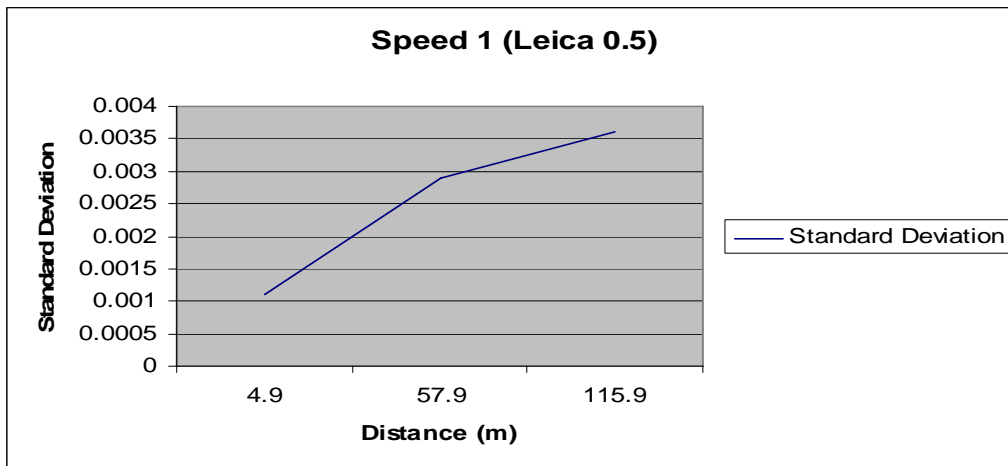


**Figure C.22:** Standard Deviation vs Distance graph, Speed 1.

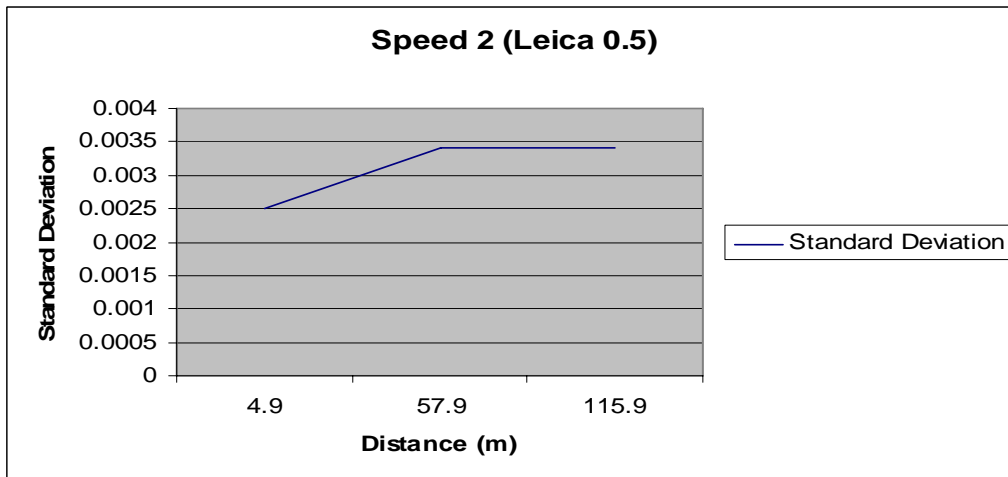


**Figure C.23:** Standard Deviation vs Distance graph, Speed 2.

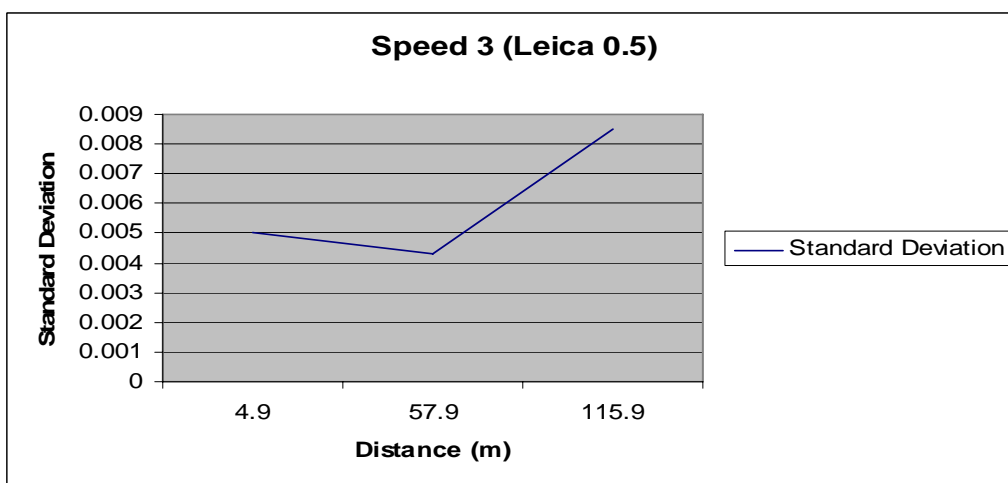


**Figure C.24:** Standard Deviation vs Distance graph, Speed 3.

## **Appendix D**

Circular Path Test Results for Trimble S6 at a recording speed of 1.0 seconds

Part A – Error vs Point Number

Part B – Absolute Error vs Tracking Speed

Part C – Standard Deviation vs Tracking Speed

Part D – Standard Deviation vs Distance

**Part A – Error vs Point Number**

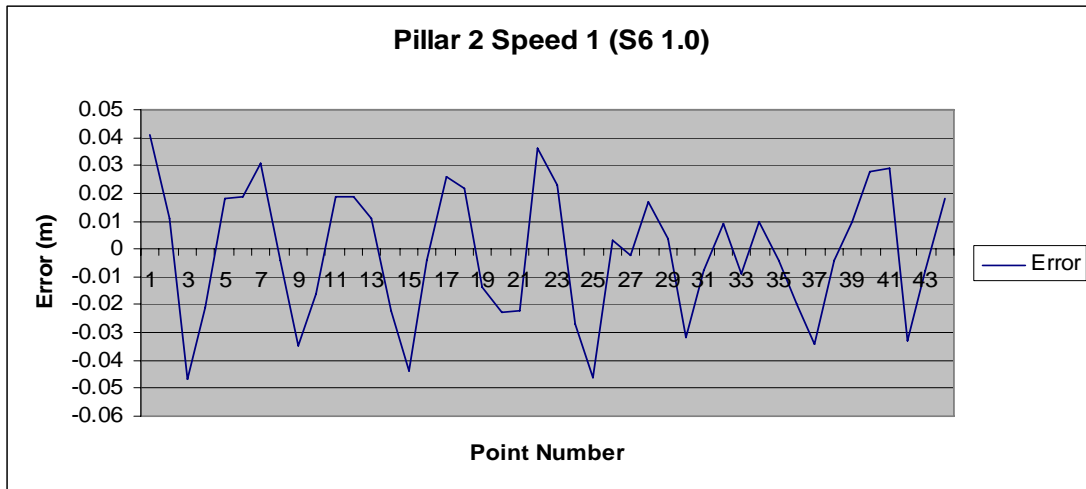


**Figure D.1:** Error vs Point Number graph, Pillar 2 Speed 1.

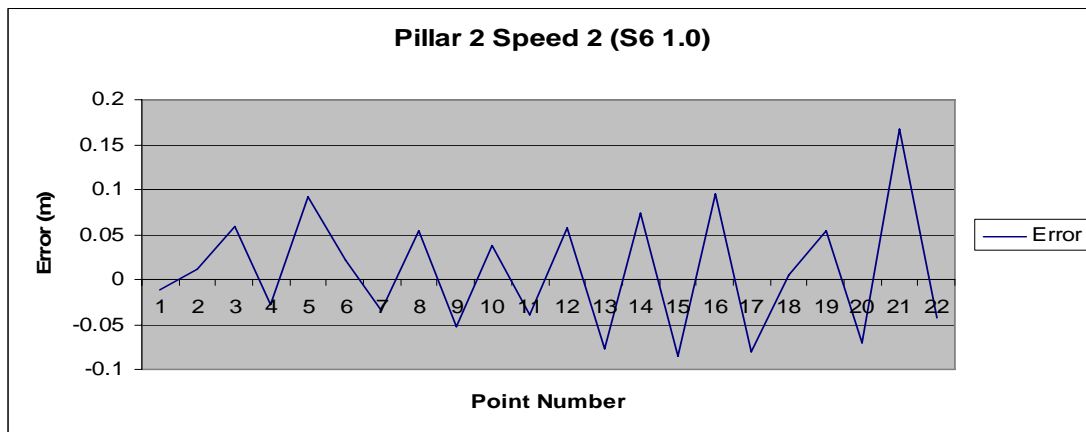


**Figure D.2:** Error vs Point Number graph, Pillar 2 Speed 2.

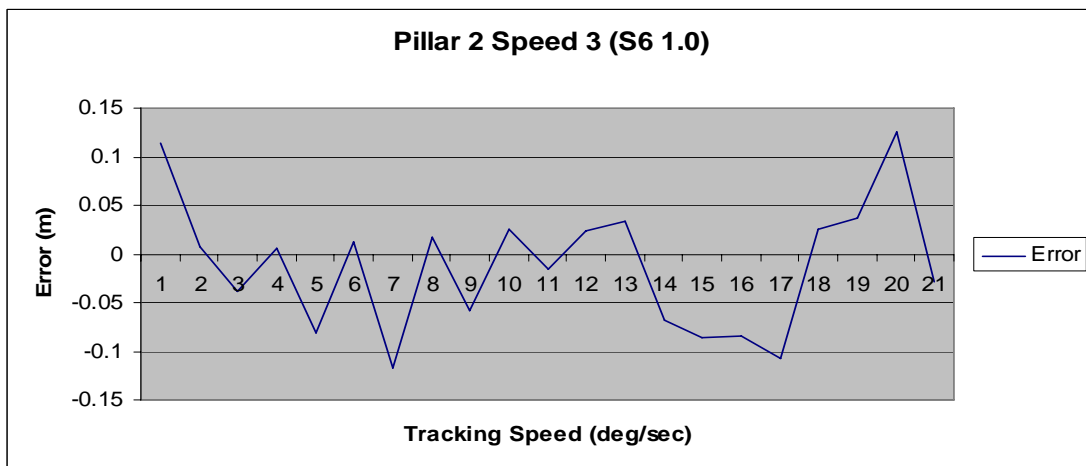


**Figure D.3:** Error vs Point Number graph, Pillar 2 Speed 3.

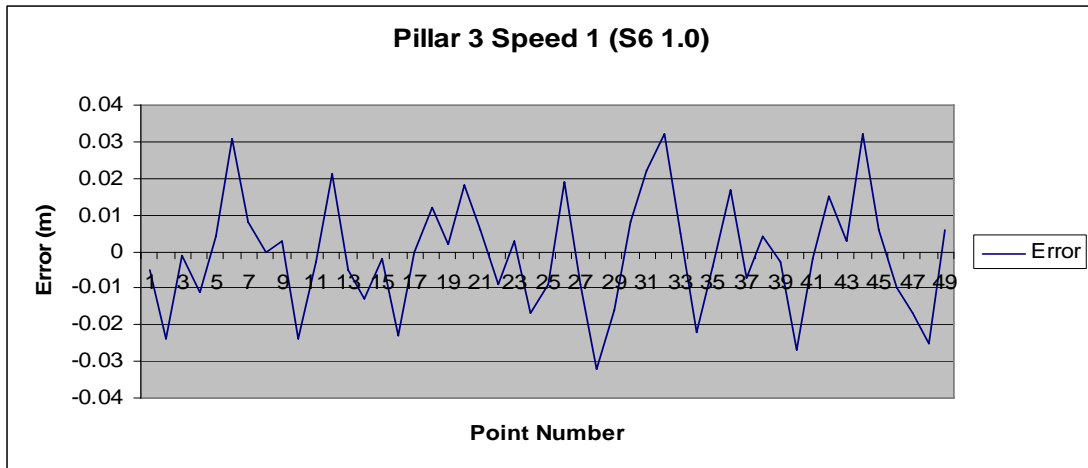


**Figure D.4:** Error vs Point Number graph, Pillar 3 Speed 1.

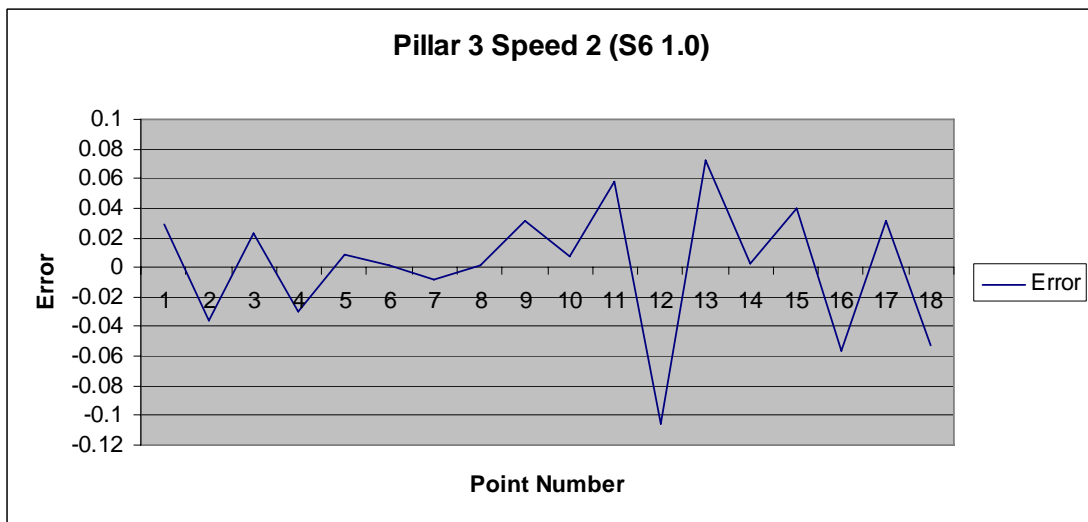


**Figure D.5:** Error vs Point Number graph, Pillar 3 Speed 2.

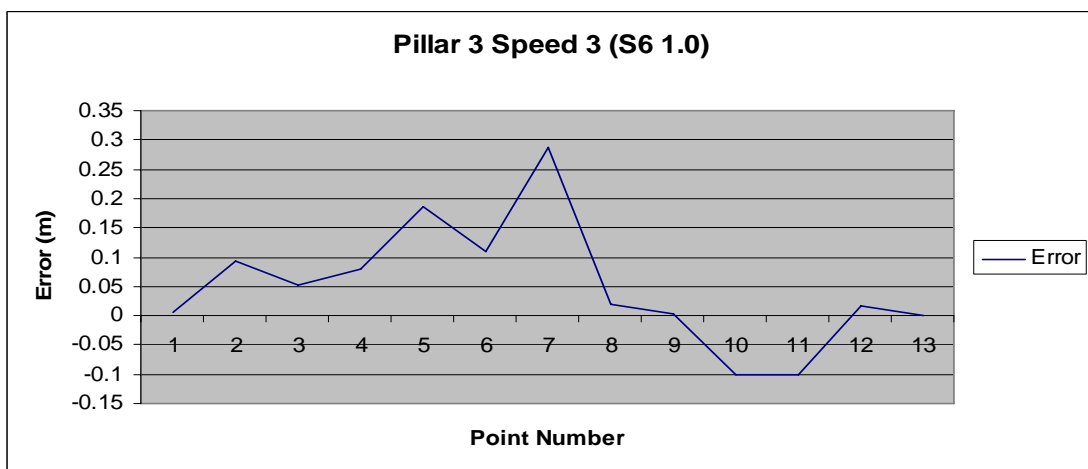


**Figure D.6:** Error vs Point Number graph, Pillar 3 Speed 3.



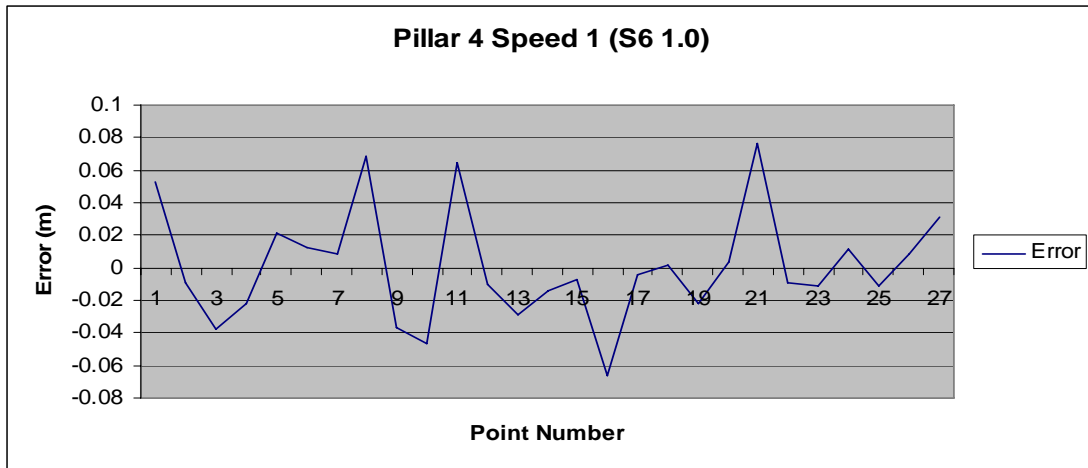


**Figure D.7:** Error vs Point Number graph, Pillar 4 Speed 1.

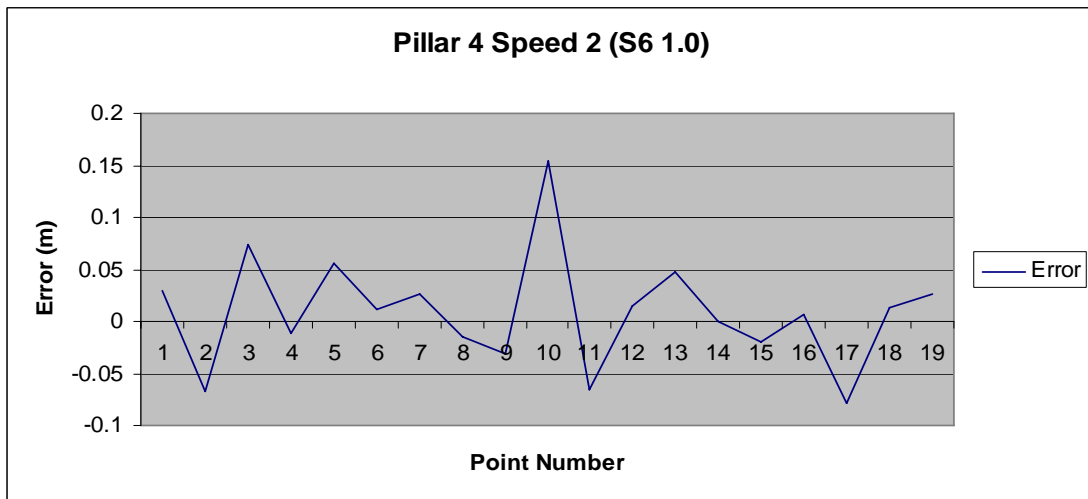


**Figure D.8:** Error vs Point Number graph, Pillar 4 Speed 2.

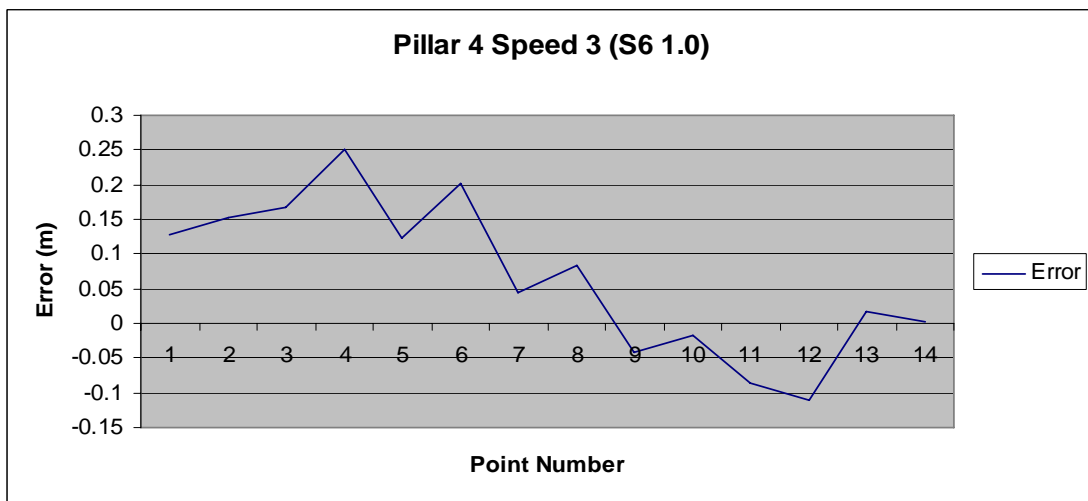


**Figure D.9:** Error vs Point Number graph, Pillar 4 Speed 3.

**Part B – Absolute Error vs Tracking Speed**

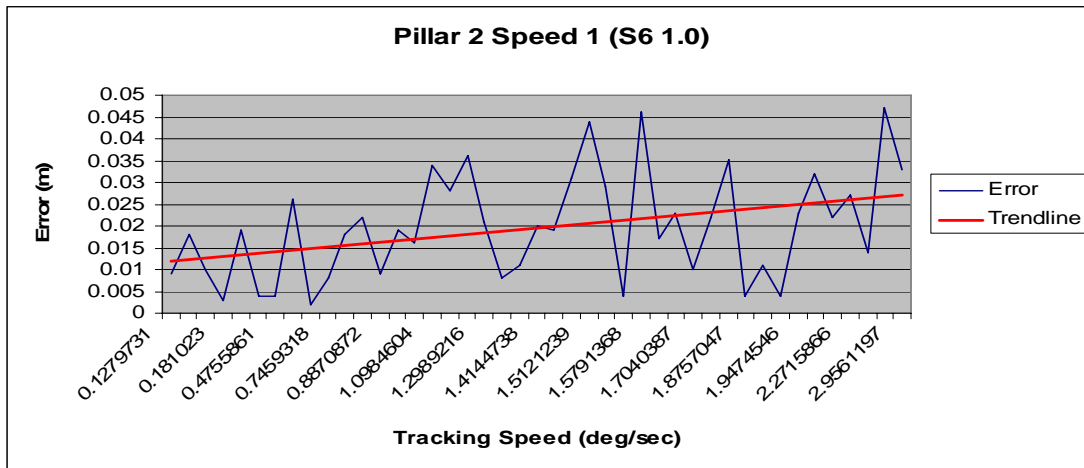


**Figure D.10:** Error vs Tracking Speed graph, Pillar 2 Speed 1.

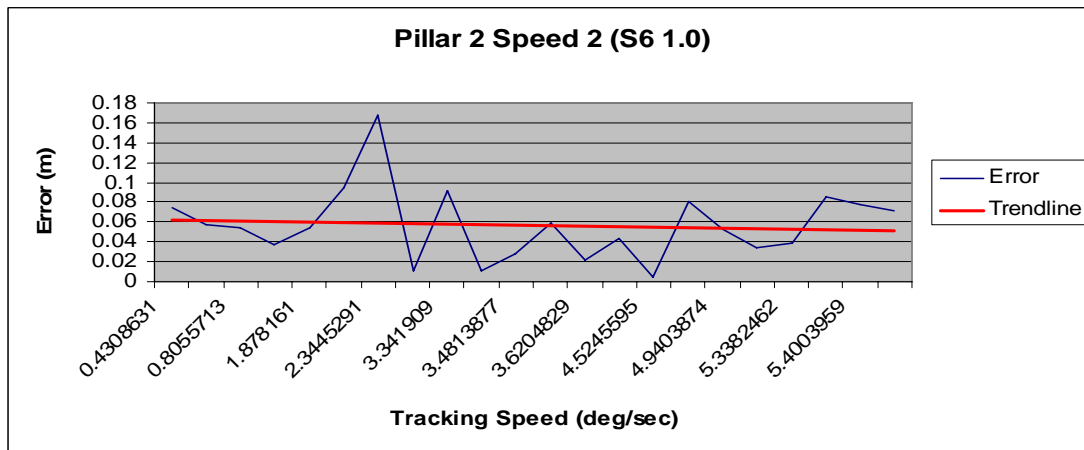


**Figure D.11:** Error vs Tracking Speed graph, Pillar 2 Speed 2.

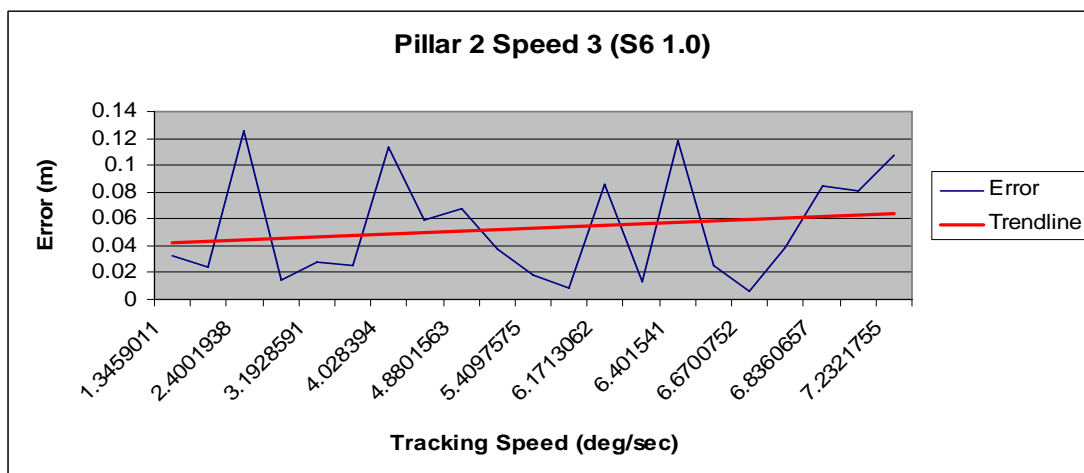


**Figure D.12:** Error vs Tracking Speed graph, Pillar 2 Speed 3.

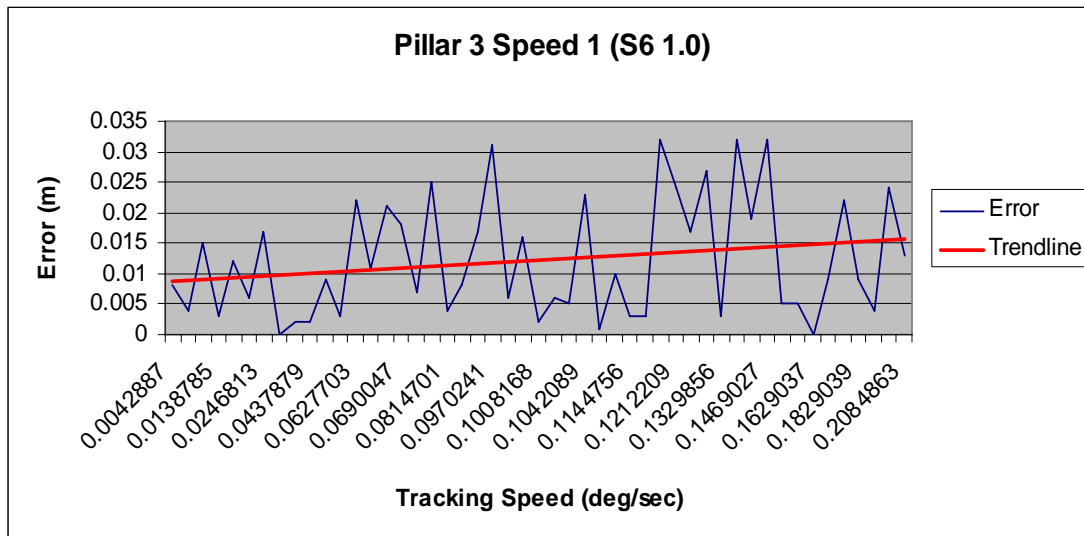


Figure D.13: Error vs Tracking Speed graph, Pillar 3 Speed 1.

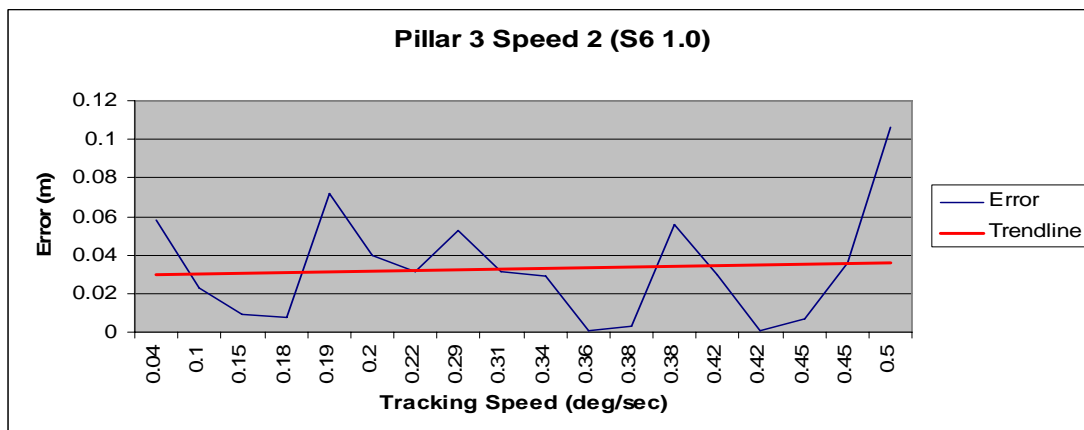


Figure D.14: Error vs Tracking Speed graph, Pillar 3 Speed 2.

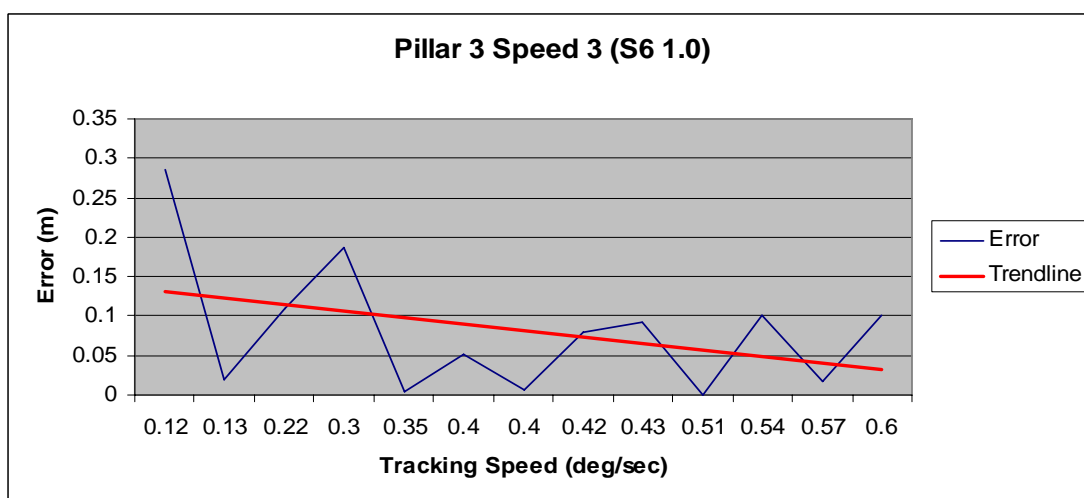


Figure D.15: Error vs Tracking Speed graph, Pillar 3 Speed 3.

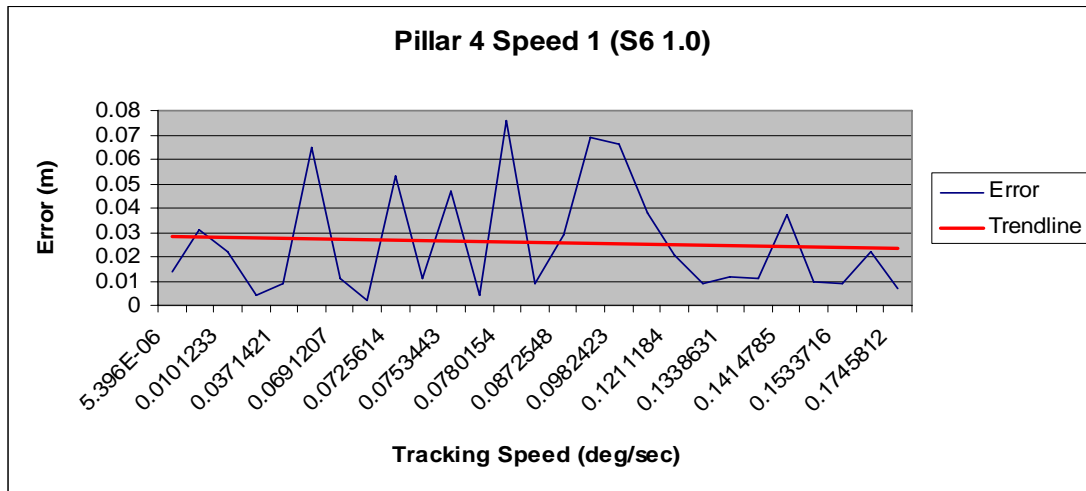


Figure D.16: Error vs Tracking Speed graph, Pillar 4 Speed 1.

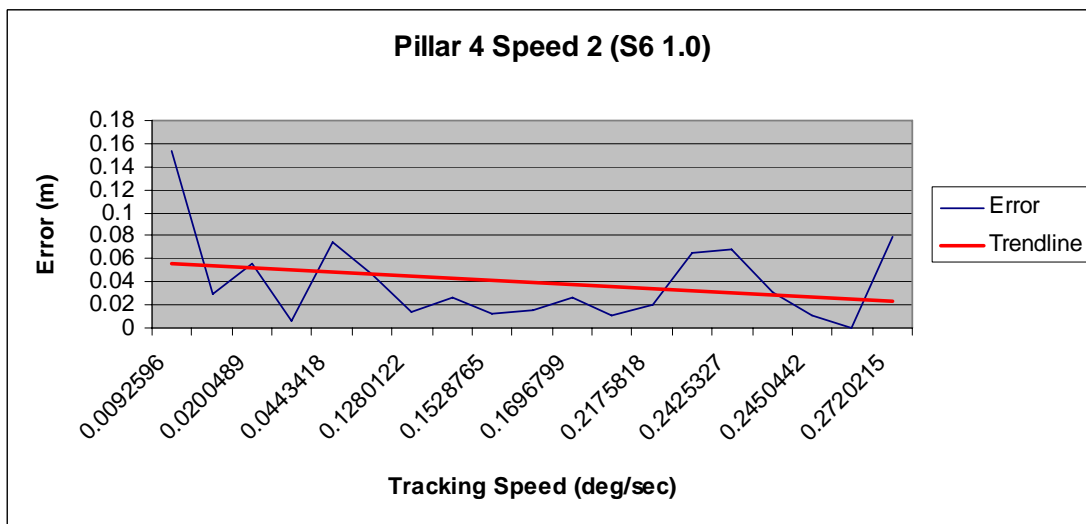


Figure D.17: Error vs Tracking Speed graph, Pillar 4 Speed 2.

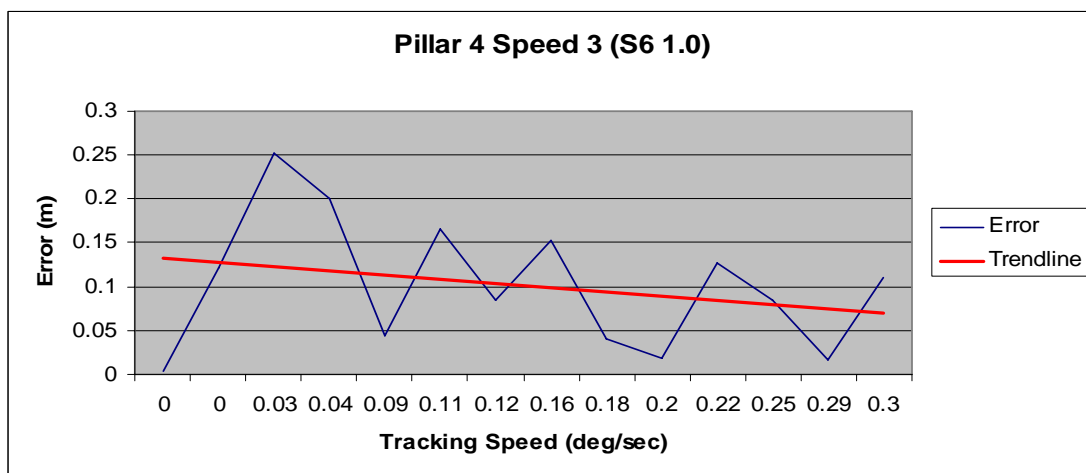


Figure D.18: Error vs Tracking Speed graph, Pillar 4 Speed 3.

Part C – Standard Deviation vs Tracking Speed

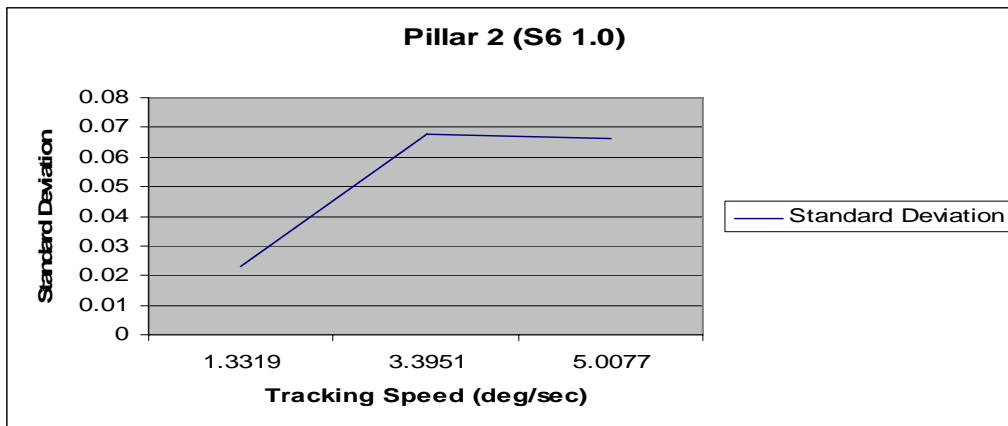


Figure D.19: Standard Deviation vs Tracking Speed graph, Pillar 2.

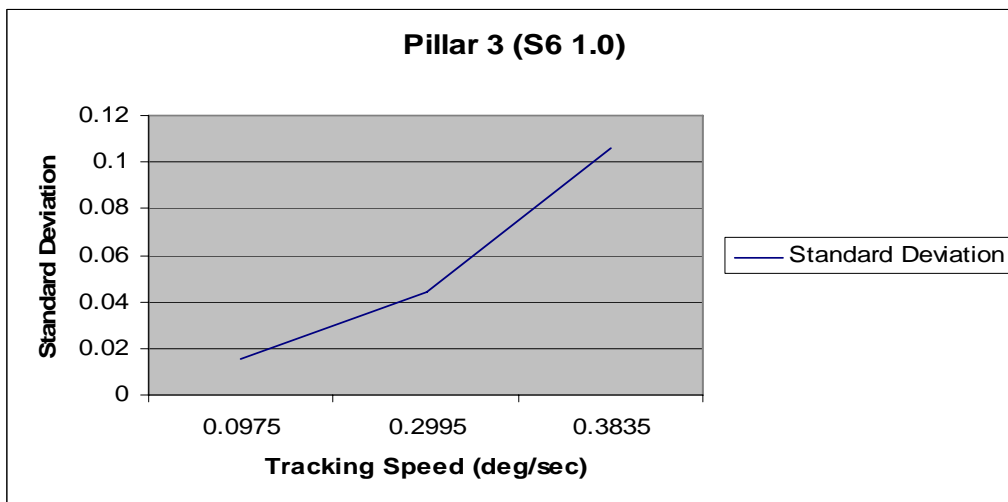


Figure D.20: Standard Deviation vs Tracking Speed graph, Pillar 3.

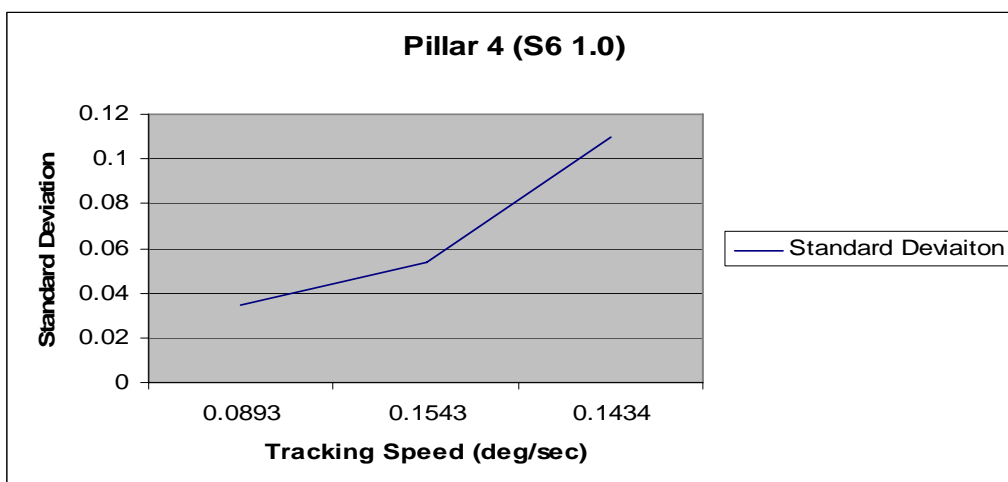
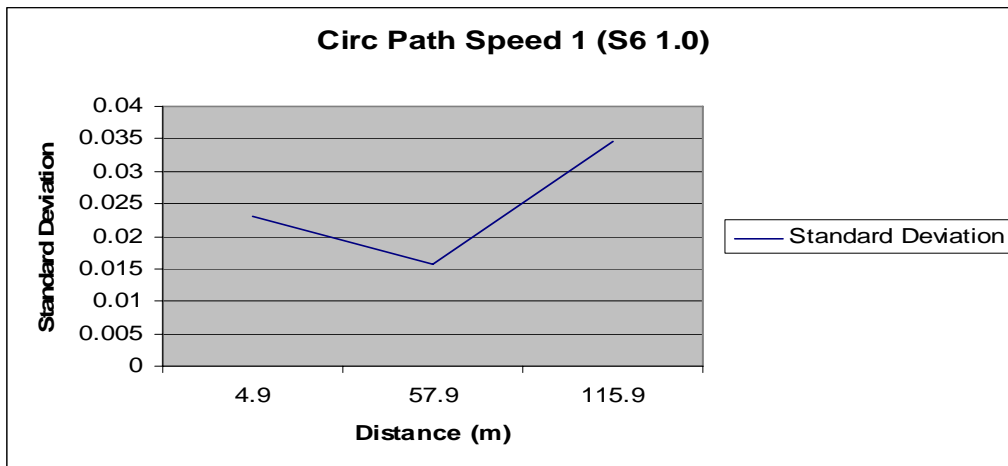
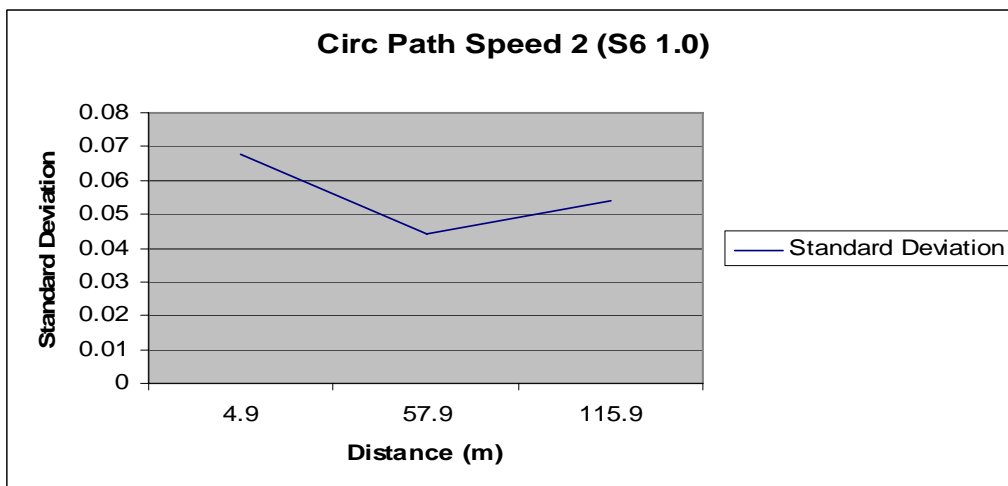


Figure D.21: Standard Deviation vs Tracking Speed graph, Pillar 4.

**Part D – Standard Deviation vs Distance**



**Figure D.22:** Standard Deviation vs Distance graph, Speed 1.



**Figure D.23:** Standard Deviation vs Distance graph, Speed 2.

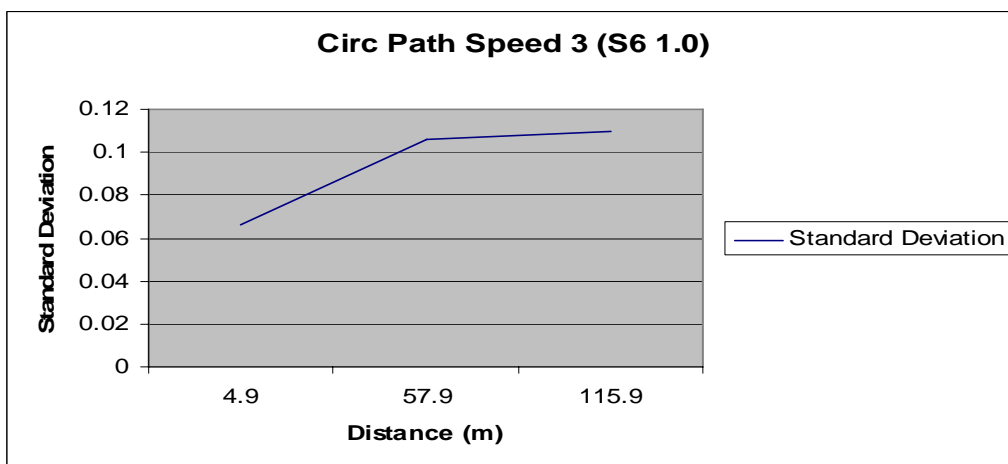


**Figure D.24:** Standard Deviation vs Distance graph, Speed 3.

## **Appendix E**

### Straight-line Test Results for Leica TPS1205 at a recording speed of 0.1 seconds

Part A – Error vs Point Number

Part B – Absolute Error vs Tracking Speed

Part C – Standard Deviation vs Tracking Speed

Part D – Standard Deviation vs Distance

**Part A – Error vs Point Number**

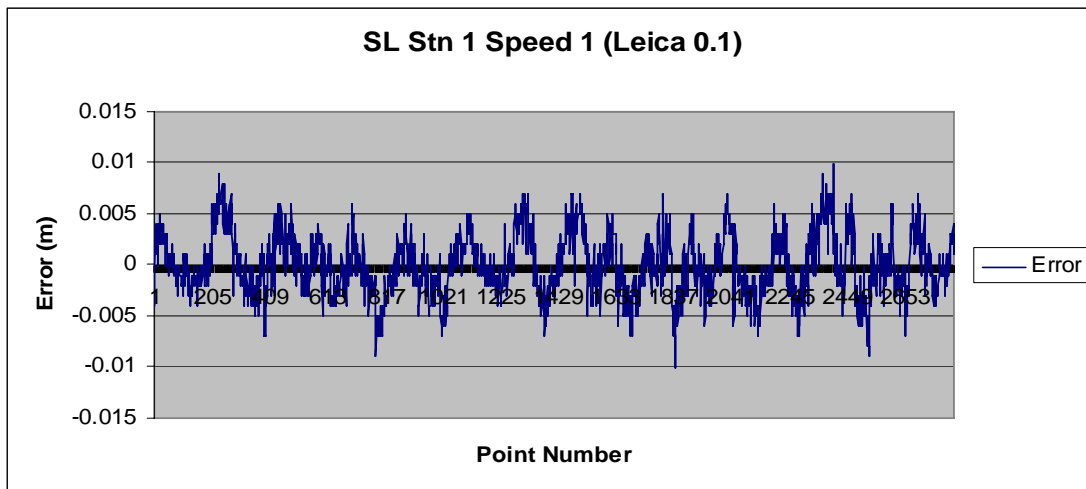


**Figure E.1:** Error vs Point Number graph, Stn 1 Speed 1.

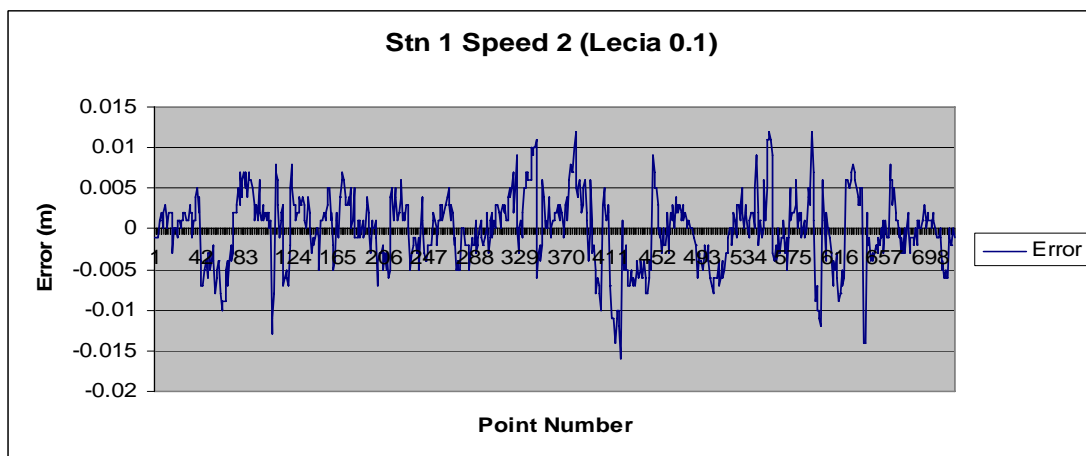


**Figure E.2:** Error vs Point Number graph, Stn 1 Speed 2.

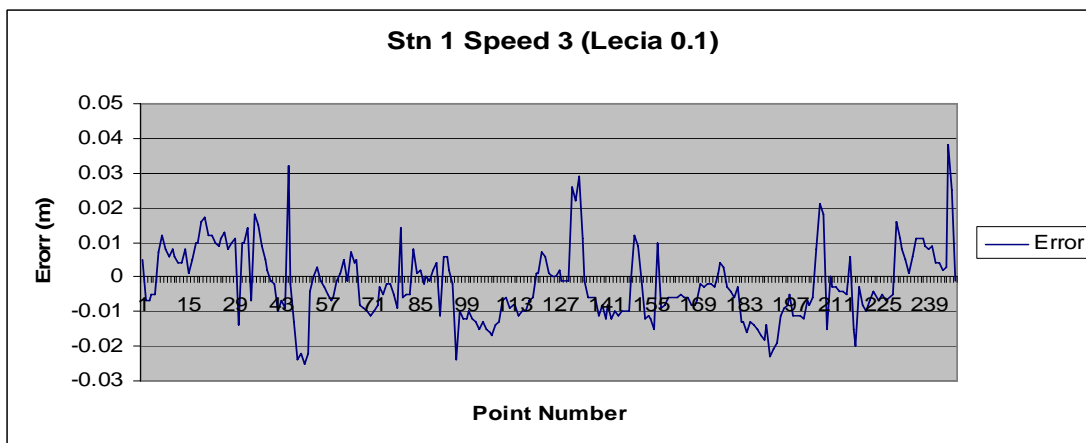


**Figure E.3:** Error vs Point Number graph, Stn 1 Speed 3.



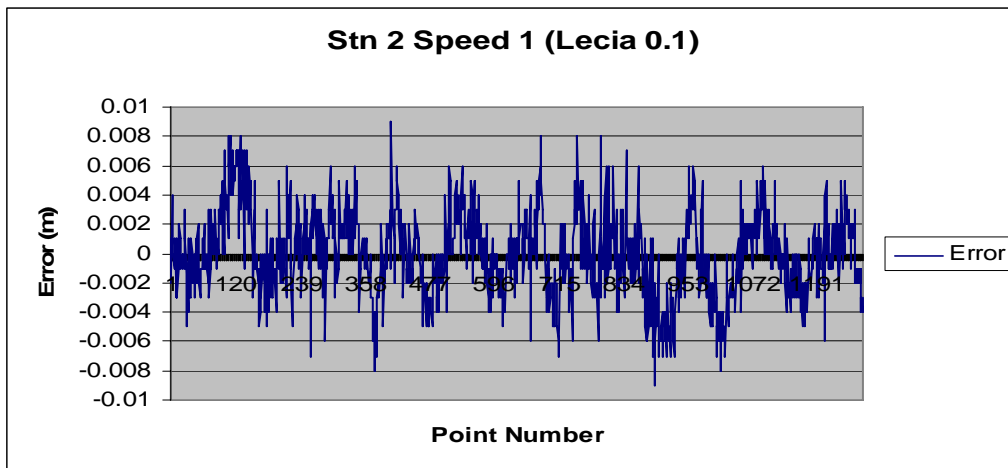


Figure E.4: Error vs Point Number graph, Stn 2 Speed 1.

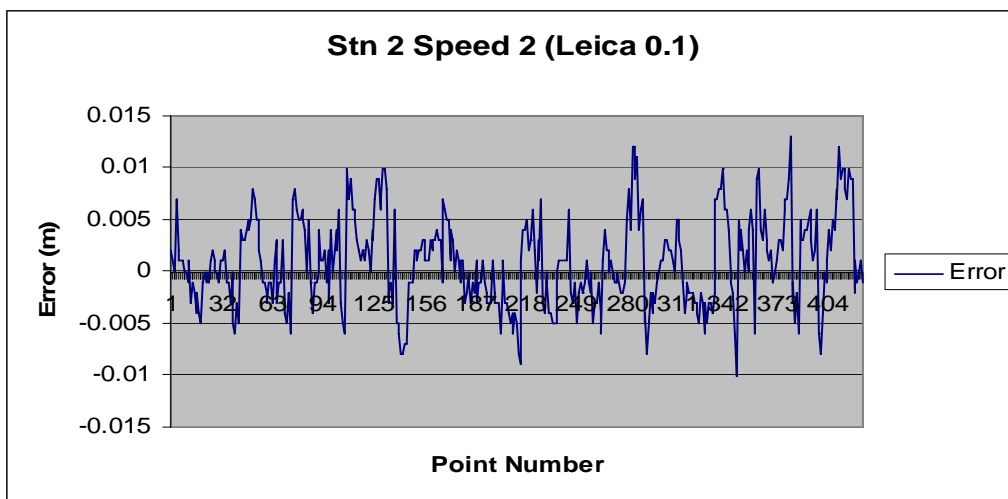


Figure E.5: Error vs Point Number graph, Stn 2 Speed 2.

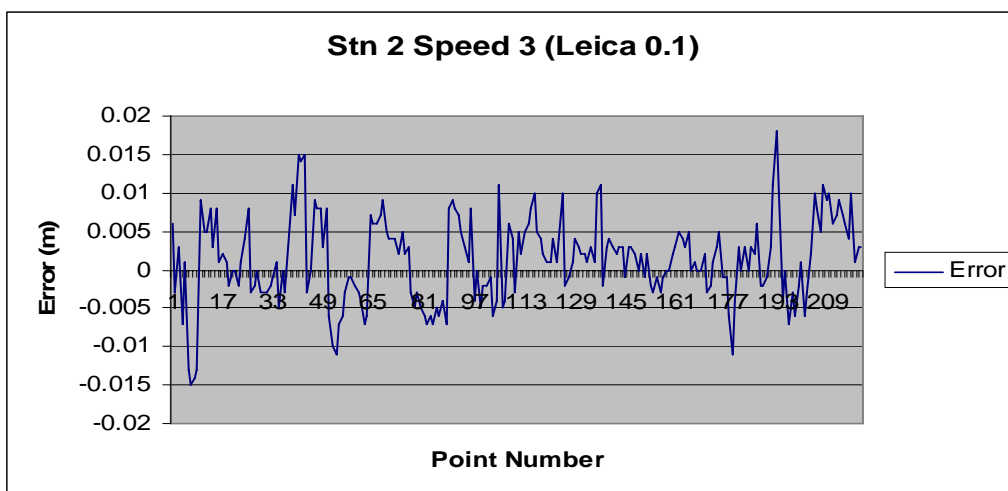
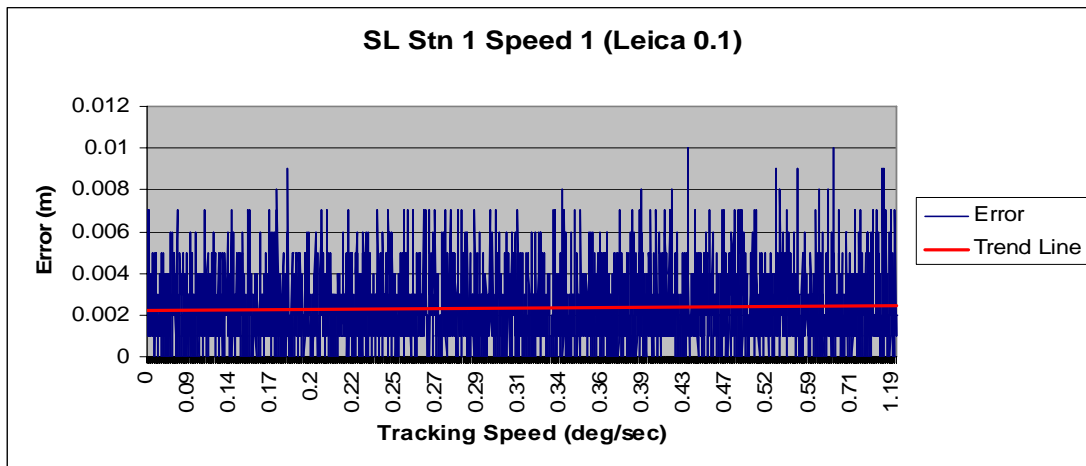
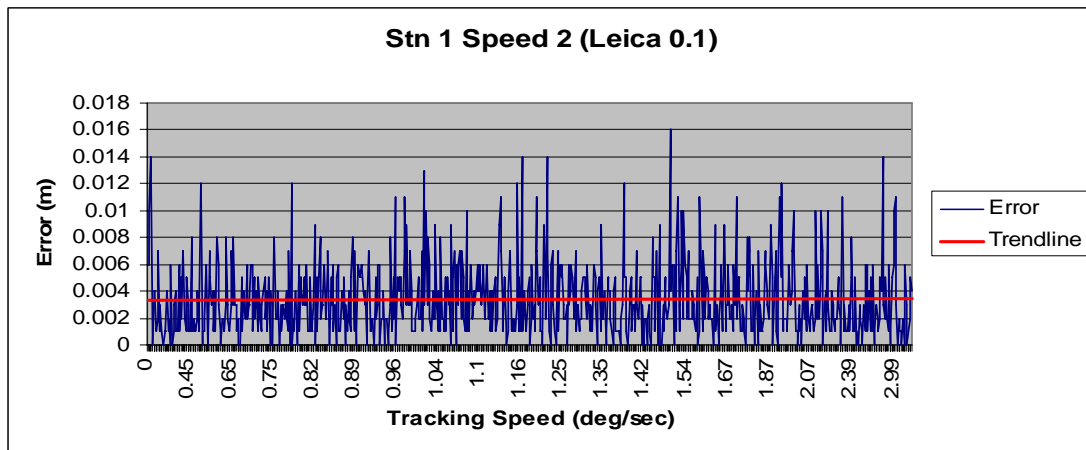


Figure E.6: Error vs Point Number graph, Stn 2 Speed 3.

**Part B – Absolute Error vs Tracking Speed**



**Figure E.7:** Error vs Tracking Speed graph, Stn 1 Speed 1.



**Figure E.8:** Error vs Tracking Speed graph, Stn 1 Speed 2.

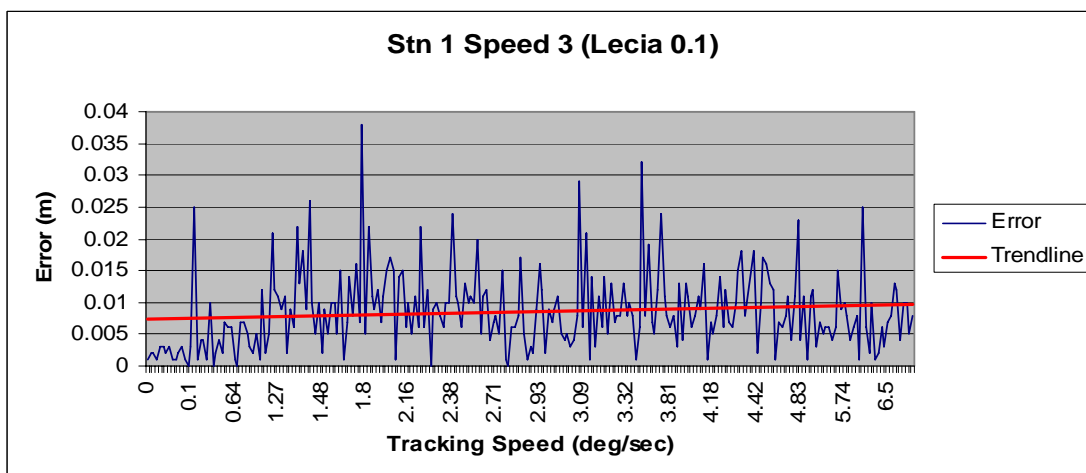


**Figure E.9:** Error vs Tracking Speed graph, Stn 1 Speed 3.

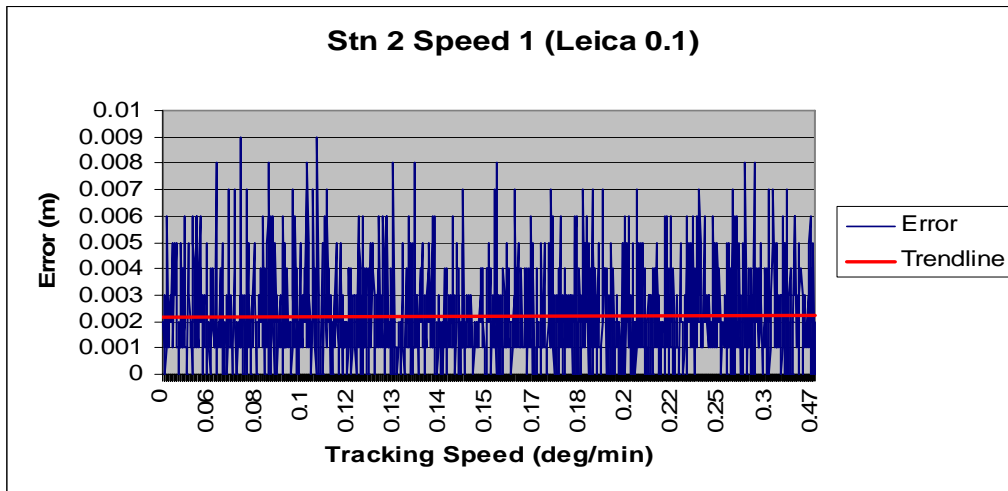


Figure E.10: Error vs Tracking Speed graph, Stn 2 Speed 1.

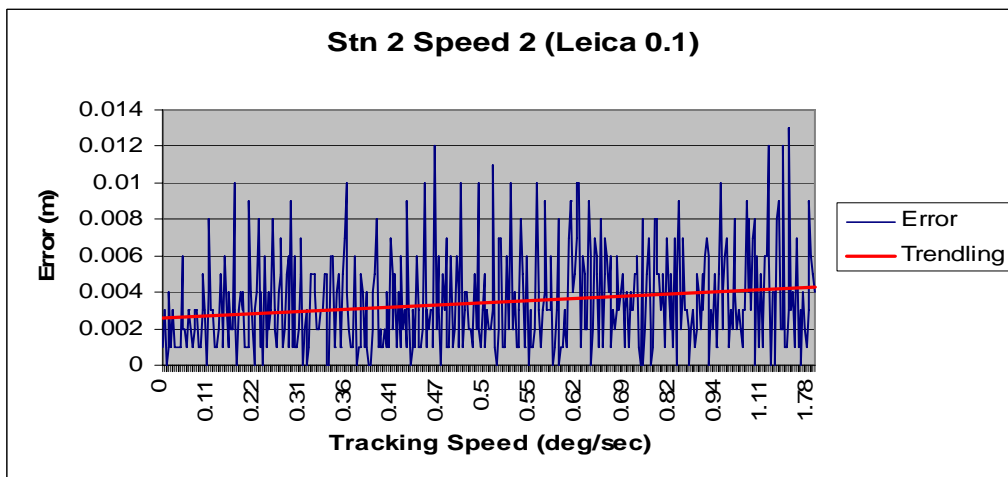


Figure E.11: Error vs Tracking Speed graph, Stn 2 Speed 2.

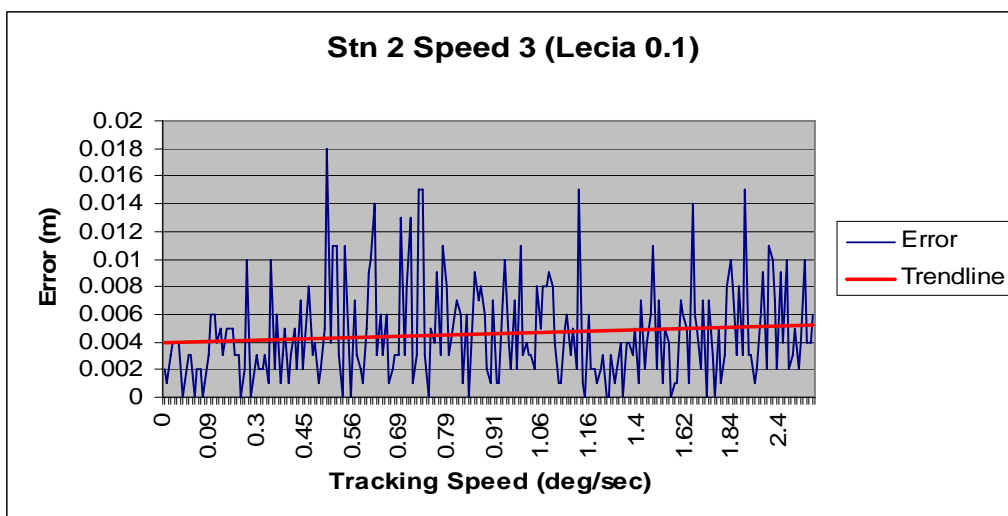
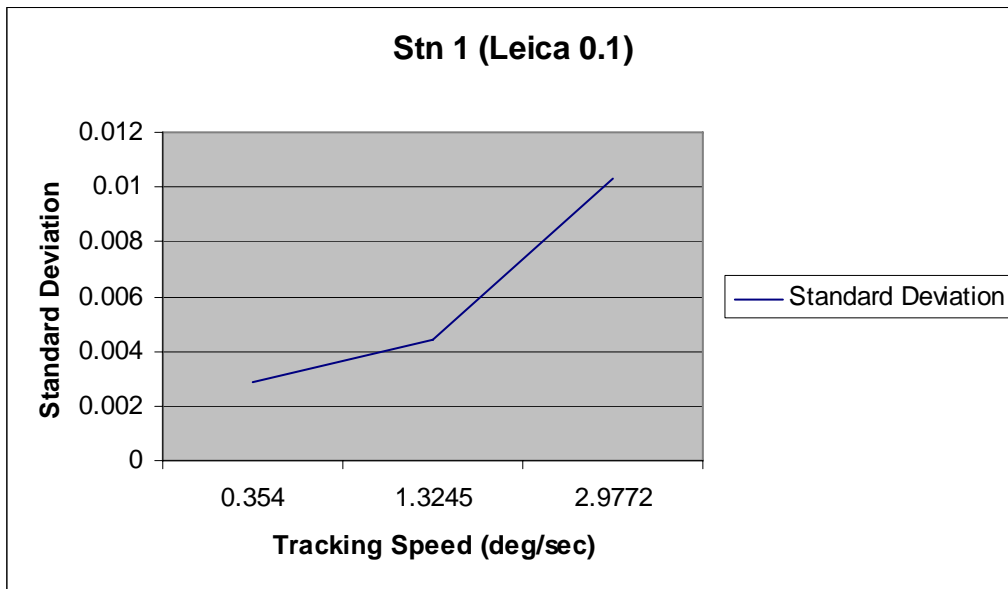
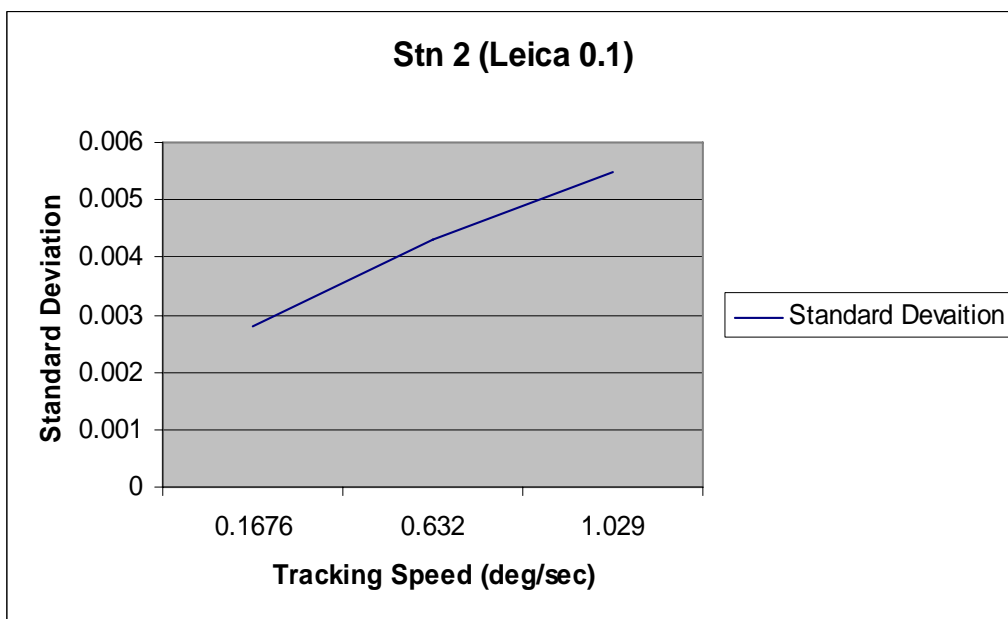


Figure E.12: Error vs Tracking Speed graph, Stn 2 Speed 3.

**Part C – Standard Deviation vs Tracking Speed**



**Figure E.13:** Standard Deviation vs Tracking Speed graph, Stn 1.



**Figure E.14:** Standard Deviation vs Tracking Speed graph, Pillar 3.

**Part D – Standard Deviation vs Distance**

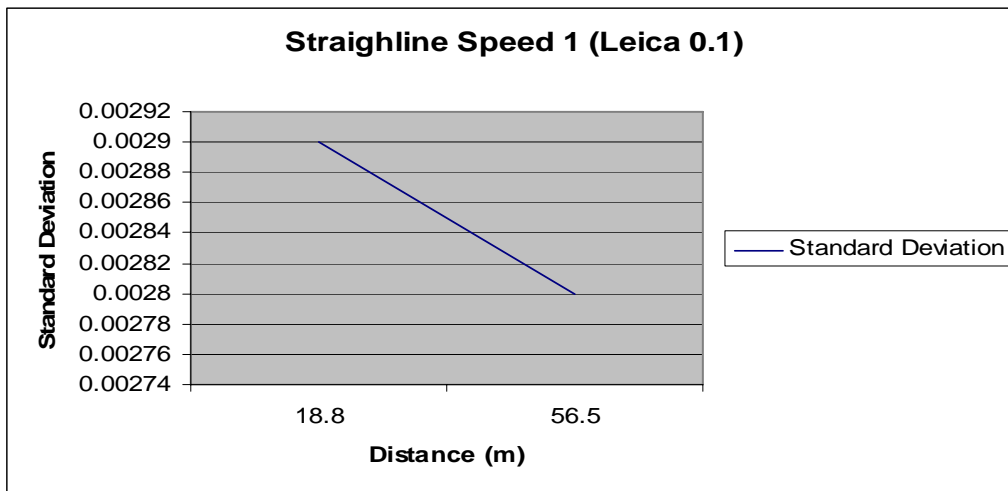


**Figure E.15:** Standard Deviation vs Distance graph, Speed 1.

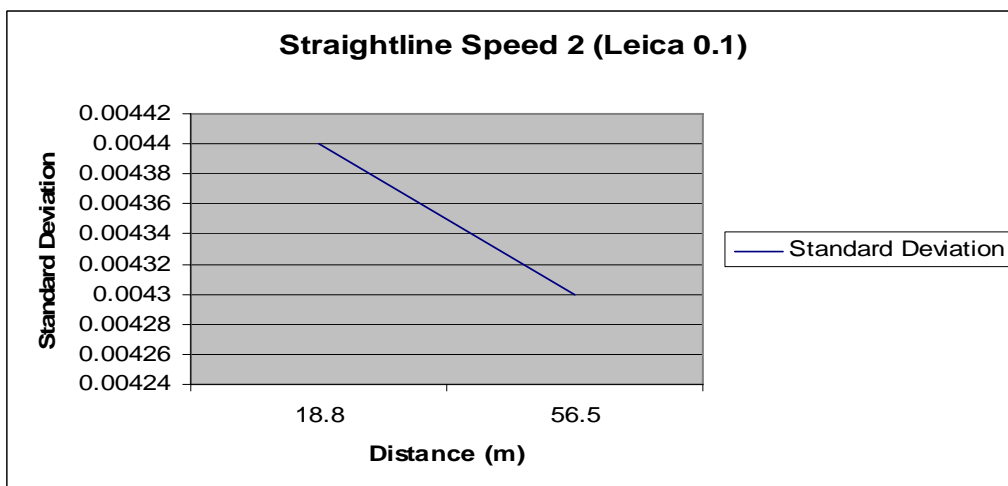


**Figure E.16:** Standard Deviation vs Distance graph, Speed 2.

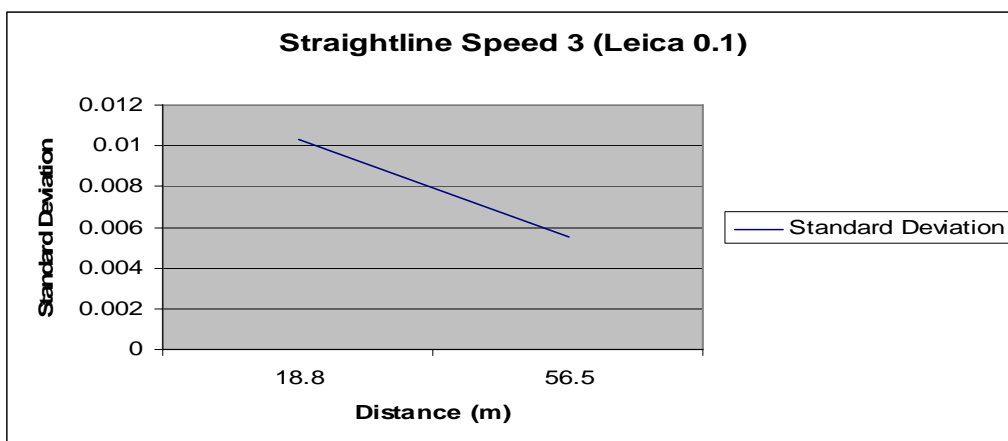


**Figure E.17:** Standard Deviation vs Distance graph, Speed 3.

## **Appendix F**

### Straight-line Test Results for Leica TPS1205 at a recording speed of 0.5 seconds

Part A – Error vs Point Number

Part B – Absolute Error vs Tracking Speed

Part C – Standard Deviation vs Tracking Speed

Part D – Standard Deviation vs Distance

**Part A – Error vs Point Number**

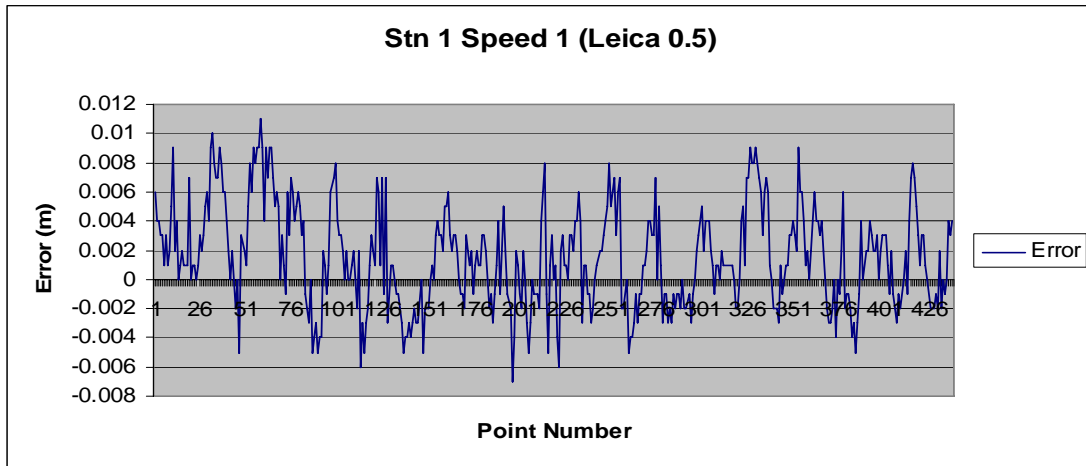


**Figure F.1:** Error vs Point Number graph, Stn 1 Speed 1.

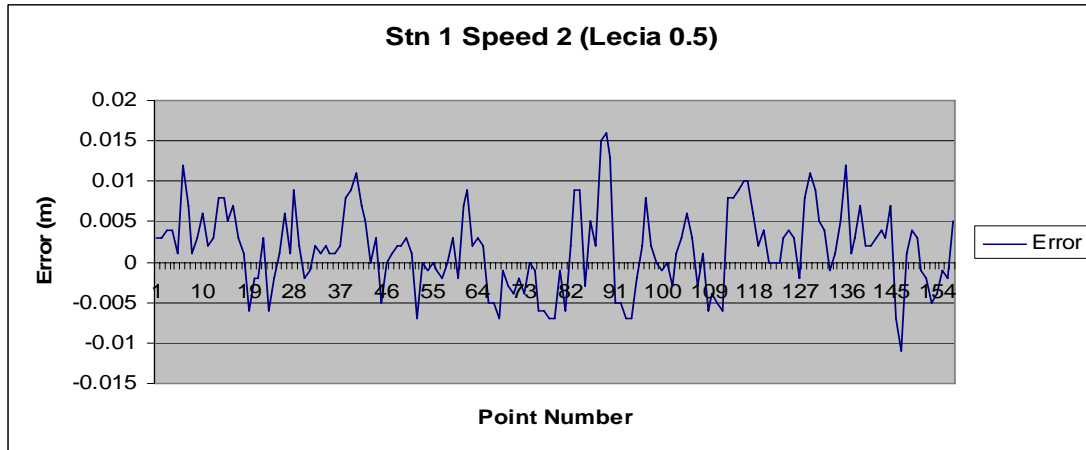


**Figure F.2:** Error vs Point Number graph, Stn 1 Speed 2.

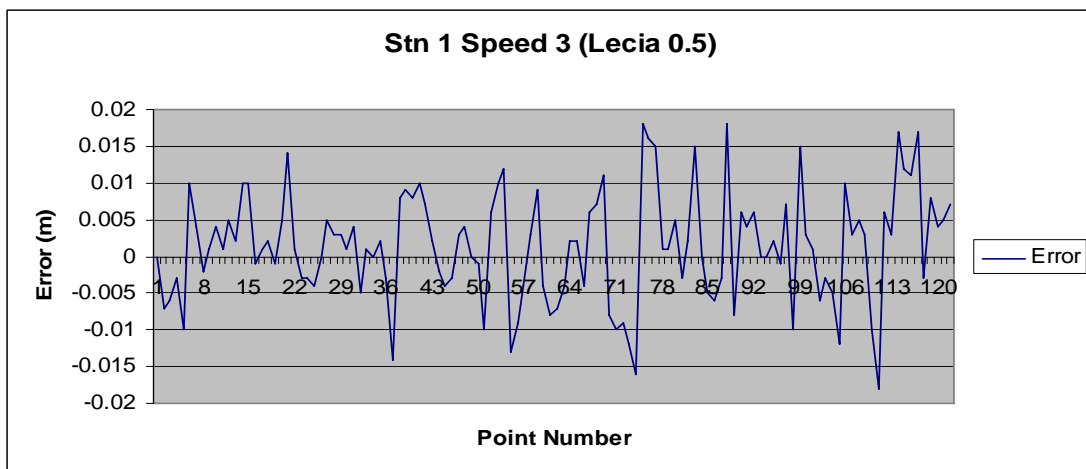


**Figure F.3:** Error vs Point Number graph, Stn 1 Speed 3.

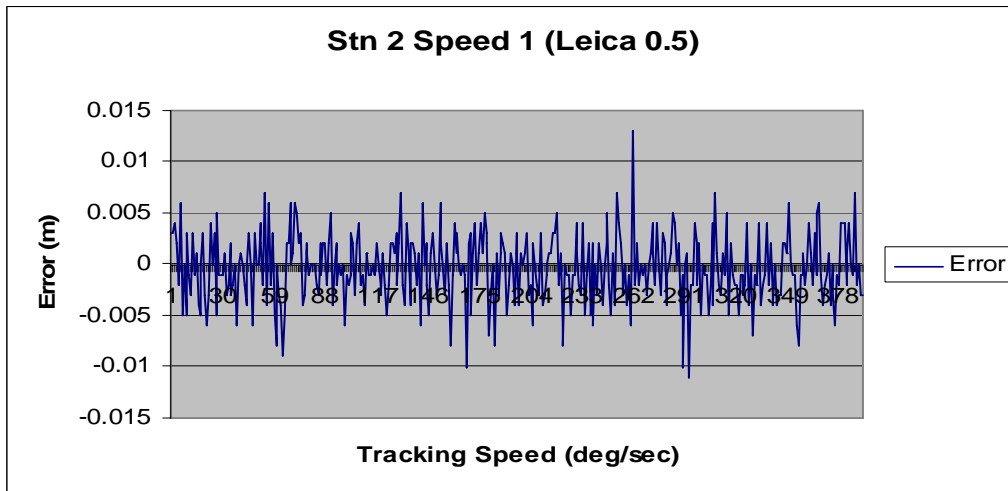


**Figure F.4:** Error vs Point Number graph, Stn 2 Speed 1.

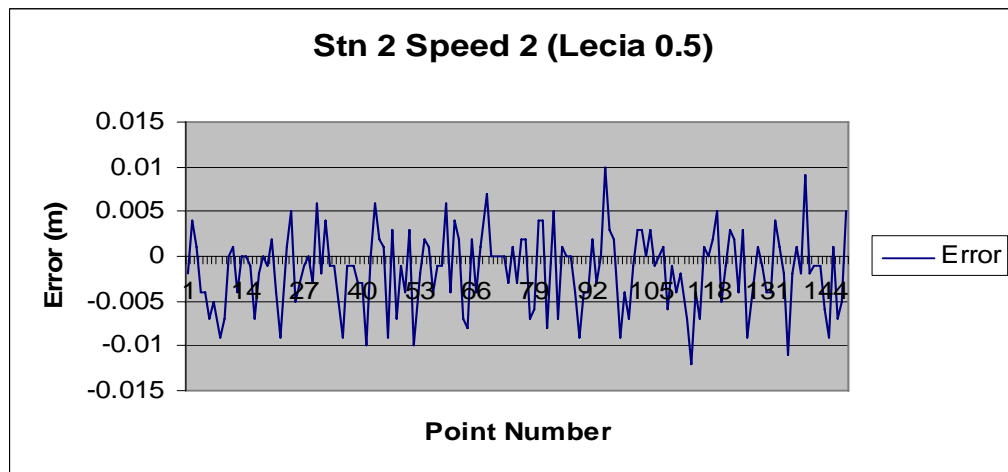


**Figure F.5:** Error vs Point Number graph, Stn 2 Speed 2.

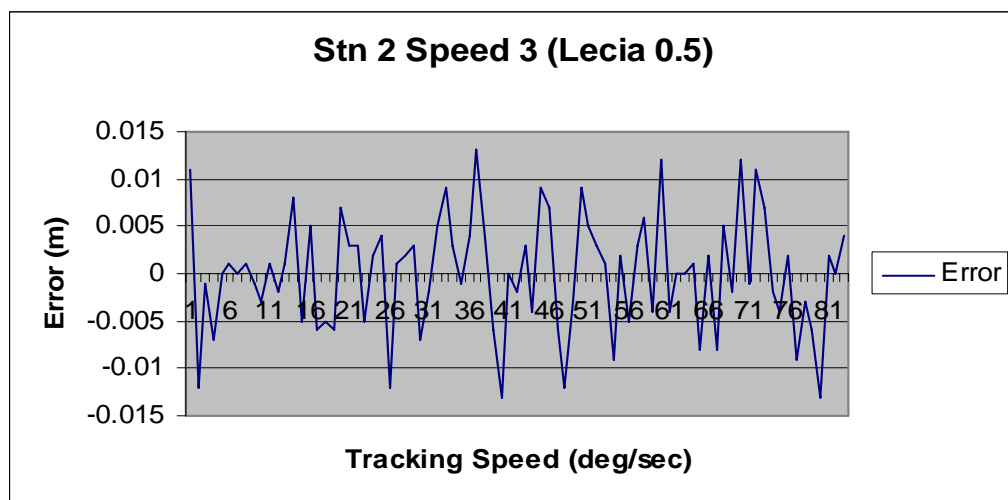


**Figure F.6:** Error vs Point Number graph, Stn 2 Speed 3.



**Part B – Absolute Error vs Tracking Speed**

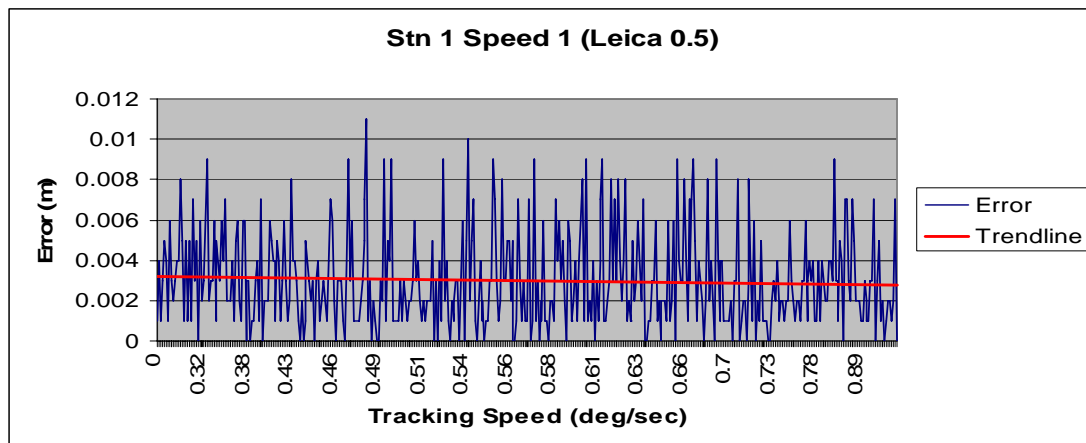


**Figure F.7:** Error vs Tracking Speed graph, Stn 1 Speed 1.

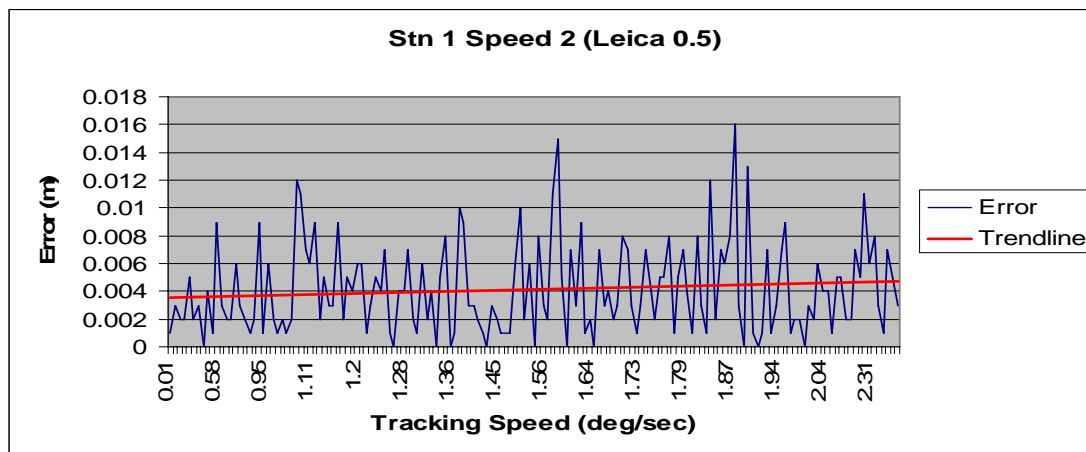


**Figure F.8:** Error vs Tracking Speed graph, Stn 1 Speed 2.

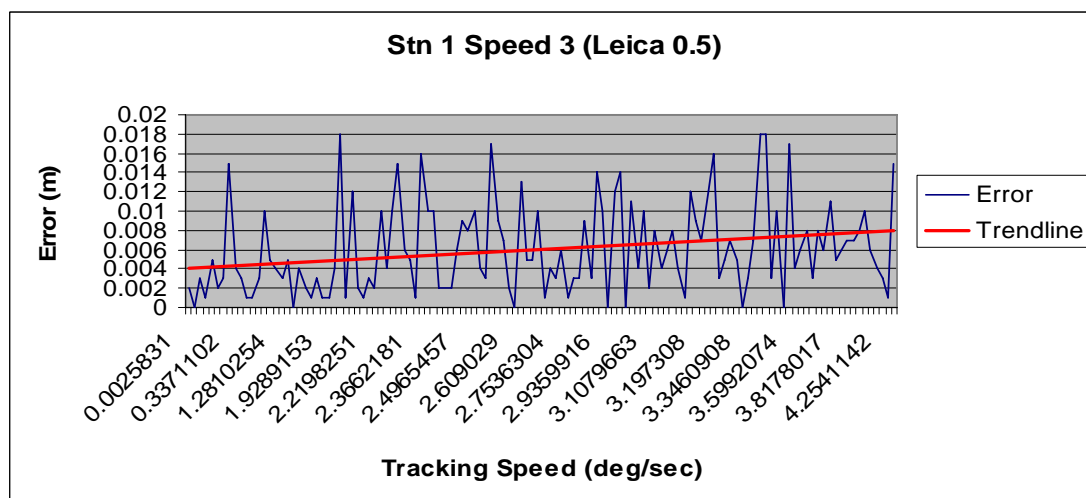


**Figure F.9:** Error vs Tracking Speed graph, Stn 1 Speed 3.

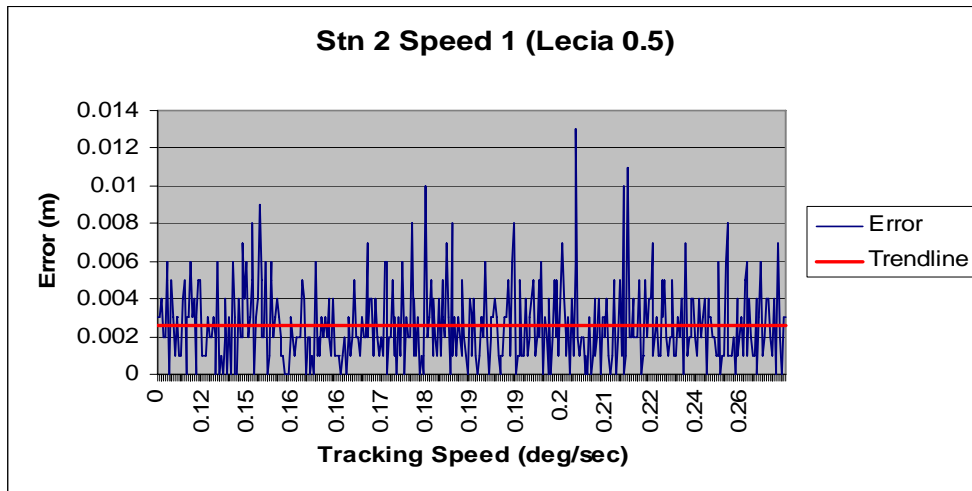


Figure F.10: Error vs Tracking Speed graph, Stn 2 Speed 1.

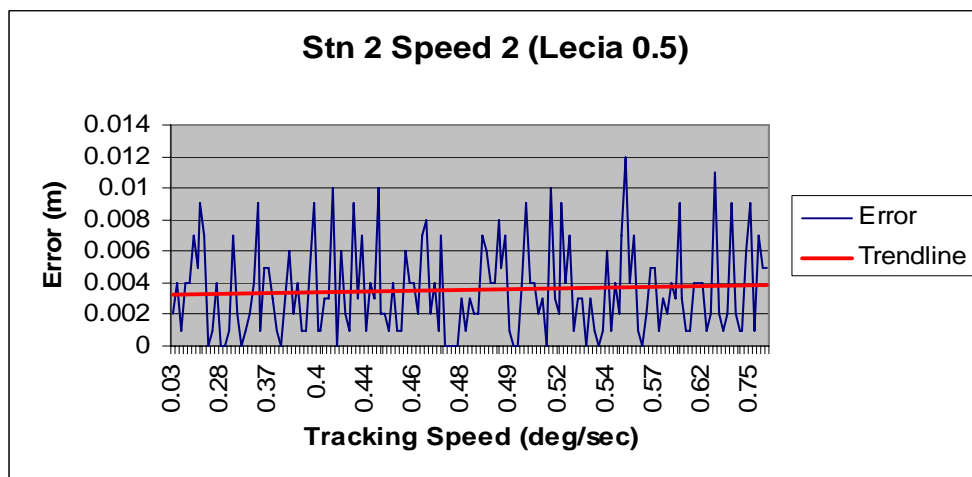


Figure F.11: Error vs Tracking Speed graph, Stn 2 Speed 2.

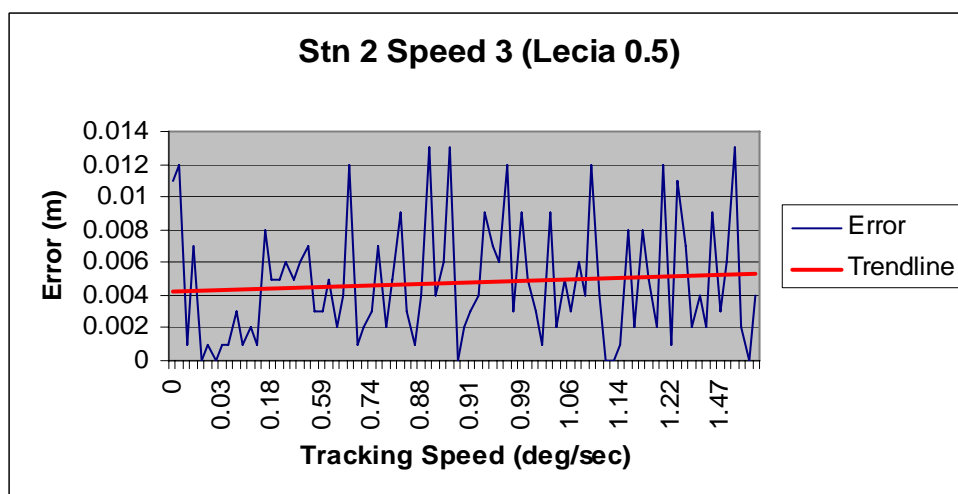
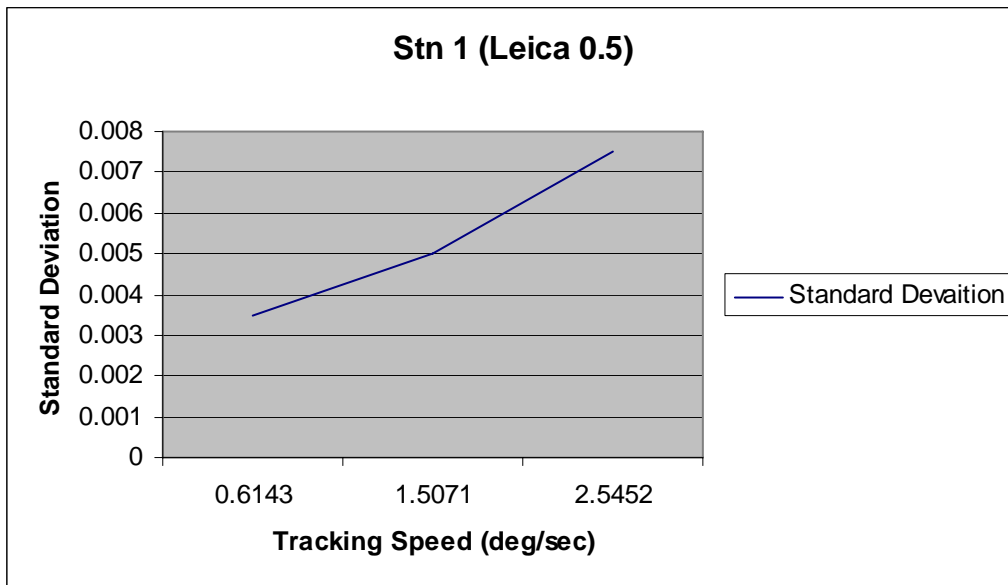
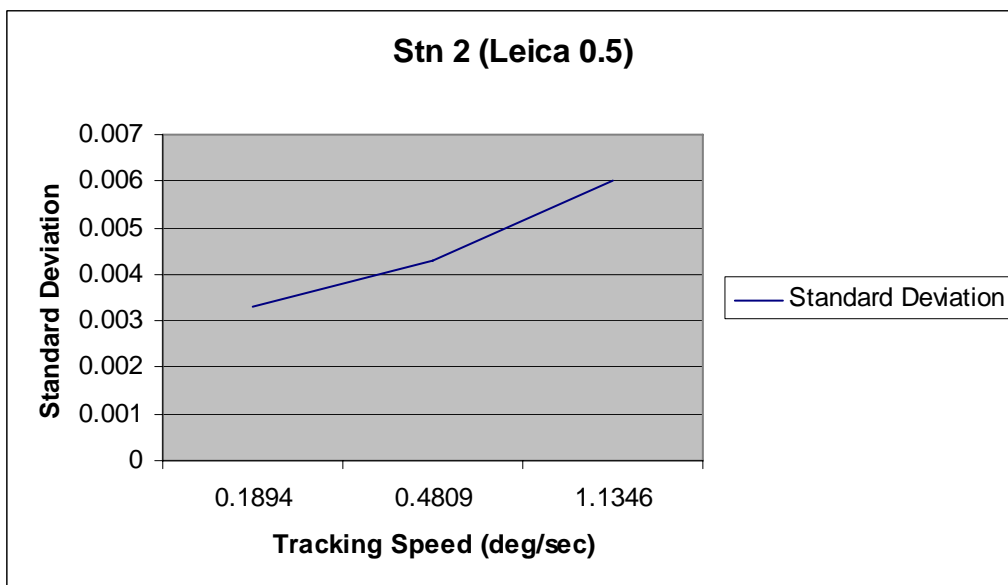


Figure F.12: Error vs Tracking Speed graph, Stn 2 Speed 3.

**Part C – Standard Deviation vs Tracking Speed**



**Figure F.13:** Standard Deviation vs Tracking Speed graph, Stn 1.



**Figure F.14:** Standard Deviation vs Tracking Speed graph, Pillar 3.

**Part D – Standard Deviation vs Distance**

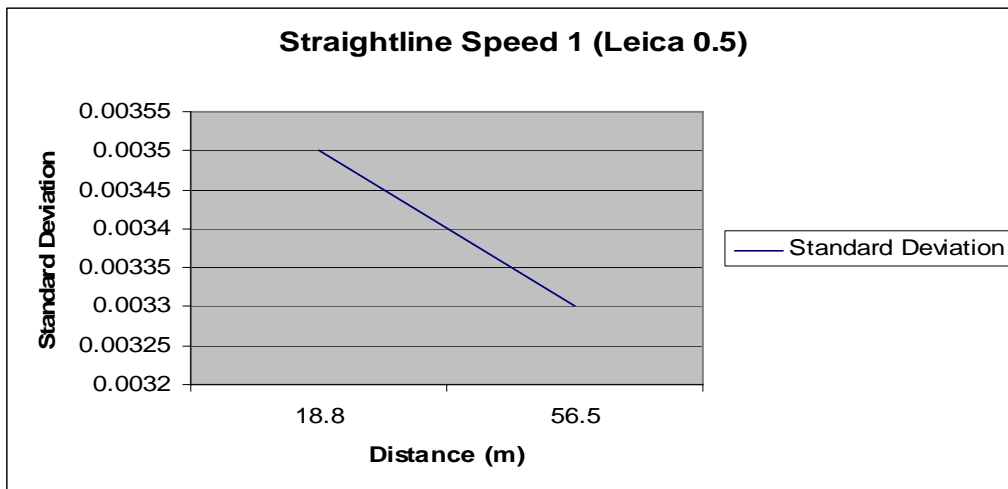


**Figure F.15:** Standard Deviation vs Distance graph, Speed 1.

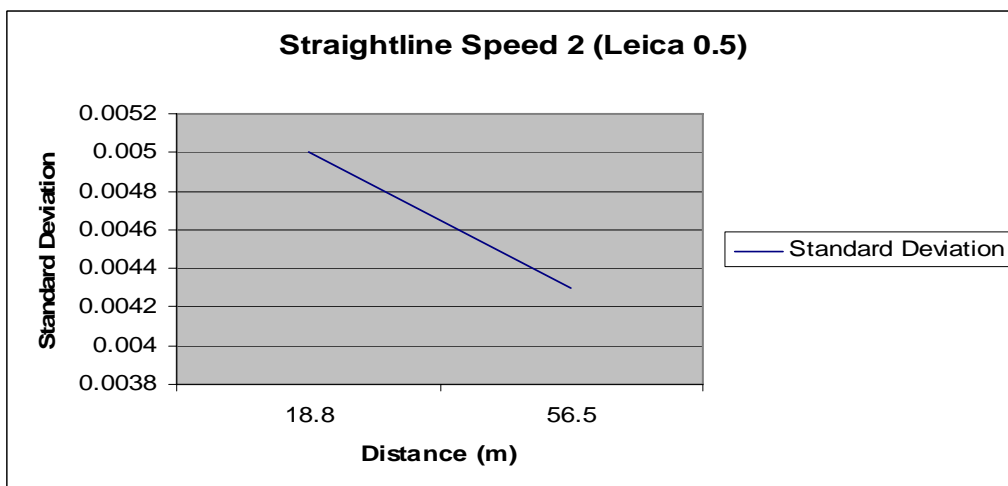


**Figure F.16:** Standard Deviation vs Distance graph, Speed 2.

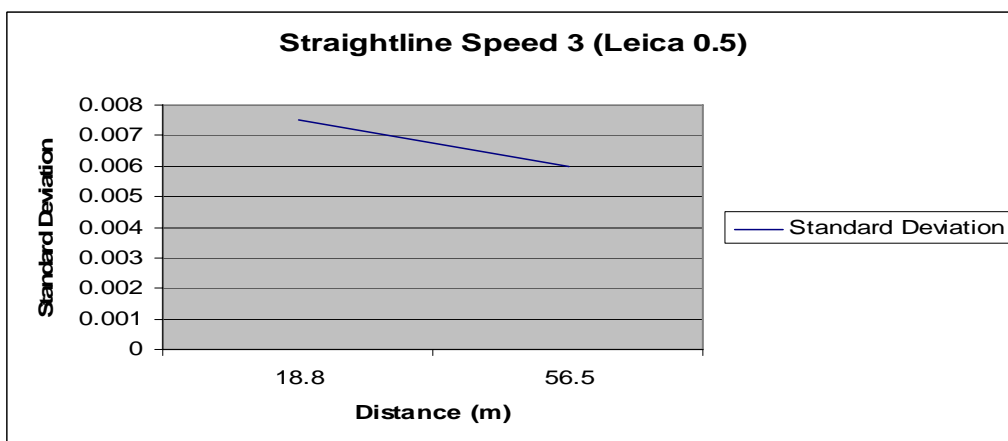


**Figure F.17:** Standard Deviation vs Distance graph, Speed 3.

## **Appendix G**

Straight-line Test Results for Trimble S6 at a recording speed of 1.0 seconds

Part A – Error vs Point Number

Part B – Absolute Error vs Tracking Speed

Part C – Standard Deviation vs Tracking Speed

Part D – Standard Deviation vs Distance

**Part A – Error vs Point Number**

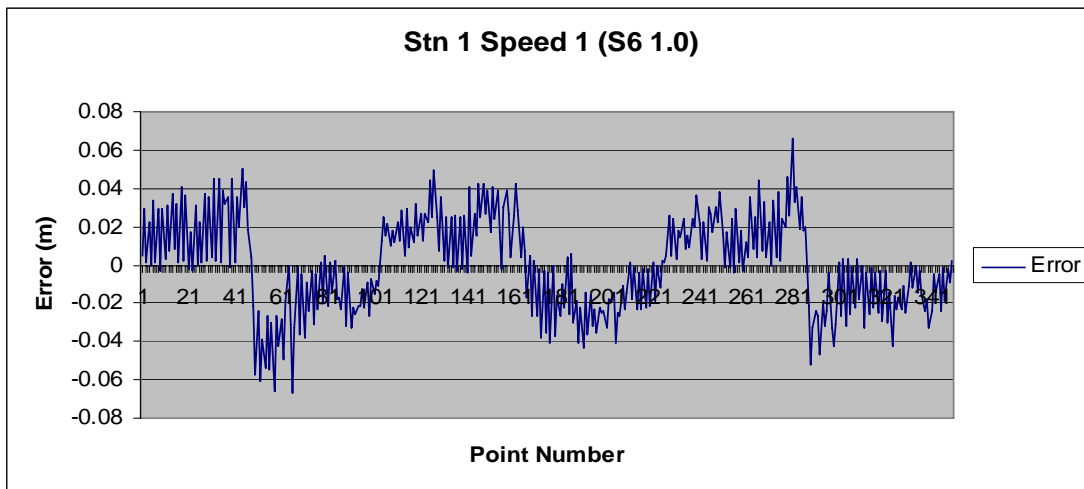


**Figure G.1:** Error vs Point Number graph, Stn 1 Speed 1.

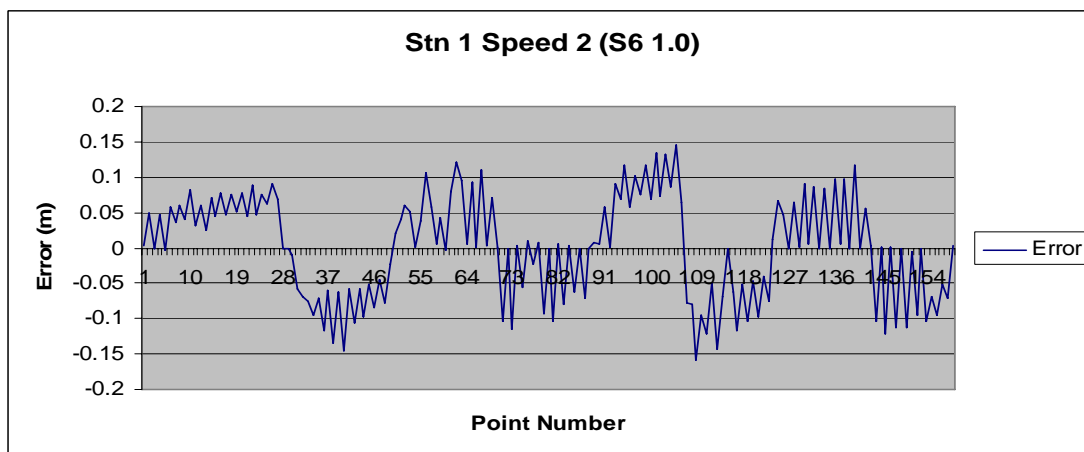


**Figure G.2:** Error vs Point Number graph, Stn 1 Speed 2.

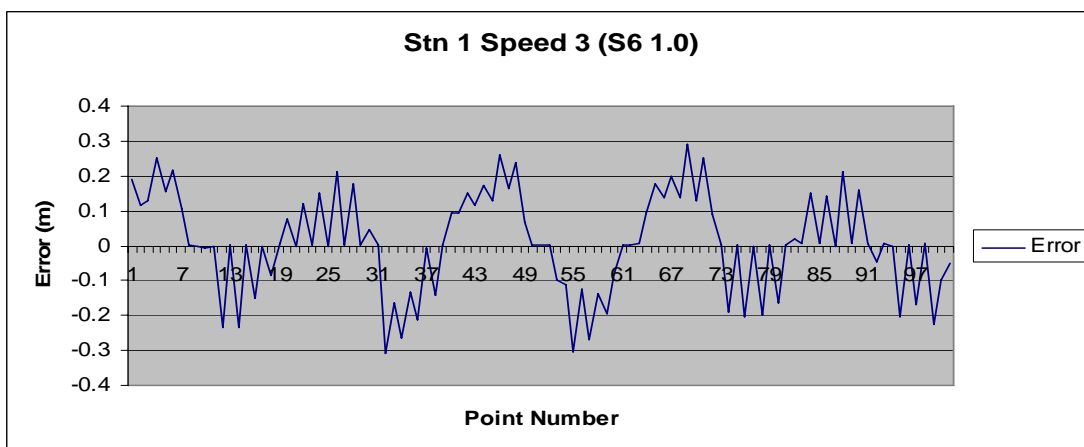


**Figure G.3:** Error vs Point Number graph, Stn 1 Speed 3.

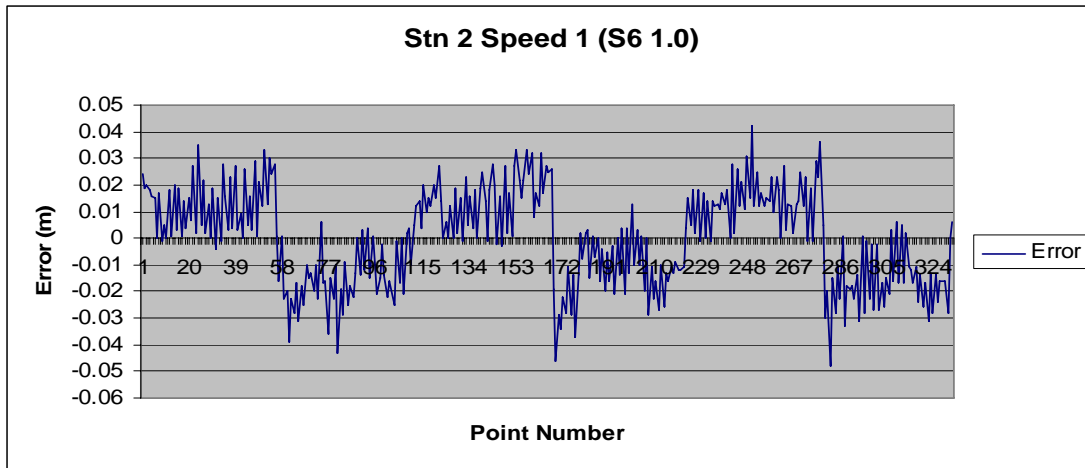


**Figure G.4:** Error vs Point Number graph, Stn 2 Speed 1.

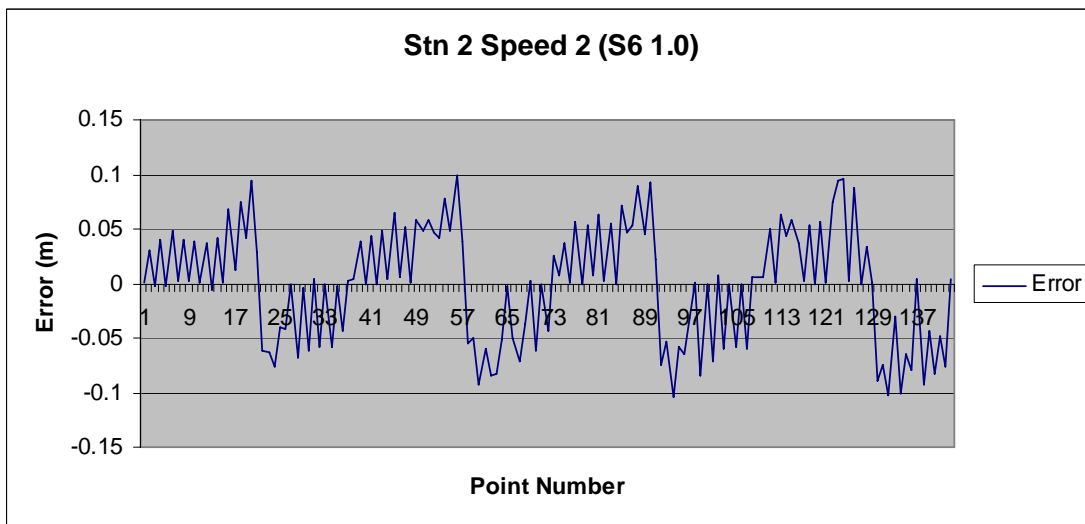


**Figure G.5:** Error vs Point Number graph, Stn 2 Speed 2.

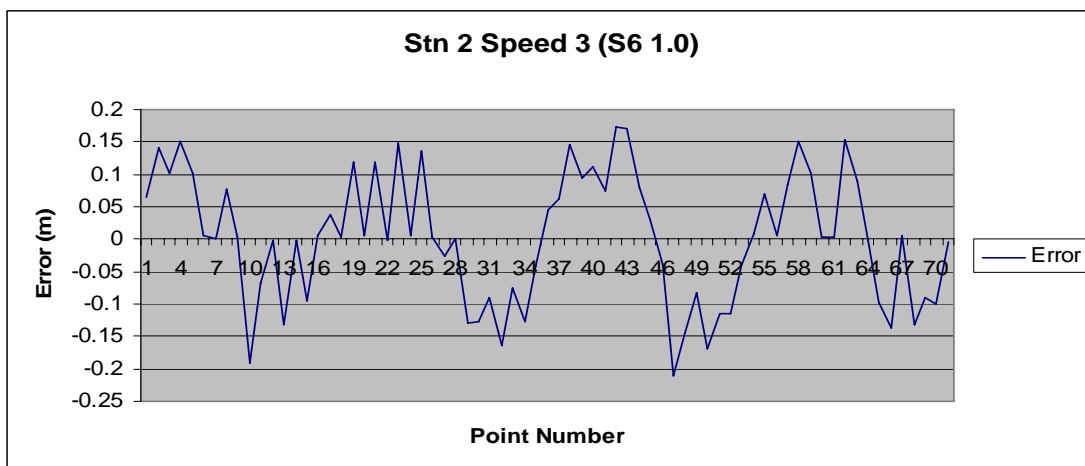


**Figure G.6:** Error vs Point Number graph, Stn 2 Speed 3.

## Part B – Absolute Error vs Tracking Speed

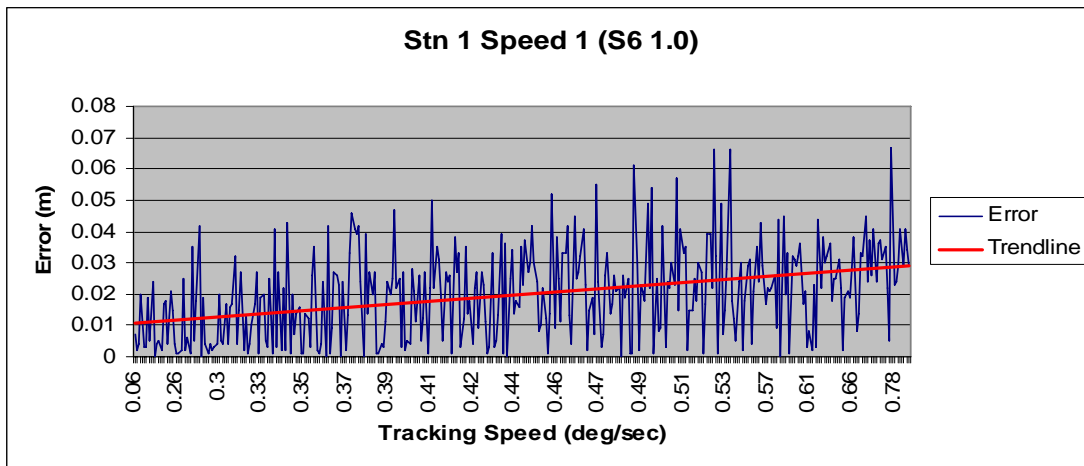


Figure G.7: Error vs Tracking Speed graph, Stn 1 Speed 1.

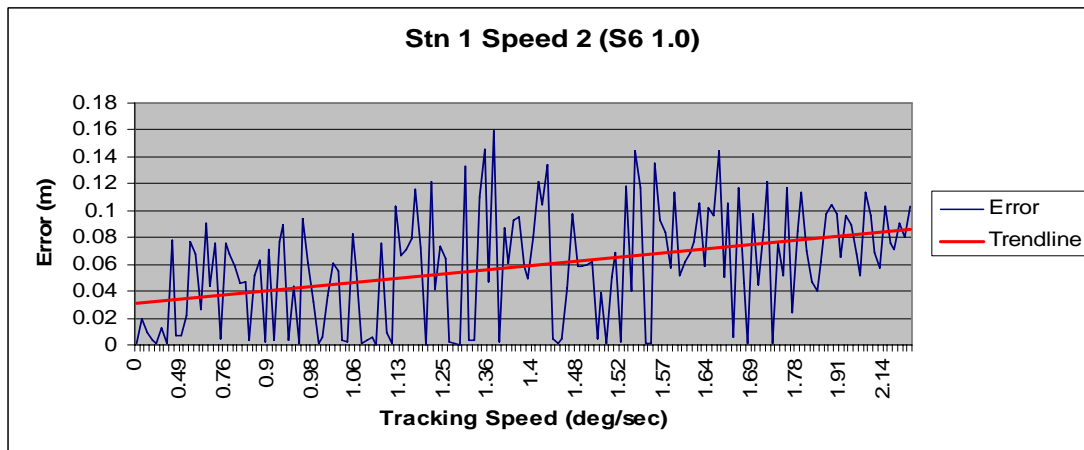


Figure G.8: Error vs Tracking Speed graph, Stn 1 Speed 2.

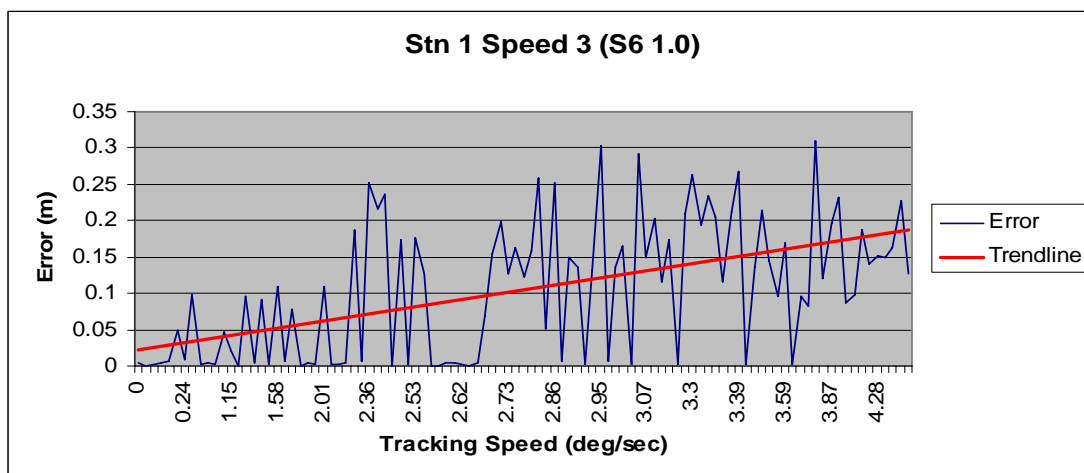
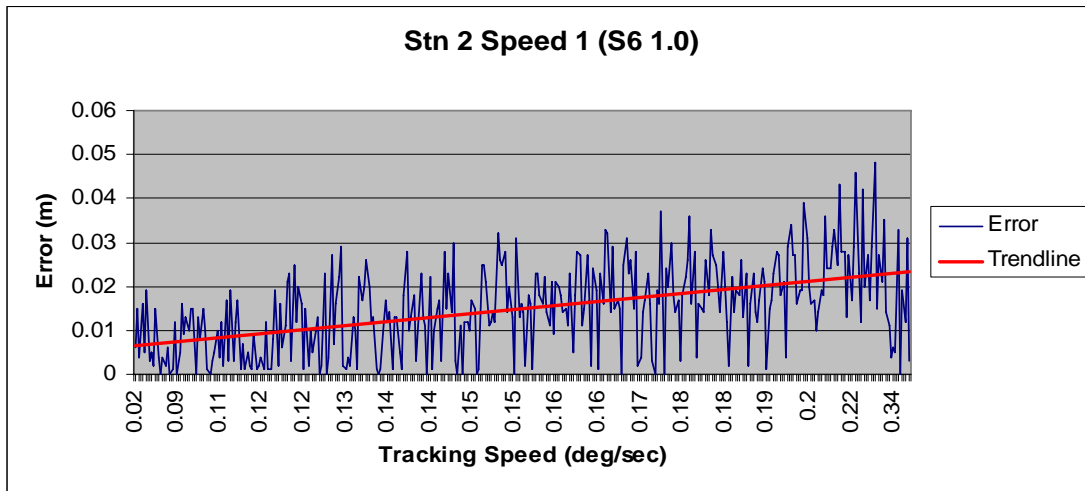
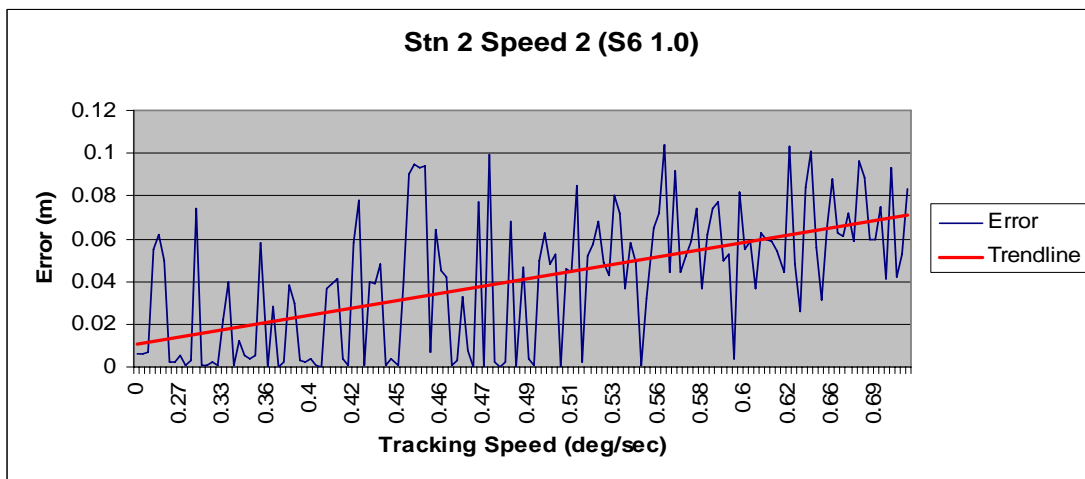


Figure G.9: Error vs Tracking Speed graph, Stn 1 Speed 3.





**Figure G.10:** Error vs Tracking Speed graph, Stn 2 Speed 1.



**Figure G.11:** Error vs Tracking Speed graph, Stn 2 Speed 2.

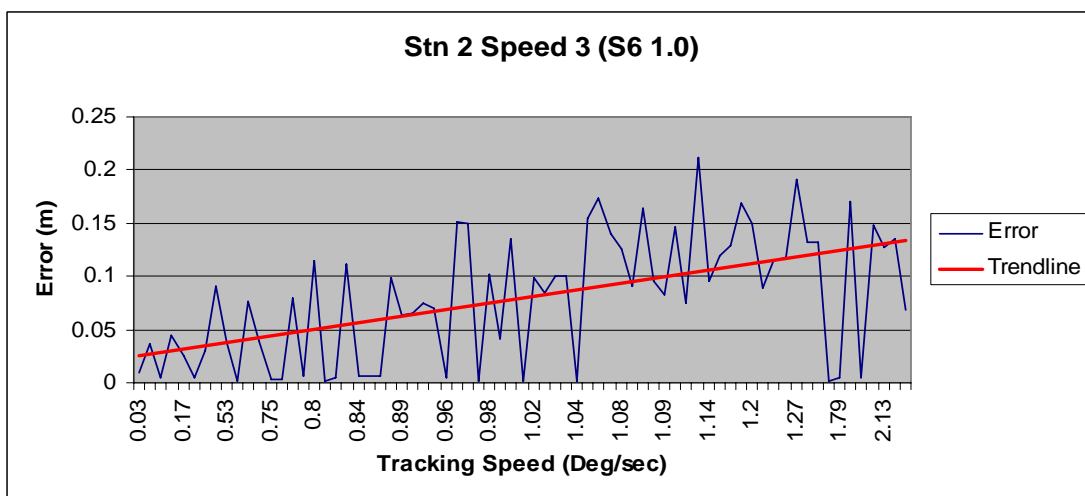


**Figure G.12:** Error vs Tracking Speed graph, Stn 2 Speed 3.

### Part C – Standard Deviation vs Tracking Speed

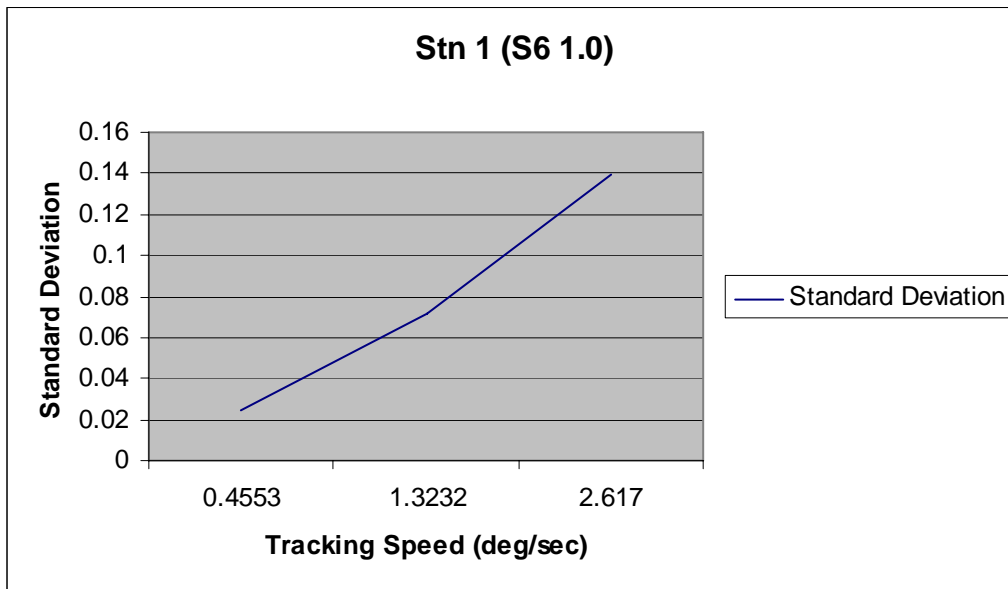


Figure G.13: Standard Deviation vs Tracking Speed graph, Stn 1.

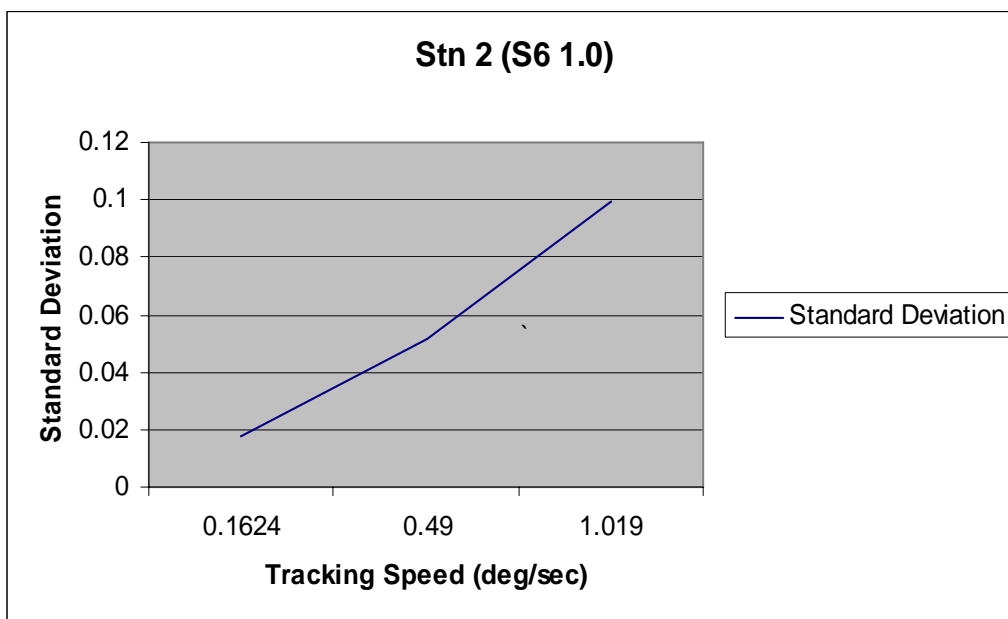


Figure G.14: Standard Deviation vs Tracking Speed graph, Pillar 3.

## Part D – Standard Deviation vs Distance

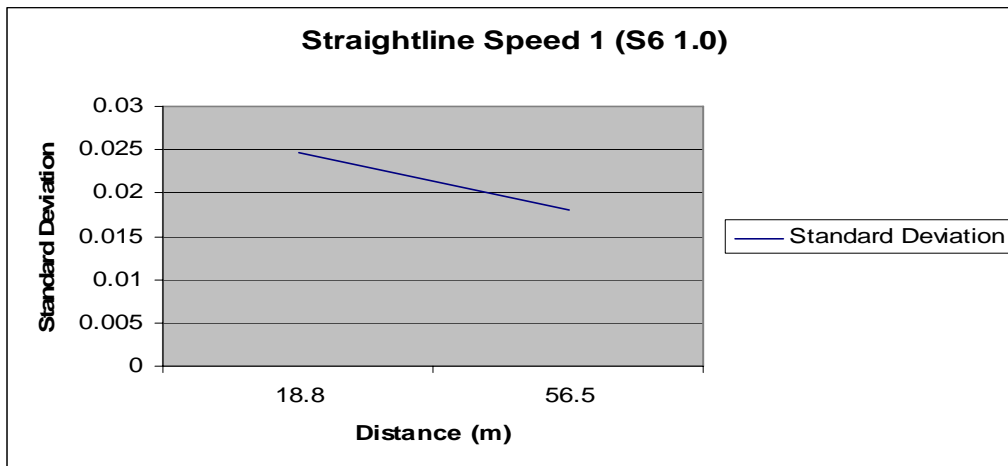


Figure G.15: Standard Deviation vs Distance graph, Speed 1.

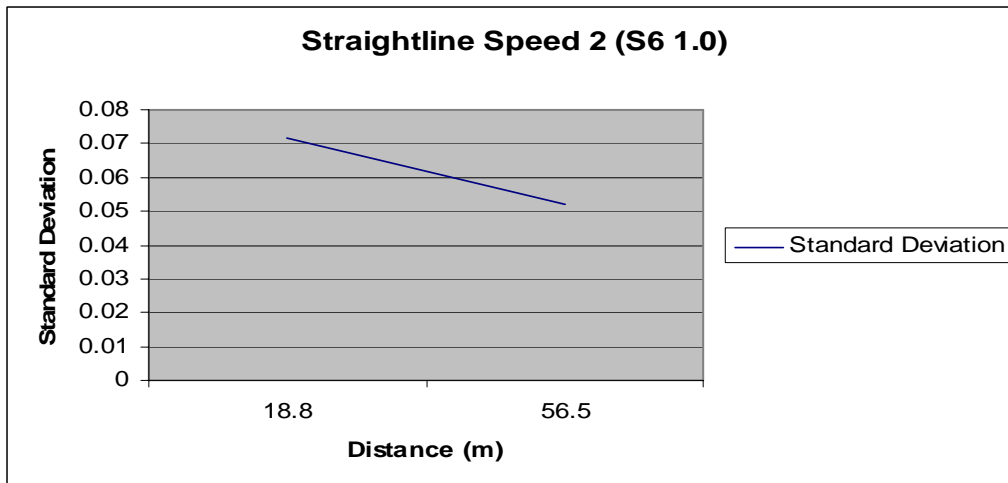


Figure G.16: Standard Deviation vs Distance graph, Speed 2.

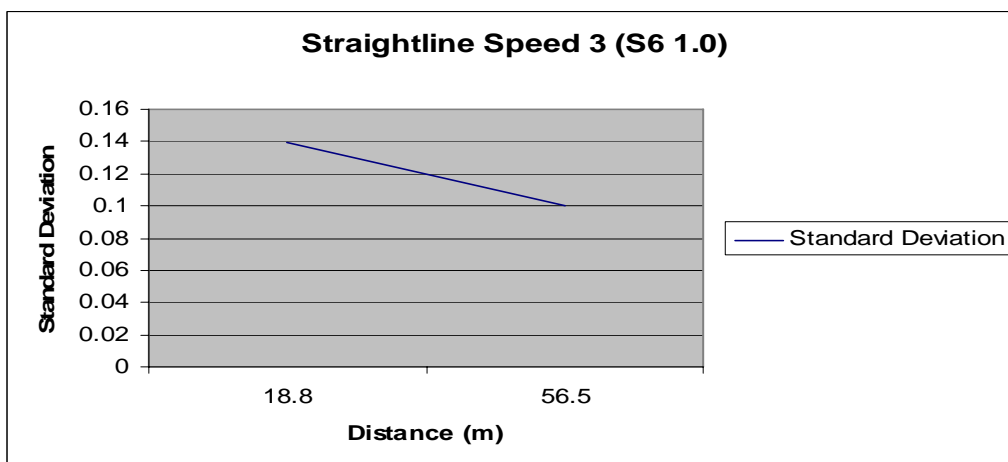


Figure G.17: Standard Deviation vs Distance graph, Speed 3.